universität wien

MASTERARBEIT / MASTER'S THESIS

Titel der Masterarbeit / Title of the Master's Thesis

„Glucose: A growth stimulator for early cancer prestages in rat liver“

verfasst von / submitted by

Christina Wernig, BSc

angestrebter akademischer Grad / in partial fulfilment of the requirements for the degree of

Master of Science (MSc)

Wien, 2017 / Vienna 2017

Studienkennzahl lt. Studienblatt / degree programme code as it appears on the student record sheet:	A 066834
Studienrichtung lt. Studienblatt / degree programme as it appears on the student record sheet:	Mastersudium Molekulare Biologie UG2002
Betreut von / Supervisor:	A.o. Univ. Prof. Dr. Bettina Grasl-Kraupp

Danksagung

Ich bedanke mich bei Prof. Dr. Bettina Grasl-Kraupp für die Finanzierung und Ermöglichung meiner Masterarbeit. Weiters bedanke ich mich für ihre fachliche Unterstützung und für die Zeit, die sie investiert hat.

Ein besonderer Dank gilt Tabea Reitinger, die mich in der Anfangszeit und darüber hinaus hervorragend eingeschult und unterstützt hat. Weiters möchte ich mich bei ihr und meinen Kollegen Max Valler und Jakob Paur für die gute Atmosphäre während der gemeinsamen Arbeitszeit und Freizeit bedanken.

Meinen Laborkolleginnen Corina Luca, Andja Gvozdenovich und Elisabeth Haslinger, sowie meinem Laborkollegen Johannes Schimming danke ich für die Unterstützung und Hilfsbereitschaft.

Ein ganz großer Dank gilt den Technikerinnen Birgit Mir-Karner und Helga Koudelka, die mir während der gesamten Zeit immer mit großer Hilfsbereitschaft zur Seite standen.

Ein besonderer und liebevoller Dank gilt meinem Partner Martin Fok, der mir immer Rückhalt gegeben hat und mich auch in schwierigen Situationen unterstützte und ermutigte.

Und zum Schluss bedanke ich mich bei meinen Eltern, sowie meinen Geschwistern und Freunden, die mich im Entstehungsprozess dieser Arbeit begleitet haben.

Table of Contents

1. Introduction **8**
1.1. The Liver 8
1.1.1. Anatomy and function 8
1.1.2. Different cells types of the liver 9
1.1.2.1. Hepatocytes (HC) 9
1.1.2.2. Kupffer cells (KC) 9
1.1.2.3. Endothelial cells (EC) 9
1.1.2.4. Hepatic stellate cells (SC) 9
1.2. Growth regulation in the liver 10
1.2.1. Regenerative growth of the liver 10
1.2.2. Adaptive growth of the liver 10
1.3 Nutrition and liver growth - glucose homeostasis 11
1.3.1. Glucose metabolism 11
1.3.1.1. Glucose transporter (GLUT) 12
1.3.2. Insulin and IGF signaling 13
1.3.2.1. Key pathways of insulin and IGF 14
1.3.3. Fuel-sensing via AMP-activated protein kinase (AMPK) 16
1.3.4. Impact of fasting and caloric restriction on liver growth 18
1.4. Development of liver cancer 19
1.4.1. Epidemiology of liver cancer 19
1.4.2. Multistage concept of hepatocarcinogenesis 20
1.4.3. Etiology of HCC: food and lifestyle 21
1.4.3.1. Ethanol 21
1.4.3.2. Aflatoxin 21
1.4.3.3. Arsenic 22
1.4.3.4. Obesity and T2DM 22
1.4.3.5. Non-alcoholic fatty liver disease (NAFLD) 23
1.4.4. Pathogenesis of liver cancer 24
1.4.4.1. Steatosis - steatohepatitis - fibrosis - cirrhosis - HCC 24
1.5. Therapies with glucose analogues 25
1.5.1. 2-Deoxyglucose (2DG) 25
2. Aims of the thesis **26**
3. Material and Methods **27**
3.1. Reagents 27
3.2. Solutions, buffers and media 29

3.2.1. Composition of culture media 32
3.3. In vivo methods 35
3.3.1. Animals 35
3.3.2. Treatment of the animals 35
3.3.2.1. N-nitrosomorpholine (NNM) 35
3.3.2.2. Phenobarbital (PB) 35
3.3.3. Perfusion of the rat liver 35
3.4. In vitro methods 36
3.4.1. Rat collagen solution 36
3.4.2. Isolation of HC 36
3.4.3. Treatment of HC 38
3.4.3.1. 2-Deoxyglucose (2DG) 38
3.4.3.2. Tritium thymidine (^{3}H-thymidine) 38
3.5. Analytical methods 39
3.5.1. Micro dissection, RNA isolation, and rat genome-array 39
3.5.2. ATP detection assay 39
3.5.3. Viability assay 40
3.5.4. Immunohistochemistry 40
3.5.4.1. Fixation of the cells 40
3.5.4.2. GSTp staining 40
3.5.4.3. Autoradiography 40
3.5.4.4. Hoechst staining 41
3.5.5. Determination of DNA replication 41
3.6. Statistical analysis 42
4. Results **43**
4.1. Transcriptome patterns of preneoplastic lesions of rat livers 43
4.1.1. Deregulation of glycolytic genes in liver foci 43
4.1.2. Deregulation of genes, involved in glycogenesis 44
4.1.3. Downregulation of genes, involved in gluconeogenesis 45
4.1.4. Upregulation of genes, involved in pentose phosphate pathway (PPP) 46
4.1.5. Preneoplastic liver lesions: summary of deregulated genes, involved in glucose metabolism 47
4.2. Comparison of different culture conditions on ATP level under treatment with 2DG 49
4.2.1. ATP level of primary HC kept in different culture media 49
4.2.2. ATP level of primary HC kept in WE_{new} (+/-G) and RPMI (+/-G) with and without food withdrawal 50
4.2.3. Vitality of primary HC in WE_{new} (+/-G) 52

4.2.4. Effect of 2DG on ATP levels of HC, kept in WE_{old} (+G), WE_{new} (+/-G) and RPMI (+/-G) 53
4.2.5. Effect of 2DG on the vitality of HC 55
4.3. Impact of 2DG on DNA synthesis of primary HC 57
4.3.1. DNA synthesis rate of 2DG treated primary HC kept in WE_{new} (+/-G) 57
4.3.2. Effect of 2DG treatment on DNA replication of unaltered and initiated primary HC in WE_{old} (+G) 58
4.3.3. Impact of 2DG treatment on unaltered and initiated primary HC in WE_{old} (+G) with and without EGF 59
4.3.4. Effect of 2DG treatment on unaltered and initiated primary HC, kept in RPMI (+/-G) 61
5. Discussion **64**
5.1. Analysis of the transcriptome pattern of enzymes involved in glucose metabolism 64
5.2. Impact of different culture media on ATP concentration, vitality and DNA replication of unaltered and initiated HC 66
5.2.1. Various compositions and components of three different culture media 66
5.2.2. Amino acid contents 67
5.2.3. Different vitamins and co-factors 69
5.2.4. Hormone additives in WE_{old} and WE_{new} (+/-G) 70
5.2.4. DNA replication of initiated HC, using different culture media 71
5.3. Inhibition of glucose supply by glucose analogue - 2-deoxyglucose (2DG) 72
5.3.1. ATP concentration, vitality and DNA replication of 2DG-treated, unaltered HC, cultured in media (+/-G) 72
5.3.2. DNA replication of 2DG-treated, initiated HC, cultured in media (+/-G) 73
6. Abstract **75**
7. Zusammenfassung **76**
8. References **78**
9. Appendices **84**
9.1. List of abbreviations 84
9.2. List of figures 89
9.3. List of tables 91
9.4. List of boxes 91

1. Introduction

1.1. The Liver

1.1.1. Anatomy and function

As one of the largest organs in the body, the liver accounts for 2% to 3% of the average body weight [1]. After digestion of food in the gastrointestinal tract, carbohydrates, lipids, proteins, vitamins and other food components are absorbed and transported via the bloodstream to the liver. There, the nutrients can be stored or used for anabolic processes. Further functions of the liver are the production of bile and the detoxification of xenobiotics [2]. The liver is a much-perfused organ, which receives approximately 25 % of total the cardiac output. It has a dual blood supply, the hepatic artery which supplies 30% of the flow and 60% of oxygen and the portal vein that supplies about 70% of the blood flow and 40% of oxygen. The hepatic artery and the portal veins together with the biliary tract form the portal triad (see figure 1) [3]. The cell types of the liver can be distinguished between parenchymal cells and non-parenchymal cells (NPC). The majority of the liver is composed of the parenchymal cells, called hepatocytes (HC) and bile epithelial cells. NPC make up the other fraction of cells in the liver [4]. The main cell types of NPC are Kupffer cells (KC), sinusoidal endothelial cells (EC) and stellate cells (SC). Other NPC types of the liver are lymphocytes and fibroblasts. EC line the sinusoidal structures, that flank the HC cords, while SC are located in the space of Disse between the HC and the sinusoidal lining cells [4], [5]. Parenchymal cells and NPC release numerous mediators, which perform paracrine and autocrine actions within the liver [6].

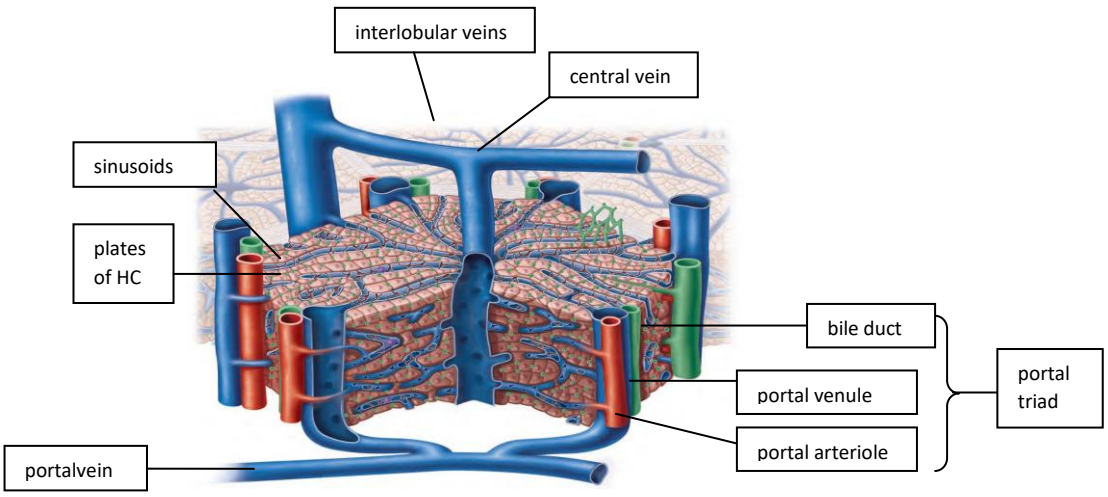


Figure 1: Scheme of the structure of sinusoids in the liver lobule and the portal triad [7].

1.1.2. Different cells types of the liver

1.1.2.1. Hepatocytes (HC)

HC occupy almost 80 % of the total liver volume and perform the majority of the liver functions, including storage and metabolism of nutrients from food, detoxification of xenobiotics and bile production. HC are particularly rich in rough endoplasmatic reticulum (ER) since they express hundreds of proteins, necessary to fulfill the numerous metabolic functions of this cell type. Furthermore, HC contain glycogen particles in the cytoplasm. HC are mononuclear or binuclear. HC divide only rarely, if at all, but after liver injury, functional load or by certain chemical compounds, HC leave the quiescent G_0-state, enter G_1-state of the cell cycle and start to proliferate. Through a cross-network between HC and the other cell types of the liver, the liver is able to fully regenerate (for further details, see chapter 1.2.) [5].

1.1.2.2. Kupffer cells (KC)

KC make up approximately 30 % of the sinusoidal cells. As the hepatic tissue macrophages, KC play an important role in the innate immune response and represent the first line in defense of particles and soluble bacterial product derived from the gut. KCs secrete numerous mediators of early phase inflammation, like reactive oxygen species (ROS) eicosanoids, nitric oxide (NO), carbon monoxide, tumor necrosis factor-α (TNF-α) and other cytokines. KCs have an endocytic and phagocytic capacity and thus prevent that pathogenic particles reach the systemic circulation. KC are the major producers of cytokines, which have both inhibitory and stimulatory effects on HC proliferation during regeneration process of the liver (for further details, see chapter 1.2.) [5], [6], [8].

1.1.2.3. Endothelial cells (EC)

EC play a protective role in the liver against pathogenic agents and a filtration system, due to the presence of fenestrations. EC also have an endocytic capacity for some ligands, such as glycoproteins, components of the extracellular matrix, immune complexes, transferrin and ceruloplasmin and function as antigen-presenting cells (APC). EC produce growth factors and cytokines, which also affect HC proliferation during liver regeneration (for further details see chapter 1.2.) [5], [6].

1.1.2.4. Hepatic stellate cells (SC)

SC, also known as fat-storing cells, ito cells, peri-sinusoidal cells or Vitamine A-rich cells, are present in perisinusoidal space and contain fat droplets in their cytoplasm. SC store vitamin A, control extracellular matrix production, regulate the contractility of sinusoids and synthesize growth factors.

After liver injury, quiescent SC change to myofibroblast-like cells, which have a key role in the inflammatory fibrotic response [5], [6].

1.2. Growth regulation in the liver

In adult rats, HC usually arrest in G_0-phase of the cell cycle. The potential of HC to replicate can be induced by two different ways: one way is regenerative growth following a massive loss of liver tissue. This may be due to partial hepatectomy or severe liver damage, as induced by cytotoxic drugs or viral infections. The other way is adaptive growth, which may be caused by functional load, like pregnancy, over nutrition, hormonal stimuli or by certain chemical compounds.

1.2.1. Regenerative growth of the liver

After partial hepatectomy or liver damage, the cells of the liver enter the cell cycle and proliferate to compensate for the lost tissue. The process of regenerative growth is based on a crosstalk between the different cell types of the liver and their released direct mitogens, priming factors and growth inhibitors. Direct mitogens are hepatocyte growth factor (HGF) and epidermal growth factor (EGF)-ligands, such as EGF, transforming growth factor-α (TGF-α) and heparin-binding EGF-like growth factor (Hb-EGF), which cause a strong mitogenic response in HC and stimulate their proliferation. Priming factors, such as interleukin-6 (IL-6), TNF-α, insulin-like growth factor (IGF), glucagon, insulin and some more, are factors, which support the action of direct mitogens. After HC and NPC had undergone several cell cycles, the liver regeneration is terminated. Termination of this process may be regulated by growth inhibitors, such as transforming growth factor-β_1 (TGF-β_1). The whole process is a well-coordinated interplay between growth stimulation (DNA synthesis) and inhibition (termination, apoptosis), which maintains the homeostasis of the normal liver size [9], [10].

1.2.2. Adaptive growth of the liver

Unlike regenerative liver growth, application of hepatomitogenic drugs exerts a direct growth stimulating effect on the liver. Xenobiotic agents, such as phenobarbitone, steroid hormones, norethisterone, organochlorine compounds, hexachlorocyclohexane or hexachlorobenzene fall into this category. These different compounds affect the liver by increasing liver growth and enhancement of specific functions, such as hepatic drug metabolizing enzyme activity.

Xenobiotic agents promote cell proliferation because they induce, that quiescent HC re-enter the cell cycle. It is assumed that the induction of proliferation is a receptor-mediated mechanism. Many hepatomitogenic xenobiotics activate nuclear receptors (transcription factor) via binding. As a consequence the receptor translocates into the nucleus, there functions as a transcription factor. In the nucleus, the receptor complex activates genes, which are involved in cell proliferation. After increased DNA replication in the cells of the liver (hyperplasia), the liver size is larger than normal, to fulfil the enhanced functional load. When the functional stimulus is withdrawn, the liver returns to its original size. Thereby the apoptosis rate is increased to establish the original number of liver cells. Thus, the growth of the liver after stimulation with xenobiotics does not serve as compensation for tissue loss but is rather an adaption to functional load [11]. The induction of DNA-synthesis may be regulated by the extent of food intake. Hoffmann and Schulte-Hermann (1979) [12] observed that α-hexachlorocyclohexane (α-HCH) failed to induce DNA-synthesis in HC if animals were fasted or subjected to protein-deprivation. They identified a period, 5 - 8 hours before the start of the cell cycle. Uptake of amino acids during this period caused to release from this block and accumulated HC entered the S-phase almost synchronously. Later on, it was speculated whether this point may be identical to the R-point (restriction point). This was first evidence, that nutritional factors are involved in the growth regulation of the liver.

1.3 Nutrition and liver growth - glucose homeostasis

1.3.1. Glucose metabolism

The monosaccharide glucose is one of the most important energy sources in the organism. Glucose in the arterial plasma derives from dietary sources, via glycogenolysis in the liver (breakdown of glycogen) or via gluconeogenesis in the liver and kidney (production of glucose from carbon compounds, such as lactate, amino acids, pyruvate or glycerol). The normal value of arterial plasma glucose throughout a 24 h period is approximately 90 mg/dL. The range of the concentration of normal blood glucose reaches from 55 mg/dL after exercise or fasting to 165 mg/dL after meal ingestion. This normoglycemic state is regulated by a hormonal system: the secretion of the hormone insulin is regulated by the amount of glucose in the blood. Pancreatic β-cells sense changes of blood glucose levels and induce insulin release into the blood, which in turn is able to lower the blood glucose level [13]. Degression of plasma glucose suppresses the release of insulin, which leads to degression of glucose uptake into the brain. The hypothalamus contains a glucose sensor system that triggers the release of hormones, such as glucagon, catecholamine, cortisol and growth hormone

(GH), which causes elevation of the blood glucose levels. When the level of blood glucose increases, the release of insulin suppresses glucagon secretion, which restores normoglycemia [14].

Intracellular glucose has four major fates (see figure 2): it is used for synthesis of complex polysaccharides, it may be stored as glycogen (glycogenesis), it may be processed to pyruvate for adenosine triphosphate (ATP) production (glycolysis) or may serve as metabolic intermediate in the pentose phosphate pathway (PPP) to generate ribose-5-phosphate (R5P) for the synthesis of nucleotides, which is required for DNA synthesis and cell proliferation. The key enzyme of glucose metabolism is hexokinase (HK), which phosphorylates incoming glucose to glucose-6-phosphate (G6P). The key enzyme of PPP, glucose-6-phosphate dehydrogenase (G6PD), catalyzes the first, rate-limiting step in this pathway, in which G6P is further processed for nucleotide synthesis [15].

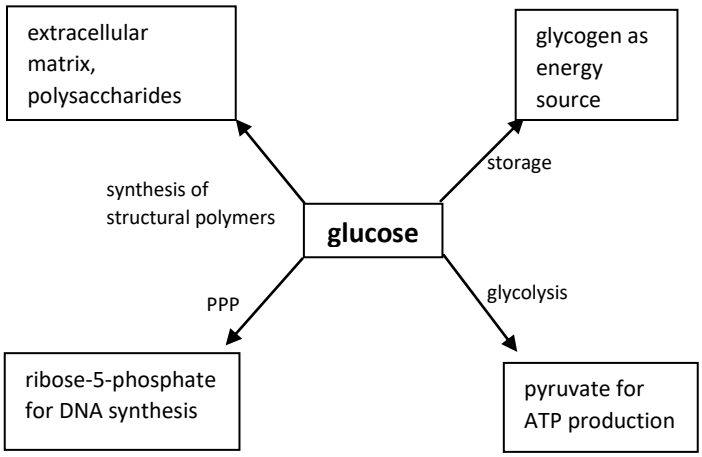


Figure 2: The four major fates of glucose. *Glucose may be used for the synthesis of polysaccharides, for glycogenesis as an energy source, for production of ATP via glycolysis or for ribose-5-phosphate synthesis via PPP.*

1.3.1.1. Glucose transporter (GLUT)

GLUT proteins are membrane transporters, which belong to the major facilitator superfamily. The fourteen members of GLUT are encoded by the solute carrier 2 (SLC2) genes. The different GLUT are expressed in various tissues and transport several hexoses, glucosamine, ascorbate and urate. The liver expresses GLUT2, GLUT8, GLUT9 and GLUT10 [16]. The major glucose transporter in HC is GLUT2. GLUT2 has low affinity for glucose, and transports also galactose, mannose, and fructose. GLUT2 is more involved in glucose efflux than in uptake of glucose.

During fasting, GLUT2 is responsible for gluconeogenesis- and glycogenolysis-derived glucose efflux to maintain normoglycemia and to prevent hypoglycemia. In the fed state, the plasma glucose and insulin concentrations increase, thereby inhibiting gluconeogenesis in HC (see chapter 1.3.2.1.1., section *inhibition of gluconeogenesis* below). Furthermore, in the fed state, GLUT2 is removed from the membrane, which results in degression of GLUT2-mediated glucose release [17], [18]. However, the glucose transport out of the cell is not fully GLUT2-dependent. In the absence of the transporter, the glucose release is mediated via a membrane traffic pathway, in which gluconeogenesis- and/or glycogenolysis- derived glucose is directly released from the endoplasmatic reticulum [19], [20]. The glucose transport into HC seems to be mediated by the insulin level in the plasma. Hyperinsulinemia elevates the hepatic glucose influx and the phosphorylation state of glucose [21] via mediating the induction of gene expression of hepatic HK (HK4) [22], [23].The insulin-mediated uptake of glucose may be partly influenced by the suppression of free fatty acid release into the plasma [21].

1.3.2. Insulin and IGF signaling

The hormone insulin is released by pancreatic β-cells in response to nutrients in the blood. Insulin regulates the uptake and storage of glucose, fatty acid, and amino acids into the liver, muscles and adipose tissue, and is involved in the regulation of protein and lipid synthesis. Furthermore, insulin inhibits ketogenesis and gluconeogenesis [24].

The insulin-like growth factor 1/2 (IGF1/2) belong to the family of insulin-related peptides and have high structural similarities to insulin. IGF1, as well as IGF2, have crucial roles in growth regulation processes within the cell, the latter especially in growth regulation of embryonic development. Low levels of IGF1 stimulate the secretion of GH from the anterior pituitary, which promotes the induction of IGF1 in the liver (negative feedback mechanism). IGF1 regulates the paracrine production of IGF1 in other tissues [25]. The bioavailability of IGF1 depends on the presence of IGF-binding proteins (IGFBPs), that limit the access of IGF1 to the IGF1 receptor (IGF1R) by forming binary complexes with IGF1 [26]. IGF2 is regulated by binding on IGF2R, which inhibits IGF2 by targeting it for degradation without signal transduction [27]. Insulin and IGFs exert this functions via the insulin receptor (IR) and/or insulin-like growth factor receptors (IGFR). IR and IGFR are heterotetrameric proteins, which contain two linked α-β-dimers. IR has two isoforms, which is a result of alternative splicing of exon 11: IR-A and IR-B. IR-A recognizes insulin and IGFs (with higher affinity for IGF2) and is mainly expressed in tumor and fetal cells and has anti-apoptotic and mitogenic effects, whereas IR-B only recognizes insulin and occurs in differentiated tissues, such as liver, muscle, and adipose tissue, where it is mainly involved in glucose homeostasis. The different types of receptors can form hybrid receptors: IR/IGFR and also IR-A/IR-B hybrid receptors (see figure 3) [28], [29].

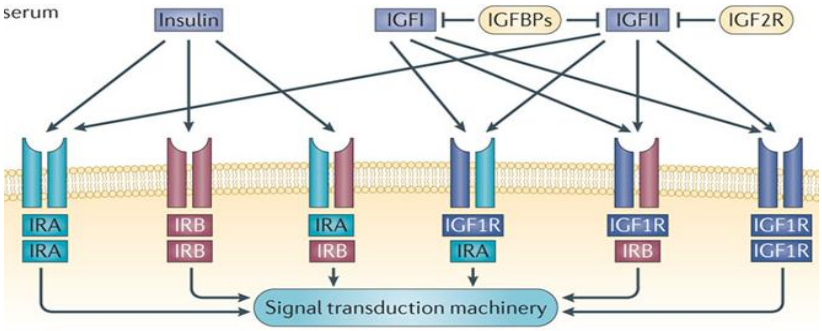


Figure 3: The insulin and IGF receptor family. *Insulin has direct access to its receptor, whereas the access of IGFs is dependent of IGFBPs and IGF2R respectively. IR has two isoforms (IR-A, IR-B), IGF1R only has one isoform. The different receptors/receptor isoforms can form receptor hybrids* [27].

1.3.2.1. Key pathways of insulin and IGF

The binding and activation of the receptors by insulin and/or IGFs and the following autophosphorylation recruits substrate adaptors, such as insulin receptor substrates (IRS1/2), Src homology 2 domain containing (SHC), Grb-2 associated protein 1 (Gab1), dedicator of cytokinesis protein 1 (Dock1), the E3-ubiquitin-protein ligase casitas B-lineage lymphoma (Cbl) or SH2B adaptor protein 2 (APS), which leads to activation of different pathways: the phosphoinositide 3-kinase (PI3K)/proteinkinase B (or AKT)/mammalian target of rapamycin (mTOR) pathway, the PI3K/AKT/forkhead box O (FOXO) pathway and the rat sarcoma G-protein (Ras) /mitogen-activated protein kinase (MAPK) pathway, which have important roles in cell growth and proliferation (see figure 4) [25], [27], [29].

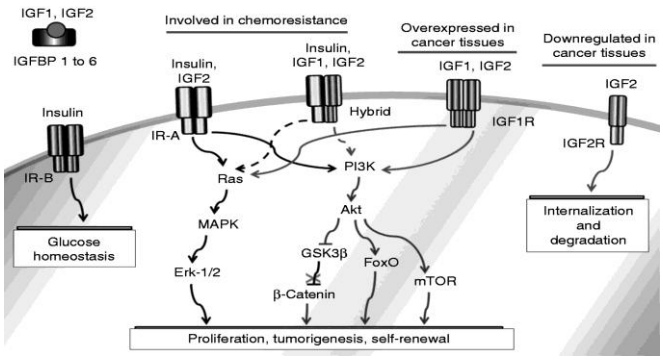


Figure 4: Insulin and IGF signaling and downstream pathways and their role in cancer. *Regulation of growth and energy balance* [29].

1.3.2.1.1. The PI3K/AKT pathway

Insulin/IGFs bind to the extracellular α-subunits of IR/IGFRs, which leads to conformational changes resulting in the autophosphorylation of the transmembrane β-subunits of the receptor. This activates IR/IGFR and recruits adaptor substrates such as insulin receptor substrate 1/2 (IRS1/2), which can bind to the receptors and gets phosphorylated. The p85 regulatory subunit of PI3K recognizes and binds to the phosphorylated IRS1/2. The catalytic subunit of PI3K, p110, converts phosphatidylinositol (4, 5) bisphosphate (PIP_2) to phosphatidylinositol (3, 4, 5) bisphosphate (PIP_3). This recruits AKT, which gets phosphorylated by phosphoinositide-dependent kinase 1 (PDK1). The activation of AKT and its downstream targets affect cell metabolism, cell growth and cell survival and are described below [24], [27], [29].

Stimulation of glucose uptake

The activation of AKT leads to the translocation of the glucose transporter 4 (GLUT4) to the plasma membrane, by which glucose gets into the cytoplasm of muscle and fat cells. [30], [31]. Insulin elevates the glucose uptake into the liver and stimulate and elevates the phosphorylation state of glucose by stimulation of HK4 transcription [21]–[23]. Further details about glucose uptake/export in the liver are described in chapter 1.3.1.1.

Promotion of glycogen storage

Activated AKT inhibits glycogen synthase kinase 3 (GSK3). Under basal conditions, the constitutive active GSK3 inhibits the enzyme glycogen synthase (GS), that catalyzes uridine diphosphate (UDP)-glucose to glycogen, the final step in glycogenesis [30].

Stimulation of amino acid uptake and protein synthesis

Another effect of the inhibition of GSK3 by AKT is the dephosphorylation and activation of the guanine nucleotide exchange factor, termed eukaryotic initiation factor 2 (eIF2B) thereby initiating protein synthesis and the storage of amino acids [30].

AKT phosphorylates the GTPase activating protein (GAP), termed tuberous sclerosis complex 2 (TSC2), which is an upstream component of mTOR complex 1 (mTORC1), which leads to TSC2 inhibition. This activates mTORC1, which promotes protein synthesis via p70 ribosomal S6 kinase (p70S6K) and inhibition of eIF4E binding protein 1 (4EBP1), which is a translation repressor protein. (For more details about mTOR pathway, see chapter 1.2.1.3) [24].

Regulation of lipid synthesis

Insulin activates the sterol regulatory element-binding protein (SREBP)-1c mTOR-dependent, which is involved in the transcriptional activation of lipogenic genes [32]. SREBP-1c also is activated by the

ligand-activated transcription factor liver X receptor (LXR)-α, whose expression is induced by insulin [33].

Inhibition of gluconeogenesis

Activated AKT by insulin/IGF signaling, phosphorylates FOXO transcription factors, causing its nuclear exclusion and subsequently the degradation of FOXO transcription factor. In the unphosphorylated state, FOXO transcription factor increases the transcription rate of glucose-6-phosphatase, an enzyme that converts G6P to glucose in the gluconeogenesis. The insulin/IGF mediated phosphorylation of FOXO therefore leads to the inhibition of gluconeogenesis [34].

1.3.2.1.2. The Ras/MAPK pathway

After binding of insulin/IGFs to the receptor, the substrate adaptor growth factor receptor-bound protein 2 (Grb2) and the guanine exchange factor son of sevenless (SOS) bind to the phosphorylated and activated receptor. SOS removes GDP that is bound to Ras. Ras is able to bind GTP and gets activated. Ras activates the protein rapidly accelerated fibrosarcoma (Raf), which activates mitogen-activated protein kinase kinase 1/2 (MEK1/2) and thus activates MAPK. This kinase cascade leads to the activation of transcription factors of the activator protein-1 (AP-1) family c-fos and c-jun, which move to the cell nucleus and form a heterodimer and bind on an AP-1 motif on the DNA. This leads to expression of several genes involved in cell growth and proliferation [35], [36].

1.3.3. Fuel-sensing via AMP-activated protein kinase (AMPK)

The nutrient-sensing enzyme AMPK represents a metabolic checkpoint, acting as an energy sensor, by re-installing energy levels by switching off energy-consuming pathways, such as protein and lipid synthesis and turning on ATP-generating processes, such as fatty acid oxidation and glycolysis [37]–[39]. AMPK is a heterotrimer, comprised of a catalytic (α) subunit and two regulatory (β, γ) subunits. During nutrient deprivation or hypoxia (conditions of low oxygen), the intracellular concentration of ATP decreases and concentrations of AMP and ADP increase. ATP, ADP and AMP try to bind to the regulatory sites of AMPK, hence, the ratios of ATP: AMP and ADP: ATP regulate the activation of AMPK. In response to energy depletion, liver kinase 1 (LKB1) phosphorylates α-subunit of AMPK, thereby activating AMPK. In response to increased intracellular Ca^{2+} levels, the upstream kinase Ca^{2+}/calmodulin-dependent kinase kinase β (CAMKKβ) phosphorylates and activates AMPK (see figure 5) [37], [38], [40], [41]. One of the main growth regulatory pathways, which are controlled by LKB1 and AMPK, is the mTOR pathway (see figure 5). The mTOR pathway regulates cell growth and proliferation. mTOR occurs in two biochemical and functional different complexes: mTOR complex 1

(C1) and mTOR complex 2 (C2). mTORC1 consists of the regulatory-associated protein of mTOR, called raptor (it is rapamycin-sensitive), which recruits downstream substrates, such as p70S6K1 (regulation of protein translation). mTORC1 regulates translation of several cell growth regulators, such as cyclin D1, hypoxia-inducible factor 1α (HIF1α) and avian myelocytomatosis viral oncogene homolog (Myc). mTORC2 comprises the rapamycin-insensitive mTOR-subunit, termed rictor. TSC2, which is upstream of mTORC1, is a GTPase activation protein (GAP) and it hydrolyzes the bound GTP of the active G protein, called Ras homolog enriched in brain (Rheb), which activates mTORC1 in its GTP-bound form. Therefore, TSC2 inhibits mTORC1 indirectly [42], [43]. Under conditions of energy stress, activated AMPK directly phosphorylates TSC2 on its serine sites and primes these serine residues for final phosphorylation by GSK3, which enhances TSC2 activity. AMPK also phosphorylates serine residues in raptor, leading to binding of raptor to 14-3-3-protein. This shows, that mTORC1 activity is inhibited by a dual mechanism [37], [38], [43].

AMPK also inhibits the enzyme of cholesterol synthesis 2-hydroxy-3-methylglutaryl-CoA-reductase (HMGCR), the key enzymes of fatty acid synthesis, termed acetyl-CoA-carboxylase 1 (ACC1) and ACC2, which is responsible for the inhibition of fatty acid oxidation (which leads to ATP generating fatty acid oxidation) [37]. The mechanisms of AMPK restore cellular energy homeostasis [37]–[41], [44].

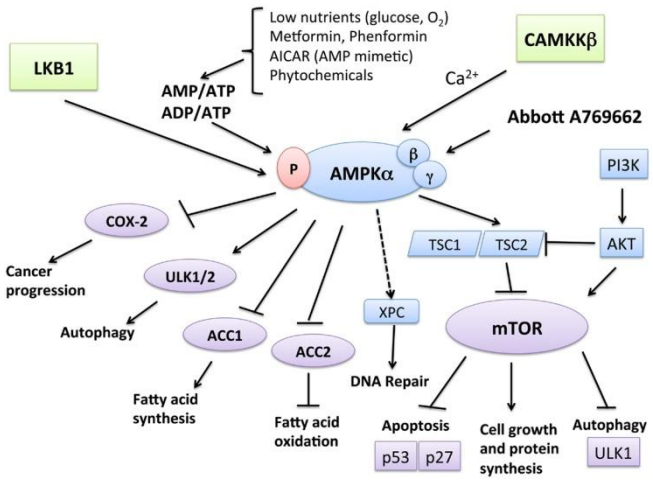


Figure 5: Mode of action and regulation of AMPK. *LKB1 and CAMKKβ phosphorylate AMPK on the α-subunit. A small molecule activator (A769662) activates AMPK both allosterically and by inhibiting its dephosphorylation. Activated AMPK acts by switching off energy consuming processes and turning on ATP-generating processes* [40].

1.3.4. Impact of fasting and caloric restriction on liver growth

Fasting or caloric restriction leads to an adaptive stress response within the cell, changes of metabolic pathways and cellular processes. The plasma glucose levels decrease and the hepatic glycogen storage depletes, which forces the cell to utilize alternative energy sources, such as free fatty acids or fatty acid-derived ketone bodies (α-hydroxybutyrate), that is produced from acetyl-CoA in β-oxidation of fatty acids or by conversion of ketogenic amino acids in HC [45]. Due to the degression of glucose during caloric restriction, the insulin levels decrease too, which result in several alterations in the metabolism and gene expression in the cell. IGF1 decreases, whereas the IGF1-repressor proteins, IGFBPs are upregulated by caloric restriction in the liver of rats. The decrease of IGF1 is due to the reduced expression of the GH receptor on liver cells, whereupon GH is no longer able to bind the GH receptor to stimulate IGF1 production [45], [46]. FOXO transcription factors play an important role during caloric restriction. FOXO is negatively regulated by AKT, which is stimulated by insulin/IGF2 signaling. AKT phosphorylates FOXO, which leads to its exclusion of the nucleus and degradation in the cytoplasm. Unphosphorylated, FOXO regulates expression of genes in various tissues, which are involved in regulation of metabolism, regulation of cell cycle, cell death and oxidative stress response. In the liver, FOXO mainly increases gluconeogenesis. One of the main regulators of FOXO, termed sirtuin 1 (SIRT1), is also upregulated during caloric restriction. SIRT1 deacetylates cytosolic FOXO, which promotes reverse translocation of FOXO into the nucleus and the upregulation of the expression of downstream genes [47], [48]. During caloric restriction, the rate of lipolysis (lipases, peroxisome proliferator-activator receptors (PPAR)) increases and the rate of lipogenesis (fatty acid synthase, SREBP-1c) decreases. PPARs (together with retinoid X receptor (RXR)) play roles in β-oxidation of fatty acids, ketone body synthesis, glucose sparing, differentiation of adipocytes, which leads to induction of the insulin-sensitizing hormone adiponectin [49]. The upregulation of PPARs during caloric restriction leads to enhanced secretion of adiponectin and the subsequent reduction of accumulation of triglycerides (TG) in liver and muscle cells, which results in enhanced insulin sensitivity of the insulin receptor [47], [50]. Protein tyrosine phosphatase 1B (PTP-1B) is a negative regulator of IR autophosphorylation, which reduces the sensitivity of the receptor to its ligand by dephosphorylation. PTP-1B is downregulated during caloric restriction, that also leads to enhanced insulin sensitivity [50]. Jiang et al (2008) showed that fasting increased phosphorylation of the energy sensor enzyme AMPK, which resulted in inhibition of the mTOR pathway, which plays a central role in growth processes. Furthermore, Prokesch et al. (2017) [51] indicated that the activation of AMPK is involved in the posttranscriptional stabilization of the hepatic p53 protein during starvation in mice.

Experiments with the hepatic p53-depleted mouse model showed that p53 is required for the maintenance of glucose homeostasis and for the expression of genes, which controls amino acid catabolism during starvation [51].

1.4. Development of liver cancer

1.4.1. Epidemiology of liver cancer

Primary liver cancer is the sixth most abundant cancer worldwide [52]. Interestingly men are more affected than woman (see figure 6). The majority of the cases occur in developing regions, with high incidence in Eastern and South Eastern Asia, Middle and Western Africa. In developed regions (except Southern Europe) the rates are lower. In 2008 nearly 700 000 death from liver cancer was estimated (far more of the half were men). Liver cancer is the second most frequent cause of death from cancer worldwide [53].

Liver cancer is categorized into several types, based on the cell type that becomes malignant: the most common form is the hepatocellular carcinoma (HCC), deriving from HC. The fibrolamellar hepatocellular carcinoma is a rare type of liver tumors and is composed of malignant HC and laminated fibrosis between the tumor cells. The cholangiocarcinoma stems from bile ducts and can be divided into an intrahepatic and an extrahepatic form. The lymph- or hemangiosarcoma derive from intrahepatic lymph or blood vessels, respectively. Secondary liver tumors develop when primary cancer cells, which are often metastasis of colorectal cancer, spread to the liver [54].

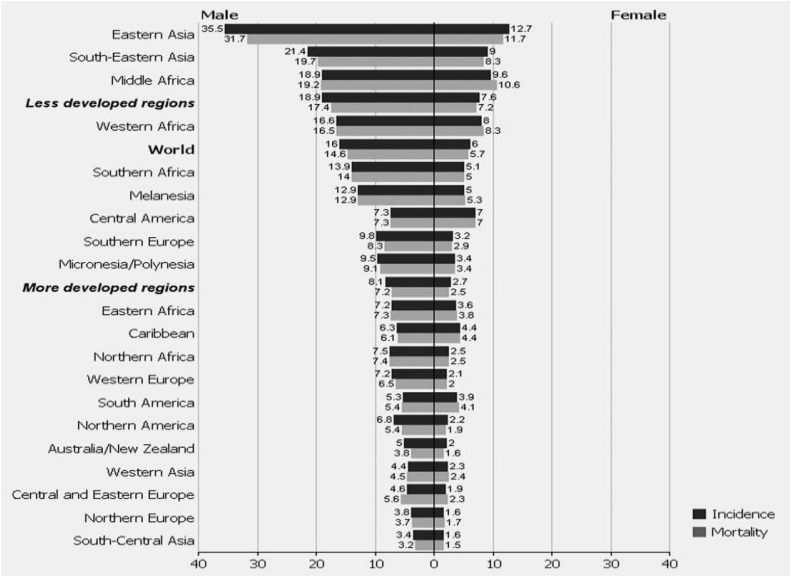


Figure 6: Estimated age-standardized incidence and mortality rates for liver cancer [55].

1.4.2. Multistage concept of hepatocarcinogenesis

The development of liver cancer is a multistage process, which comprises initiation, promotion, and progression (see figure 7): The stage of initiation involves gene mutations, which may emerge either spontaneously or after chronic inflammation or exposure to carcinogenic agents. The mutations may comprise alterations in a single gene (point mutations, frame shift mutations, gene amplification or deletion), aberrations in single chromosomes (chromosome breaks, translocations) or changes in the genome (changes in the number of chromosomes - aneuploidy). These mutations mainly affect genes, involved in the regulation of cell growth and/or cell death (tumor suppressor genes/oncogenes). More than two rounds of the cell cycle and an impaired DNA repair system are necessary to establish mutations in these genes [56]–[58].

Tumor promotion describes the selective clonal expansion of initiated cells that have acquired growth advantages. In this phase, DNA replication increases and the apoptosis rate decreases, this leads to a net gain of initiated/preneoplastic cells. Extended exposure toward growth stimuli, the preceding loss of function of tumor suppressor genes and the gain of function mutations of oncogenes promote this increase of DNA replication and the decrease of apoptosis. Promotion is a slow and long-lasting process but is reversible by the withdrawal of the growth stimulator. Then the tumor prestages shrink by enhanced apoptotic activity [56]–[58].

Further mutations and proliferation of the cells, as a consequence of genetic instability, lead to the progression phase, which represents a late stage of carcinogenesis. The progression phase defines the transition from premalignant to malignant cells. Then, the tumor cells are acquiring the potential for destructive and invasive growth and the formation of metastasis [56]–[58].

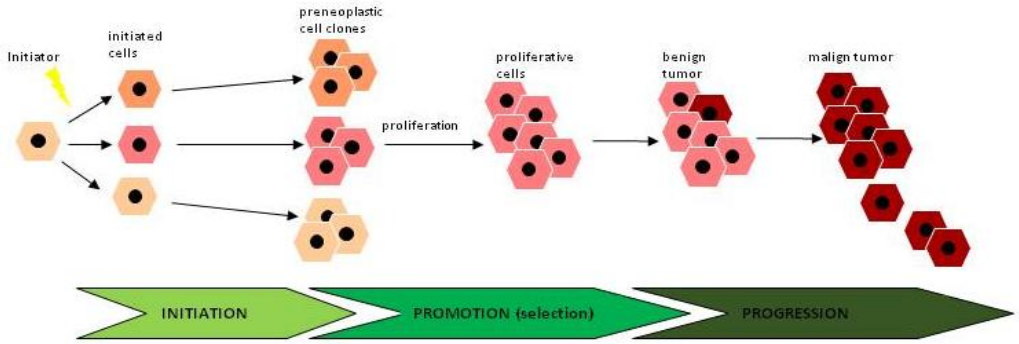


Figure 7: The Multistage process of hepatocarcinogenesis. *The multistage concept comprises the initiation phase, in which gene mutations occur, the promotion phase of clonal expansion and selective growth of initiated cells and the progression phase, which represents the transition from premalignant to malignant cells.*

1.4.3. Etiology of HCC: food and lifestyle

The western lifestyle is characterized by the consumption of fat-rich food and easily digestible carbohydrates with high glycemic indices. This diet may lead to obesity, type-2 diabetes mellitus (T2DM) and associated diseases, such as metabolic syndrome, which is characterized by dyslipidemia (high TG levels and low high-density lipoprotein (HDL)- levels), central obesity, insulin resistance and hypertension [59]. With regard to further food and lifestyle factors, excessive ethanol abuse shows a high prevalence in industrial countries and increases the risk of HCC. In developed countries, other HCC risk factors are important, such as aflatoxin-contaminated food and arsenic in the drinking water.

The impact of these factors on the development of HCC is outlined in the following.

1.4.3.1. Ethanol

A risk factor for developing liver cancer is the excessive consumption of ethanol. The persistent intake of ethanol leads to liver damage, due to gut-derived endotoxins, oxidative stress, and inflammation. In detail, the oxidation of ethanol takes place in the liver. Alcohol dehydrogenase (ADH) generates acetaldehyde which is further metabolized to acetate by the enzyme aldehyde dehydrogenase (ALDH). The first step, catalyzed by ADH, generates NADH, which changes the mitochondrial redox potential, resulting in oxidative stress. This, in turn, influences tricarboxylic acid cycle (TCA) and β-oxidation of fatty acids, accelerating the accumulation of lipids in the liver. The toxic acetaldehyde, in combination with ethanol, impairs the intestinal epithelial tight junctions, resulting in enhanced permeability to endotoxins. Endotoxemia triggers KC to produce ROS and cytokines, which lead to inflammatory processes in the liver [60], [61]

1.4.3.2. Aflatoxin

In sub-Saharan Africa, Eastern Asia and South America, food (maize, ground nuts, rice) often is contaminated with aflatoxin B1, B2, G1, and G2, which are metabolites of the fungi *Aspergillus flavus* and *Aspergillus parasiticus*. The mycotoxins are produced as a result of food storage at high temperature and humidity. In the liver, aflatoxins are converted into several electrophilic intermediates by cytochrome p450 enzymes. These intermediates are mutagenic and carcinogenic, by causing loss of function mutations in the DNA-binding domain of the tumor suppressor gene p53. Aflatoxin B1 has the highest hepatocarcinogenic potential [62].

1.4.3.3. Arsenic

Another dietary risk factor for liver cancer is the contamination of drinking water with organic arsenic. Millions of people in Bangladesh and other countries are chronically exposed to arsenic in the drinking water, leading to higher mortality due to liver, lung, skin, kidney and bladder cancer. Arsenic disturbs processes, such as energy metabolism, signal transduction, DNA repair, and may change DNA methylation patterns, which may lead to carcinogenesis [63], [64].

1.4.3.4. Obesity and T2DM

Most of the obese individuals have a higher risk to develop T2DM. This link between obesity and the pathogenesis of T2DM can be explained by the portal/visceral hypothesis: adipocytes of obese individuals have increased rates of lipolysis, which causes an overflow of the liver with free fatty acids. This affects the cells´ capability of glucose uptake and metabolism, which results subsequently in insulin resistance of the liver, skeletal muscle and the adipose tissue [65].

Insulin resistance is the main characteristic of T2DM. Glucose is no longer able to enter the cells, which leads to high blood glucose levels. As a consequence of high blood glucose levels and insulin resistance, pancreatic β-cells produce insulin in excessive amounts. This is the attempt to compensate the insulin resistance, which leads to hyperinsulinaemia and hyperglycaemia [29]. High levels of insulin increase levels of bioavailable IGF1, due to suppression of IGFBP1/2. These high levels of insulin and IGF1 lead to enhanced insulin/IGF1 signaling, which promotes cell proliferation, cell growth, antiapoptotic pathway activation, alterations in carbohydrate metabolism and protein synthesis stimulation via the PI3K/AKT and/or Ras/MAPK signaling pathways. It is assumed that insulin resistance and the following hyperinsulinaemia may represent the link between obesity, T2DM, and cancer [28], [29], [66].

Additionally to hyperinsulinaemia, blood levels of adipokines (such as leptin or adiponectin) and cytokines (TNFα and IL6) are abnormal in persons suffering from obesity and T2DM. The proinflammatory cytokines TNFα and IL6 are increased. The leptin levels, which correlate positively with white adipose tissue mass, are elevated as well. The enhanced action of leptin includes regulation of energy homeostasis and stimulation of cell growth. Adiponectin, that inhibits inflammation, insulin resistance and cell growth via AMPK activation, is downregulated in obese individuals and patients with T2DM. It is obvious, that obesity and T2DM are proinflammatory conditions, which may contribute to chronic liver diseases, such as non-alcoholic fatty liver disease (NAFLD) and/or development of cancer [28].

1.4.3.5. Non-alcoholic fatty liver disease (NAFLD)

Non-alcoholic fatty liver disease (NAFLD) is one of the most common forms of chronic liver diseases and is the hepatic manifestation of the metabolic syndrome, including dyslipidemia, central obesity, insulin resistance and hypertension. Obese individuals and patients with T2DM have a high risk to develop NAFLD. NAFLD comprises two stages of the disease. The first stage is non-alcoholic fatty liver (NAFL), which involves steatosis (lipid accumulation in HC). NAFL may turn into non-alcoholic steatohepatitis (NASH), showing not only steatosis but also hepatic inflammation [67].

The pathogenesis of NAFLD is based on 2 hits (see figure 8): the first hit is a consequence of insulin resistance in obese individuals. Then lipolysis is hyperactivated and β-oxidation is inhibited in adipocytes, which leads to elevated levels of free fatty acids in the plasma and accumulation into HC. Other sources of lipids, which may accumulate within HC, are dietary sources and de novo lipogenesis, due to upregulation of SREBP-1c. The excessive accumulation of fat (TG) within HC leads to hepatic insulin resistance and steatosis, in further consequence to increased susceptibility of the liver to injuries, mediated by pro-inflammatory cytokines/adipokines, oxidative stress and mitochondrial dysfunction (ROS production), which is known as the second hit in the pathogenesis of NAFLD. This second hit leads to hepatic inflammation (steatohepatitis), fibrosis, cirrhosis and subsequently to the development of liver cancer [68]–[71].

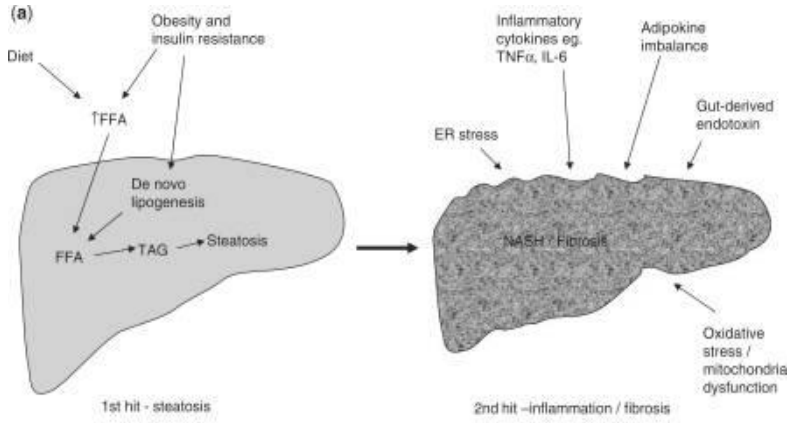


Figure 8: The two hit hypothesis in the pathogenesis of NAFLD. *Accumulation of fat within HC leads to steatosis, which represents the 1st hit. Proinflammatory cytokines and adipokines, oxidative stress and mitochondrial dysfunction lead to the 2nd hit, hepatic inflammation and fibrosis* [69]

1.4.4. Pathogenesis of liver cancer

1.4.4.1. Steatosis - steatohepatitis - fibrosis - cirrhosis - HCC

The development of steatosis to steatohepatitis is described in detail above (see chapter 1.4.3.5.). In response to liver injury, a wound healing process in the liver is occurring. HC try to compensate for the lost tissue and undergo regenerative DNA synthesis (see chapter 1.2.1.). Thereby proinflammatory mediators (cytokines, growth factors, and ROS) are generated by injured HC, neighbouring cells and infiltrating immune cells, leading to the activation of hepatic SC and their transformation into highly proliferative myofibroblast. Myofibroblasts regulate the secretion and degradation of extracellular matrix (ECM) at the sites of tissue repair. In liver fibrosis, the ECM composition (ECM contains macromolecules, such as collagen (I, III and IV), undulin, fibronectin, elastin, proteoglycans, laminin, and hyaluronan) and the ECM quantity are altered. Myofibroblasts secrete large amounts of ECM proteins (collagen) and inhibit ECM degradation. The emerging collagen bands replace more and more HC, which destructs the normal hepatic architecture and function [72]–[74]. This stage represents the transition from fibrosis to cirrhosis. Liver cirrhosis is characterized by the formation of nodules, which consist regenerative parenchyma surrounded by fibrotic septae (see figure 9) [72], [75]. During cirrhosis, the liver continues to regenerate, i.e. the cell turnover rate is highly elevated in this stage. At the same time, many HC die, this recruits inflammatory cells. Due to this chronic inflammation, the genomic DNA of HC suffers oxidative and nitrosative damages, which may lead to the accumulation of mutations. Mutations, which occur in genes, involved in regulation of proliferation and apoptosis, may lead to growth advantages of HC. This stage is characterized by the occurrence of phenotypically altered and dysplastic HC with increased proliferation rate and decreased apoptosis rate. Dysplastic HC may give rise to the development of dysplastic nodules, which represent tumor prestages. In the long phase of HCC development, which takes 10 - 30 years, the cells have to acquire several features to become malignant and develop several strategies to survive and invade surrounding tissues [76].

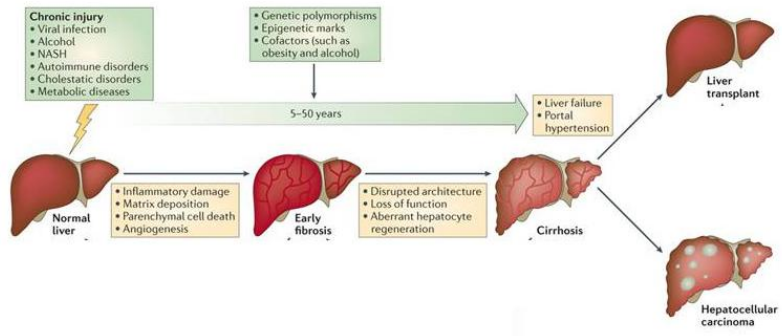


Figure 9: Pathogenesis of liver cancer. *After preceding liver injury, fibrosis and cirrhosis occur, which may lead to the development of HCC* [72].

1.5. Therapies with glucose analogues

Reprogramming of cellular metabolism belongs to the hallmarks of cancer and fulfills the energy needs of cancer cells. Due to elevated glucose metabolism, cancer cells consume the bioenergetic intermediates to build up biomass and nucleotides for DNA replication (see chapter 1.3.1.). The deprivation of tumor bioenergetics by inhibition of energy pathways turned out as a novel strategy to fight cancer [77]–[79]. Therefore glucose analogues, such as 2-deoxyglucose (2DG) and others, are promising agents, which may inhibit glycolysis and pathways involved in cell growth. Other glucose analogues, which target the glucose metabolism, are 5-thioglucose and D-mannoheptulose, both inhibiting the enzyme HK [80], [81].

1.5.1. 2-Deoxyglucose (2DG)

2DG is a synthetic glucose analogue, which has the C2 hydroxyl group replaced by hydrogen. The high structural similarity to glucose allows the transport of 2DG into the cell via glucose transporter (GLUT). Then, 2DG is converted by HK to phosphorylated 2DG (2DGP), which accumulates in the cell, leading to inhibition of HK, which is the rate-limiting enzyme in the glycolysis (see figure 10). This inhibition decreases the production of ATP and lactate and leads to cell cycle arrest and apoptosis [81], [82].

Some reports revealed that the 2DG-based therapy may be more effective in combination with other antitumoral agents [77], [83], [84]. These antitumoral agents include among others, tephrosin [83] or AMPK agonist (such as metformin) [77] or sorafenib, a multi-kinase inhibitor, used for therapy of advanced HCC [84].

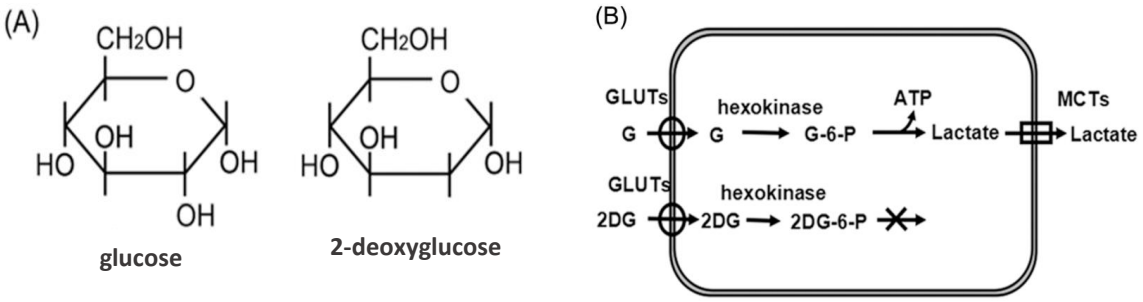


Figure 10: (A) Molecular structure of glucose and 2DG. (B) 2DG and the inhibition of HK*. The high structural similarity of 2DG with glucose allows the 2DG transport into the cell by GLUT. HK phosphorylates 2DG. 2DG-P accumulates in the cell and thereby inhibiting HK, leading to inhibition of glucose metabolism* [85].

2. Aims of the thesis

Metabolic syndrome and type 2 diabetes (T2DM) are established risk factors leading to the development of hepatocellular carcinoma (HCC). Both risk factors are characterized by elevated blood glucose levels. For this purpose, we addressed the question whether blood glucose may be involved in the process of hepatocarcinogenesis.

In the present work, we addressed the following issues:

1. First, we characterized and analyzed the transcriptome patterns of preneoplastic liver lesions with a focus on enzymes, which are involved in the glucose metabolism.

2. We investigated whether glucose supply may act as a growth-stimulating factor for unaltered and preneoplastic hepatocytes.

3. Hexokinase turns glucose to glucose-6-phosphate which enables the cells to use glucose-6-phosphate as an energy source, for the pentose-phosphate pathway and/or for glycogen-storage. We addressed the question whether blockade of hexokinase may affect the use of glucose as fuel for the growth of unaltered and preneoplastic hepatocytes.

3. Material and Methods

3.1. Reagents

Name	Supplier
2-Deoxyglucose	*Sigma (St. Louis, MO, USA)*
Ascorbat	*Merck (Darmstadt, Germany)*
Bovine serum albumin (BSA)	*Sigma (St. Louis, MO, USA)*
Calcium chloride	*Merck (Darmstadt, Germany)*
Chloroform	*Merck (Darmstadt, Germany)*
Collagenase, Type II	*CLS2 Worthington (Lakewood, NJ, USA)*
Dexamethasone	*Sigma (St. Louis, MO, USA)*
FCS (Fetal calf serum)	*PAA (Pasching, Austria)*
Formalin	*Merck (Darmstadt, Germany)*
Gentamycin	*Serva (Heidelberg, Germany*
Glucagon	*Sigma (St. Louis, MO, USA)*
Glucose monohydrate	*Merck (Darmstadt, Germany)*
Glutamax	*Gibco (Carlsbad, CA, USA)*
Glycerol	*Sigma (St. Louis, MO, USA)*
Glycine	*Sigma (St. Louis, MO, USA)*
Goat-anti rabbit AP antibody	*Dako (Glostrup, Denmark)*
GST-Yp	*Biotrin (Dublin, Irelad)*
Heparin sodium salt	*Serva (Heidelberg, Germany)*
HEPES	*Sigma (St. Louis, MO, USA)*
Hoechst 33258	*Sigma (St. Louis, MO, USA)*
Ilford Hypam (fiaxtion solution)	*Harman Technology Ltd (Cheshire, England)*
Ilford Nuclear Emulsion K.5	*Harman Technology Ltd (Cheshire, England)*
Ilford Phenisol (developer)	*Harman Technology Ltd (Cheshire, England)*
Insulin	*Sigma (St. Louis, MO, USA)*
Kaiser's glycerol gelatine	*Merck (Darmstadt, Germany)*
Minimum Essential Medium Eagle	*Sigma (St. Louis, MO, USA)*
Natrium chloride	*Sigma (St. Louis, MO, USA)*
Natrium dihydrogen phosphate monohydrate	*Merck (Darmstadt, Germany)*

*(NaH_2PO_4*H_2O)*	
*Natrium hydrogen phosphate dihydrate (Na_2HPO_4*$2H_2O$)*	*Merck (Darmstadt, Germany)*
*Natrium hydrogen phosphate monohydrate (Na_2HPO_4*H_2O)*	*Sigma (St. Louis, MO, USA)*
N-Nitrosomorpholine (NNM)	*Sigma (St. Louis, MO, USA)*
Penicillin G sodium salt	*Sigma (St. Louis, MO, USA)*
Percoll	*GE Healthcare (Chalfont St. Gilles, Great Britain)*
Phenobarbital (PB)	*Sigma (St. Louis, MO, USA)*
Potassium chloride (KCl)	*Merck (Darmstadt, Germany)*
Potassium dihydrogen phosphate (KH_2PO_4)	*Merck (Darmstadt, Germany)*
Recombinant human EGF	*Sigma (St. Louis, MO, USA)*
RPMI 1640	*Sigma (St. Louis, MO, USA)*
RPMI 1640 w/o glucose	*Gibco (Carlsbad, CA, USA)*
Sigma ^{3}H-Thymidine	*Hartmann Analytics (Braunschweig, Germany)*
Streptomycin sulfate salt	*Sigma (St. Louis, MO, USA)*
Triiodthyronin	*Serva (Heidelberg, Germany)*
Tris	*Sigma (St. Louis, MO, USA)*
Trypan blue	*Merck (Darmstadt, Germany)*
Tween 20	*Sigma (St. Louis, MO, USA)*
Williams´ E medium	*Gibco (Carlsbad, CA, USA)*
Williams´ E medium w/o glucose	*Biomol GmbH (Hamburg, Germany)*

Table 1: *List of used reagents including suppliers.*

3.2. Solutions, buffers and media

Solution	Composition
AP-1-solution (pH 9.5)	*per 1 L:* *12.1 g Tris* *5.84 g NaCl* *2.04 g MgCl2*6H_2O* *1 mL Tween 20* *482 mg tetramisole hydrochloride*
AP-staining solution	*1 mL AP-1 solution* *3.5 µL NBT stock* *4.5 BCIP stock*
AP-stop solution (pH 9.5)	*per 1 L:* *12.1 g Tris* *5.84 g NaCl* *37.22 g EDTA*
Ascorbat (100x)	*265 mg ascorbat* *100 mL distilled H_2O*
BCIP stock	*50 mg BCIP* *1 mL N,N-dimethylformamide*
BSA-solution	*296 mg BSA* *237 mL 0.9 % NaCl*
$CaCl_2$ (100x)	*2.94 g $CaCl_2$* *100 mL distilled H_2O*
Collagenase buffer (pH 7.5)	*per 200 mL:* *174 mL H_2O bidest* *20 mL salt buffer (10x)* *2 mL pen-strep (100x)* *2 mL H_2-Mix (100x)* *0.4 mL pyruvate (500x)* *One hour before perfusion:* *2 mL $CaCl_2$ (100x)* *80 mg collagenase type II*
DEPC H_2O	*1 mL diethylprocarbonate (DEPC)*

	1 L distilled H_2O
Dexamethason-solution	*53.2 mg dexamethasone* *10 mL 0.9 % NaCl*
Formalin according to Lillie (pH 7.0)	*per 1 L:* *100 mL formaldehyde (37-40%)* *4 g $NaH_2PO_4*H_2O$* *8.125 g $Na_2HPO_4*2H_2O$* *1 L distilled H_2O*
Gentamycin (100x)	*1 g gentamycin* *100 mL 0.9 % NaCl*
Glucagon-solution	*7 mg glucagon* *100 µL 0.1 M HCl* *9.9 mL 0.9 % NaCl with 15 mg BSA/10 mL*
H2-Mix (100x)	*100 µL insulin-solution* *84 µL glucagon-solution* *237 mL BSA-solution* *2.4 mL T_3-solution* *240 µL dexamethasone-solution*
HBSS 10x – Hank´s balanced salt solution	*per 1 L:* *80 g NaCl* *4 g KCl* *2 g $MgSO_4*7H_2O$* *0.6 g KH_2PO_4* *10 g D-glucose* *0.6 g $Na_2HPO_4*2H_20$*
Heparin 2	*12 mg heparin* *50 mL 0.9 % NaCl*
Heparin 3 (100x)	*62 mg heparin* *50 mL 0.9 % NaCl*
Hepes (100x)	*23.8 mg HEPES* *6-8 mL 4 M NaOH* *50 mL distilled H_2O*
Hoechst-solution (8 µg/mL)	*2 mg Hoechst 33258* *250 mL distilled H_2O*

Insulin-solution	*0,92 mg insulin* *100 µL 0.1 N NaOH*
NBT stock	*75 mg NBT* *700 µl N,N -Dimethylformamide*
PBS (1x) – phosphate buffered saline (pH 7.4)	*per 1 L:* *1.44 g Na_2HPO_4*2H_2O* *2.62 g NaH_2PO_4*H_2O* *5.86 g NaCl*
Pen-Strep (100x)	*300 mg penicillin* *500 mg streptomycin* *50 ml 0.9 % NaCl*
Perfusion buffer (pH 7.4)	*per 500 mL:* *434 mL H_2O bidest* *50 mL salt buffer (10x)* *5 mL pen-strep (100x)* *5 mL H_2-Mix (100x)* *5 mL heparin 3 (100x)* *1 mL pyruvate (500x)*
Pyruvat (500x)	*1.1 g pyruvate* *20 mL 0.9 % NaCl*
R10	*per 400 mL:* *400 mL RPMI 1640 w/o D-glucose* *11.1 mM D-glucose* *0.444 mL gentamycin* *10 % FCS*
RPMI 1640 w/o D-glucose	*per 400 mL:* *0.4 mL gentamycin*
Salt buffer (10x)	*34 g NaCl* *2 g KCl* *5 g HEPES* *5 g D-glucose* *1 mL 4 M NaOH* *add 500 mL distilled H_2O*
SIP-solution – Standard isotonic percoll solution	*45 mL Percoll*

	5 mL HBSS-buffer
T_3-solution	*1.35 mg triiodothyronin* *200 µL 0.1 M NaOH* *19.8 mL 0.9 % NaCl*
TBS 1x – Tris buffered saline (pH 7.4)	*0.05 M Tris* *0.3 M NaCl*
Wash medium	*per 400 mL:* *391.6 mL minimum essential medium (MEM)* *4 mL HEPES* *0,4 mL gentamycin* *4 mL glutamax*
Williams´ E culture medium	*per 500 mL:* *480 mL Williams´ E medium* *5 mL glutamax (100x)* *5 mL HEPES (100x)* *0.5 mL gentamycin (1000x)* *5 mL H_2-mix (100x)* *5 mL ascorbat (100x)*
Williams´ E plating medium	*per 500 mL:* *Williams´ E culture medium* *10 % FCS*

Table 2: *List of used solutions, buffers and media.*

3.2.1. Composition of culture media

For cultivation and plating, three different media were used: Williams´ E medium (gibco, termed as WE_{old} in the text below), Williams´ E medium w/o D-glucose (Biomol GmbH termed as WE_{new} in the text below) and RPMI 1640w/o D-glucose (termed RPMI in the text below).

Before usage of the WE_{old} and WE_{new} glutamax, HEPES, gentamycin, H_2-mix (for details about the composition of H_2-mix, see table 2 above) and ascorbate (for details about amounts of the additives, see table 2 above) had to be added to the medium. RPMI was mixed with gentamycin (for details about the amount of gentamycin, see table 2 above). The amounts of different components in WE_{new}, WE_{old} and RPMI are described in table 3.

Components	WE_{new}	WE_{old}	RPMI
concentration in mg / L			
Amino acids			
Glycine	*50*	*50*	*10*
L-Arginine	*50*	*50*	*200*
L-Alanine	*90*	*90*	*/*
L-Asparagine H_2O	*20*	*20*	*50*
L-Aspartic acid	*30*	*30*	*20*
L-Cysteine	*40*	*40*	*/*
L-Cystine 2HCl	*20*	*26*	*65*
L-Glutamic Acid	*44.5*	*50*	*20*
L-Histidine	*15*	*15*	*15*
L-Hydroxyproline	*/*	*/*	*20*
L-Isoleucine	*50*	*50*	*50*
L-Leucine	*75*	*75*	*50*
L-Lysine HCl	*87.46*	*87.46*	*40*
L-Methionine	*15*	*15*	*15*
L-Phenylalanine	*25*	*25*	*15*
L-Proline	*30*	*30*	*20*
L-Serine	*10*	*10*	*30*
L-Threonine	*40*	*40*	*20*
L-Tryptophan	*10*	*10*	*5*
L-Tyrosine 2Na $2H_2O$	*50.45*	*50.65*	*29*
L-Valine	*50*	*50*	*20*
L-Glutamine	*292*	*/*	*300*
Vitamins			
Ascorbic Acid	*2.27*	*2*	*/*
Biotin	*0.5*	*0.5*	*0.2*
Choline chloride	*1.5*	*1.5*	*3*
D-Calcium pantothenate	*1*	*1*	*0.25*
Ergocalciferol	*0.1*	*0.1*	*/*
Folic Acid	*1*	*1*	*1*
Menadione ($NaHSO_4$)	*0.01*	*0.01*	*/*

Niacinamide	*1*	*1*	*1*
Pyridoxal hydrochloride	*1*	*1*	*1*
Riboflavin	*0.1*	*0.1*	*0.2*
Thiamine hydrochloride	*1*	*1*	*1*
Vitamin A (acetate)	*0.1*	*0.1*	*/*
Vitamin B_{12}	*0.2*	*0.2*	*0.005*
α-Tocopherol phos. 2Na	*0.01*	*0.01*	*/*
i-Inositol	*2*	*2*	*35*
Para-Aminobenzoic Acid	*/*	*/*	*1*
Inorganic salts			
Calcium Chloride ($CaCl_2$) $2H_2O$/(anhyd.)	*265*	*200*	*/*
Cupric sulfate ($CuSO_4$ $5H_2O$)	*0.0001*	*0.0001*	*/*
Ferric nitrate ($Fe(NO_3)$ $9H_2O$)	*0.0001*	*0.0001*	*/*
Magnesium Sulfate ($MgSO_4$) (anhyd.)	*97.7*	*97.67*	*48.84*
Manganese chloride ($MnCl_2$ $4H_2O$)	*0.0001*	*0.0001*	*/*
Potassium Chloride (KCl)	*400*	*400*	*400*
Sodium Bicarbonate ($NaHCO_3$)	*/*	*2200*	*2000*
Sodium Chloride (NaCl)	*6800*	*6800*	*6000*
Sodium Phosphate monobasic (NaH_2PO_4) (anhyd.)	*122*	*140*	*/*
Sodium Phosphate dibasic (Na_2HPO_4 $7H_2O$)	*/*	*/*	*1512*
Zinc sulfate ($ZnSO_4$ $7H_2O$)	*0.0002*	*0.0002*	*/*
Calcium nitrate ($Ca(NO_3)_2$ $4H_2O$)	*/*	*/*	*100*
Other components			
D-glucose	*/*	*2000*	*/*
Glutathion	*0.05*	*0.05*	*1*
Methyl linoleate	*0.03*	*0.03*	*/*
Phenol red, sodium	*10.7*	*10*	*5*
Pyriuvic acid, sodium	*25*	*25*	*/*

Table 3: *List of components of WE_{old}, WE_{new} and RPMI.*

3.3. In vivo methods

3.3.1. Animals

Wistar rats were obtained from Charles River laboratories and kept in the "Division for Decentralized Biomedical Facilities of the Medical University of Vienna" in the standardized specific-pathogen-free (SPF) conditions (Makrolon cages, 20 ± 3°C, 40-70 % humidity). The rats were kept in a 12 hours light/dark rhythm (e.g. from 6 am until 6 pm rats were exposed to light). Diet (ssniff® R/M-H Extrudate, ssniff, Soest, Germany) and water were obtainable ad libitum. All experimental protocols were approved by the "Committee of Animal Protection" of the Austrian government and were performed in agreement with Austrian regulations.

3.3.2. Treatment of the animals

3.3.2.1. N-nitrosomorpholine (NNM)

Four - six weeks old male Wistar rats were treated with a single dose of NNM by gastrogavage. Since two rats had died after treatment with 167 mg NNM/ 10 ml PBS/ kg body weight, 125 mg NNM/ 10 ml PBS/ kg body weight was used to generate initiated HC. After 21 days of recovery time, the livers of NNM treated rats were perfused.

3.3.2.2. Phenobarbital (PB)

The long-term treatment with PB was carried out by Teresa Riegler.
Three weeks old male Wistar rats were pre-treated with 250 mg/ 10 ml PBS/ kg body weight of NNM by gastrogavage to create initiated HC. After 3 weeks, the rats were treated with PB (50 mg PB / kg body weight per day) via food for a period of 17 months to promote tumor growth. The rats were sacrificed and the liver and tumor samples were obtained.

3.3.3. Perfusion of the rat liver

Perfusion was carried out by Prof. Dr. Bettina Grasl-Kraupp and Elisabeth Haslinger, except the preparation of the required buffers and solutions.
Rats were anesthetized with a mixture of chloroform, dinitrogen oxide and oxygen. To avoid blood coagulation, heparin 2 solution (1 mL/ kg body weight) was injected into the leg vein. Collagenase and perfusion buffers were heated to 37° C and pumped into a cannula. After opening the abdomen, a cannula was inserted into the portal vein to free the liver from the blood. The vena cava inferior

was cut for exsanguination and the liver was perfused for approximately 10 min with the perfusion buffer until the whole amount of blood in the liver was washed out. Then, the liver was perfused with the collagenase buffer for further 5 - 10 min, which made the liver soft and swollen. The liver was excised and put into a beaker glass, filled with 20 mL wash medium and ready to isolate HC (see chapter 3.4.2.).

3.4. In vitro methods

3.4.1. Rat collagen solution

The preparation of the rat collagen solution was carried out by Birgit Mir-Karner.
Rat tails were broken into small pieces and collagen filaments were pulled and dried on a filter paper for 24 - 48 h at room temperature. The dry filaments were cut into pieces (0.5 - 1 cm) and 1.66 g were sterilized in a culture dish under UV-light for 2 h. The filaments were stirred in 500 ml distilled H_2O and 2 mL acetic acid for 3 days at 4° C. The solution was filled into falcon tubes and centrifuged for 60 min at 43000 g and 4° C. After that, the rat collagen solution was ready to use as a coating for of culture dishes.

3.4.2. Isolation of HC

One day before perfusion, the rat collagen solution was mixed 1: 1 with distilled and autoclaved H_2O and 100 µL / cm^2 area of the culture dish were coated. The coated culture dishes were dried in the hood with open lids over night.
The perfused liver, which had been placed into a beaker glass with 20 mL wash medium, was cut with a sterile pair of scissors and the cells were shaken out of the liver capsule. The cells were filtered through a mesh with 100 µm pores and collected in a glass. The beaker glass with the liver was refilled with 20 mL wash medium and the isolation procedure was repeated until 100 mL of cell suspension was obtained. The suspension was filled into tubes and centrifuged for 5 min at 500 rpm and 4° C. The NPC-containing fraction on the top was removed and the HC-containing pellet was resuspended in about 20 mL of wash medium. The suspension was centrifuged again for 5 min at 300 rpm and 4° C. During the 2nd centrifugation step, SIP-solution was prepared, by mixing 21.6 mL of Percoll with 2.4 mL of 10xHBSS per rat. The pellet obtained was resuspended in 25 mL of wash medium and mixed with SIP. The 3rd centrifugation step for 12 min at 500 rpm and 4° C separated dead from living cells. The dead cells on the top of the falcon were removed and the pellet was resuspended in 40 mL of wash medium and centrifuged for 2 min at 500 rpm and 4° C. After

removing the supernatant, the pellet was resuspended in 30 mL of wash medium and centrifuged again for 5 min at 300 rpm and 4° C. After the last centrifugation step, the pellet was resuspended in approximately 20 mL of wash medium, depending on the size of the pellet.

To determine the number of dead cells (stained) and living cells (unstained) a trypan blue exclusion test was performed. Therefore, trypan blue was diluted with NaCl in a ratio of 1: 2. Then, 4.8 mL of the diluted trypan blue solution was filled in a tube and 200 µL of cell suspension was added. The Neubauer counting chambers were filled with the mixture and 10 quadrates were counted under the microscope.

The following formula was used to calculate the amount of cell suspension necessary for plating of $4x10^4$ of living HC / cm^2:

$$counted\ HC\ number\ x\ 1000\ x\ 25\ = ①\ HC\ number/mL$$

$$①\ HC\ number/mL\ x\ a\ mL\ = ②\ \Sigma\ of\ HC\ in\ mL$$

$$(4x10^4\ HC/cm^2)\ x\ number\ of\ wells\ =\ ③\ \Sigma\ of\ HC\ for\ all\ wells\ in\ mL$$

$$\frac{③\ \Sigma\ of\ HC\ for\ all\ wells\ in\ mL}{①\ HC\ number/mL}\ = ④\ HC\ suspension\ for\ all\ wells\ in\ mL$$

$$number\ of\ wells\ x\ 0.5\ mL\ =\ b\ mL$$

$$b\ mL\ -\ ④\ HC\ suspension\ for\ all\ wells\ in\ mL\ =\ plating\ medium\ (in\ total)\ in\ mL$$

a: amount of wash medium in mL, in which HC were resuspended

b: amount of HC suspension diluted in plating medium for all wells

Box 1: *Calculation for plating of living HC after trypan exclusion test.*

The calculated amount of cell suspension was diluted in plating medium containing 10 % FCS and 11.11 mM of D-glucose (R10 / Williams´ E medium). HC were plated as duplicates on collagen-coated culture dishes. After 90 - 120 min incubation at 37° C and 5 % CO_2, HC were attached to the culture dish.

3.4.3. Treatment of HC

3.4.3.1. 2-Deoxyglucose (2DG)

After incubation of unaltered/preneoplastic HC in serum-containing plating medium for 90 - 120 min, the medium had to be changed to serum-free medium with or without D-glucose, containing 0 mM, 0.5 mM, 1 mM and 1.5 mM of 2DG (two wells per treatment and animal). In detail, HC were washed with culture medium and treatment solutions were prepared. For that purpose, crystalline 2DG was solved in distilled and autoclaved H_2O to obtain a stock concentration of 10 mM. The stock-solution of 2DG was diluted in the appropriate serum-free culture medium. Unaltered/preneoplastic HC were treated with appropriate amounts of treatment solution per well and incubated for different time points at 37° C and 5 % CO_2. After these different time spans, the treated unaltered/preneoplastic HC were used for further analysis.

If required, HC were treated with the epidermal growth factor (EGF, solved in BSA/acetic acid; stock concentration of 10 µg / mL), which stimulates DNA synthesis. Therefore, 6 h after the start of 2DG-treatment, 10 ng / 30 ng EGF per mL and well were added to the treatment solution and incubated at 37° C and 5 % CO_2 for 48 h and/or 72 h.

For cultivation time spans of 72 h, the medium and the treatment solution were changed after 48 h after the start of 2DG-treatment.

3.4.3.2. Tritium thymidine (^{3}H-thymidine)

Twenty-four or 48 h after the start of 2DG-treatment, HC were treated with ^{3}H-thymidine and if required, medium with or without treatment solution was changed before the procedure. Then, 2.5 µCi / mL of ^{3}H-thymidine (stock concentration ^{3}H-thymidine: 1 µCi / mL) were added in each well. The incorporated ^{3}H-thymidine was visualized by autoradiography (see chapter 3.5.4.).

3.5. Analytical methods

3.5.1. Micro dissection, RNA isolation, and rat genome-array

The micro dissection and RNA isolation was carried out by Teresa Riegler.

The tumor samples, obtained from NNM and PB treated rats (see chapter 3.3.2.2.) were used afterward for transcriptome analysis. For this purpose, 10 x 7 µm serial sections and 1 x very thin section of tumor samples were cut (RNAse free). Then the sections were put on slide-OT and were dried for 10 min. Afterwards the slides were deparaffinated in xylol at 50 ° C for 4 min and were put 2 times in 100 % EtOH for 2 min. The slides were dried in a desiccator over night. At the next day, the very thin section on the slide was colored with GSTp immunostaining. Foci of GSTp stained section were searched on the 7 µm sections. Next, foci were fixed on slides with infrared and were cut with UV (LCM - laser capture microdissection). The RNA was extracted using miRNeasy mini Kit (Quiagen). The extracted RNA was processed, labelled for application and applied on a rat genome 230 2.0 array (Affymetrix) by members of the core facility genomics of the Medical University of Vienna. For further details see [86].

3.5.2. ATP detection assay

To determine the ATP levels a luminescence ATP detection assay system (ATP lite™ - Perkin Elmer®) was used. It is an ATP monitoring system based on the firefly (*Photinus pyralis)* enzyme luciferase, which catalyzes the following reaction:

$$ATP + D\text{-}luciferin + O_2 \xrightarrow[Mg^{2+}]{\textbf{\textit{Luciferase}}} Oxyluciferin + AMP + PP_i + CO_2 + Light$$

The emitted light is measured by a plate reader and is proportional to the ATP concentration.

After incubation of HC with 2DG for different time points, cells were washed with 1xPBS. Fifty µL of mammalian cell lysis buffer was added and the cells were scraped off and transferred to a white 96-well plate. The plate was shaken for 5 min at 700 rpm and room temperature to lyse the cells. After that, the lyophilized substrate solution was solved in substrate buffer solution. At the next step, 50 µL of the solved substrate solution was added to each well and the plate was shaken again for 5 min at 700 rpm at room temperature. Then, the plate was dark adapted for 10 min and the luminescence was measured using the program Gen5.

3.5.3. Viability assay

To test the effect of 2DG on the vitality of primary HC, a viability assay was performed. The viability assay is based on the reduction of 3-(4, 5-dimethylthiazol-2yl)-2, 5-diphenyltetrazolium bromide (MTT) to a water-soluble purple colored formazan product by viable cells with active metabolism. Formazan can be detected by spectrophotometry.

Cells were seeded at a density of $2x10^3$ cells/ well in a 96-well and treated with 0 mM or 0.5 mM of 2DG. After incubation of HC with 2DG for 24 h and 48 h, a non-toxic tetrazolium salt (yellow-colored EZ4U reagent, Biomedica immunoassays) diluted in serum-free culture medium at a concentration of 10 % was added to the cells. After approximately 3 h of incubation at 37° C the absorbance was measured at a wavelength of 450nm in a microplate reader (Asys Expert Plus, Biochrom).

3.5.4. Immunohistochemistry

3.5.4.1. Fixation of the cells

Twenty-four hours after ^{3}H-thymidine treatment, HC were fixed. Therefore, HC were washed three times with 0.9 % NaCl and then fixed with approximately 1 mL of 4 % Lillie´s buffered formalin per well for 90 min at 4° C. After 90 min, formalin was removed and HC were washed twice with distilled H_2O. The fixed HC were covered with distilled H_2O and kept in the fridge at 4° C until staining.

3.5.4.2. GSTp staining

For the GSTp staining, the fixed HC were washed with TBS for 10 min and then blocked with 2.5 % BSA / TBS for 30 min. The 1st antibody, GST-Yp (1: 1000 with 2.5 % BSA / TBS) was applied on HC overnight at 4° C. At the next day, the wells were washed six times with TBS and blocked with 2.5 % BSA/TBS. After blocking the 2nd antibody, the goat-anti-rabbit AP antibody (1: 100 with 2.5 % BSA / TBS), was added for 1 h at room temperature. Next, the wells were washed six times with TBS again and incubated with an AP-1 solution and stained with an AP-staining solution. The staining process was controlled under the microscope. When staining was sufficient, the process was terminated by an AP-stop solution. The wells were washed with distilled H_2O and dried at room temperature.

3.5.4.3. Autoradiography

For autoradiography, unsolved photo emulsion snippets (Ilford Nuclear emulsion K.5) were mixed with distilled H_2O. Therefore, 15 mL of distilled H_2O was filled in a volumetric flask. The photo

emulsion snippets were added until the 25 mL mark on the volumetric flask was reached. The mixture was solved in a water bath in the dark chamber.

The wells with the fixed HC were coated with the solved photo emulsion and incubated over night at 4° C in complete darkness. At the next day, a developer (Ilford Phenisol) was diluted in a ratio of 1: 4 with distilled H_2O. The wells with fixed HC were incubated in the developer for 5 min. After termination of this process with 2 % acetic acid for a few seconds, HC were exposed to a fixation solution (Ilford Hypam) for 5 min. Then, the wells were washed under running tap water for at least 1 h, and after that, the cells were stained by Hoechst 33258.

3.5.4.4. Hoechst staining

The wells were stained with 0.5 mL of Hoechst 33258 (80 µg bisbenzimide / mL distilled H_2O) for 5 min and washed with distilled H_2O for another 5 min. These steps were made in light-excluded conditions. After drying of the wells at room temperature, the bottom of the well was punched out and the cells were covered with a round glass cover slide by Kaiser´s glycerol gelatine.

3.5.5. Determination of DNA replication

This radio-labelled nucleotide ^{3}H-thymidine was incorporated into the DNA during S-phase of the cell cycle. After autoradiography and Hoechst staining, the incorporated ^{3}H-thymidine became visible under the microscope as black dots over nuclei, which represented HC in S-phase. A thousand nuclei of HC were counted per well and the labelling index (LI %) were determined by the following formula:

$$\frac{average\ of\ counted\ marked\ nuclei}{1000}\ x\ 100\ =\ LI\ \%$$

In the case of the LI-determination of preneoplastic HC, 300 GSTp-positive cells, which appeared as purplish cells, were counted per well. The LI % was calculated with the following formula:

$$\frac{average\ of\ counted\ GSTp\ pos.marked\ nuclei}{300}\ x\ 100\ =\ LI\ \%$$

3.6. Statistical analysis

The statistical analysis of the data sets was performed with GraphPad Prism 5.0 software (GraphPad Software Inc). All experiments are illustrated as means ±SEM of ≥ two independent cell preparations. One-sample t-test and Kruskal-Wallis test were used to test for significances.

4. Results

4.1. Transcriptome patterns of preneoplastic lesions of rat livers

Our special interest was focused on the transcriptome patterns of preneoplastic liver foci, which represent an early stage in carcinogenesis. To obtain these lesions, male rats received a single dose of the genotoxic hepatocarcinogen N-nitrosomorpholine (NNM) and were treated subsequently with phenobarbital (PB) for 17 months. The liver foci obtained were used to extract RNA, which was subjected to analyses by rat oligo arrays. This part was performed by Teresa Riegler, as described in detail in chapter 3.5.1. Several pathways were altered in preneoplastic liver foci, including glycolysis, gluconeogenesis, glycogenesis and pentose-phosphate pathway (PPP) (see figure 16).

4.1.1. Deregulation of glycolytic genes in liver foci

Previous results of array data showed that the key enzyme for glycolysis, namely hexokinase (HK), was upregulated about 2-fold in hepatocellular adenomas of rats (data not shown). The enzyme HK catalyzes the first step of glycolysis, i.e., HK phosphorylates glucose to G6P, which can be further processed by other metabolic pathways, such as glycogenesis, gluconeogenesis, and PPP. The transcriptome of liver foci revealed upregulation of HK1, as observed in adenomas (see figure 11).

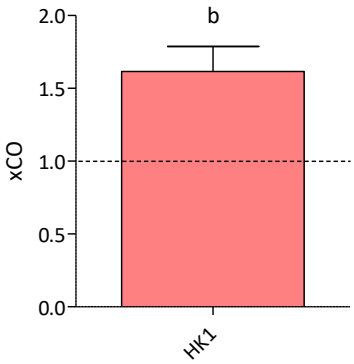


Figure 11: The level of HK1-mRNA in liver foci. *Male rats were treated with a single dose of NNM (250 mg/ kg of body weight), for tumor initiation. After 3 weeks recovery time, rats were treated with PB (50 mg/ kg body weight per day) for 17 months. RNA was extracted and analyzed by rat oligo arrays. Data are expressed as fold surrounding tissue. The mean ± SEM from 9 foci is given. Statistics by one-sample t-test: (b) $p < 0.01$. Abbreviations: HK1 - hexokinase1.*

Our findings show that important glycolytic genes were deregulated in liver foci (see figure 12), i.e., aldolase A (ALDO A) was upregulated in liver foci. Aldolase A catalyzes fructose-1, 6-bipohosphate (F1,6BP) to glyceraldehyde-3-phosphate (G3P) and dihydroxyacetone phosphate (DHAP). Another glycolytic enzyme, phosphoglycerate mutase 1 (PGAM 1), is slightly elevated. PGAM 1 catalyzes the conversion of 3-phosphoglycerate (3PG) to 2-phosphoglycerate (2PG) and controls the intracellular levels of 2PG and 3PG. The enzymes pyruvate kinase (PKLR) and lactate dehydrogenase B (LDH B) are not upregulated in liver foci.

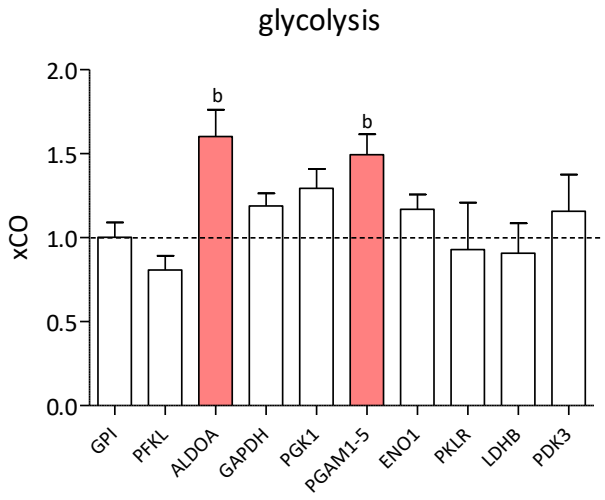


Figure 12: Deregulated genes, involved in glycolysis. *Male rats were treated with a single dose of NNM (250 mg/ kg of body weight), for tumor initiation. After 3 weeks recovery time, rats were treated with PB (50 mg/ kg body weight per day) for 17 months. RNA was extracted and analyzed by rat oligo arrays. Data are expressed as fold surrounding tissue and are means ± SEM from 9 foci. Statistics by one-sample t-test: (b) p < 0.01. Abbreviations: GPI - glucose-6-phosphate isomerase, PFKL - phosphofructokinase, ALDOA - aldolase A, GAPDH - glyceraldehyde-3-phosphate dehydrogenase, PGK1 - phosphoglycerate kinase 1, PGAM1 - phosphoglyceratemutase 1, ENO1 - enolase, PKLR - pyruvate kinase (liver and RBC), LDHB - lactate dehydrogenase B, PDK3 - pyruvate dehydrogenase kinase 3.*

4.1.2. Deregulation of genes, involved in glycogenesis

The array data of liver foci revealed that several enzymes, which are heavily involved in glycogenesis, are upregulated (see figure 13). This includes UTP glucose-1-phosphate uridylyltransferase 2 (UGP2), glycogenin 1 (GYG1) and the glucan-(1, 4-α) branching enzyme 1 (GBE1).

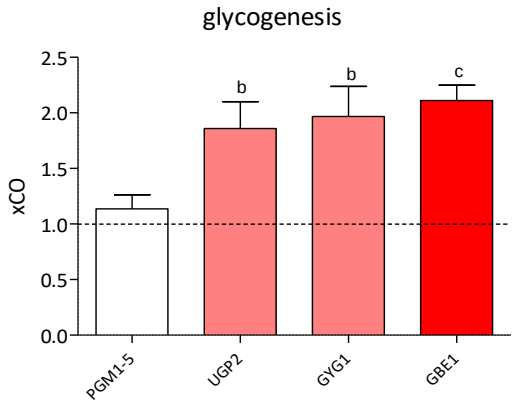


Figure 13: Deregulated genes, involved in glycogenesis. *Male rats were treated with a single dose of NNM (250 mg/ kg of body weight), for tumor initiation. After 3 weeks recovery time, rats were treated with PB (50 mg/ kg body weight per day) for 17 months. RNA was extracted and analyzed by rat oligo arrays. Data are expressed as fold surrounding tissue and are means ± SEM from 9 foci. Statistics by one-sample t-test: (b) p < 0.01, (c) p < 0.001. Abbreviations: PGM1-5 - phosphoglucomutase 1-5, UGP2 - UTP glucose-1-phosphate uridylyltransferase 2, GYG1 - glycogenin 1, GBE1 - glucan-(1, 4-α) branching enzyme 1.*

4.1.3. Downregulation of genes, involved in gluconeogenesis

Gluconeogenesis is the process in which non-carbohydrates, such as pyruvate or oxalacetate (OAA), are used to generate glucose in order to maintain glucose homeostasis. The enzymes, involved in gluconeogenesis, are downregulated in liver foci (see figure 14). This includes phosphoenolpyruvate carboxykinase 1 (PCK1), glucose-6-phosphatase (G6PC) and fructose-1, 6-bisphosphatase 1 (FBP1).

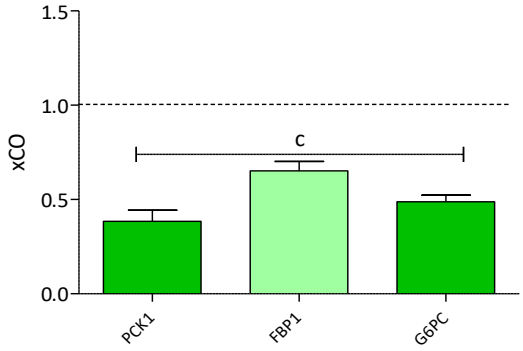


Figure 14: Downregulation of genes, involved in gluconeogenesis. *Male rats were treated with a single dose of NNM (250 mg/ kg of body weight), for tumor initiation. After 3 weeks recovery time, rats were treated with PB (50 mg/ kg body weight per day) for 17 months. RNA was extracted and*

analyzed by rat oligo arrays. Data are expressed as fold surrounding tissue and are means ± SEM from 9 foci. Statistics by one-sample t-test: (c) p < 0.001. Abbreviations: PCK1 - phosphoenolpyruvate carboxykinase 1, FBP1 - fructose-1, 6-bisphosphatase 1, G6PC - glucose-6-phosphatase.

4.1.4. Upregulation of genes, involved in pentose phosphate pathway (PPP)

One of the products, generated in the PPP, is ribose-5-phosphate (R5P). Further metabolizing of R5P generates phosphoribosyl-phosphate, which functions as the backbone for nucleotide synthesis. Nucleotides are required for DNA replication, allowing cells to proliferate. Figure 15 shows the upregulation of three crucial enzymes, which are involved in the PPP. The enzyme glucose-6 phosphate dehydrogenase (G6PD), which catalyzes the entry step of PPP, is highly elevated in liver foci. The enzymes transketolase (TKT) and transaldolase 1 (TALDO 1) are also upregulated in liver foci. TKT and TALDO are involved in a step of the PPP, in which glycolytic intermediates are generated, which can be further used for glycolysis and/or may utilize in the PPP again.

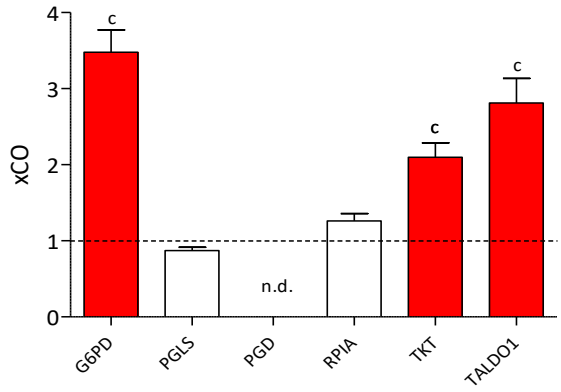


Figure 15: Upregulation of genes, involved in PPP. *Male rats were treated with a single dose of NNM (250 mg/ kg of body weight), for tumor initiation. After 3 weeks recovery time, rats were treated with PB (50 mg/ kg body weight per day) for 17 months. RNA was extracted and analyzed by rat oligo arrays. Data are expressed as fold surrounding tissue and are means ± SEM from 9 foci. Statistics by one-sample t-test: (c) p < 0.001. Abbreviations: G6PD - glucose-6-phosphate dehydrogenase, PGLS - 6-phosphate gluconolactonase, PGD - phosphoglyconate dehydrogenase, RPIA - ribose-5-phosphate isomerase A, TKT - transketolase, TALDO1 - transaldolase 1.*

4.1.5. Preneoplastic liver lesions: summary of deregulated genes, involved in glucose metabolism

Figure 16 summarizes deregulated genes involved in the glucose metabolism. Several glycolytic enzymes, such as HK1, ALDO A, and PGAM 1-5, are upregulated in preneoplastic liver foci. Genes, which play crucial roles in glycogenesis, such as GBE1, GYG1, and UGP2 are also highly expressed in prestages of cancer. The enzymes G6PC, PCK1, and FBP1, which are involved in gluconeogenesis, are downregulated in liver foci. The PPP is involved in the nucleotide synthesis, which is required for DNA replication. The levels of G6PD-mRNA, TKT-mRNA and TALDO-mRNA, which are important enzymes of the PPP, are highly increased in preneoplastic liver lesions.

The deregulations in genes in preneoplastic liver lesions indicate a general shift of the usage of glucose for glycogen storage (glycogenesis) and DNA replication (PPP), while the level of newly synthesized glucose is decreased.

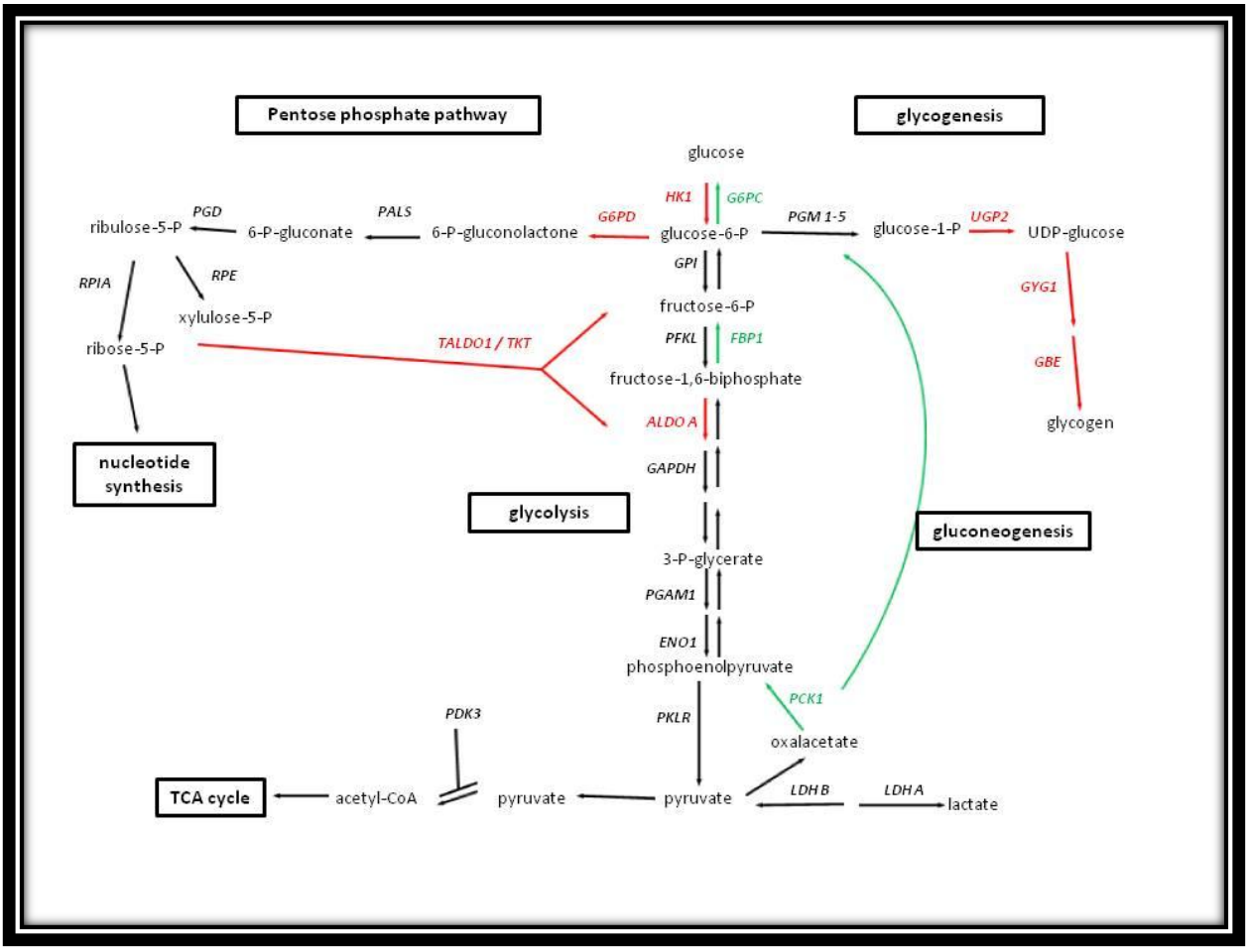


Figure 16: Summary of deregulated key enzymes in the glucose metabolism of preneoplastic lesions. *Male rats were treated with a single dose of NNM (250 mg/ kg of body weight), for tumor initiation. After 3 weeks recovery time, rats were treated with PB (50 mg/ kg body weight per day) for 17 months. RNA was extracted and analyzed by rat oligo arrays.*

Red: upregulation. Green: downregulation. Data are means from 9 foci. Abbreviations: HK1 - hexokinase1, GPI - glucose-6-phosphate isomerase, PFKL - phosphofructokinase, ALDO A - aldolase A, GAPDH - glyceraldehyde-3-phosphate dehydrogenase, PGK1 - phosphoglycerate kinase 1, PGAM1 - phosphoglyceratemutase 1, ENO1 - enolase, PKLR - pyruvate kinase (liver and RBC), LDH A, B - lactate dehydrogenase A,B, PDK3 - pyruvate dehydrogenase kinase 3, G6PC - glucose-6-phosphatase, PGM 1-5 - phosphoglucomutase 1-5, UGP2 - UTP glucose-1-phosphate uridylyltransferase 2, GYG1 - glycogenin 1, GBE1 - glucan-(1,4-α) branching enzyme 1, PCK1 - phosphoenolpyruvate carboxykinase 1, FBP1 - fructose-1,6-bisphosphatase 1, G6PD - glucose-6-phosphate dehydrogenase, PGLS - 6-phosphate gluconolactonase, PGD - phosphogluconate dehydrogenase, RPIA - ribose-5-phosphate isomerase A, RPE - ribulose-5-phosphate-3-epimerase, TALDO 1 - transaldolase, TKT - transketolase.

4.2. Comparison of different culture conditions on ATP level under treatment with 2DG

As described in chapter 4.1., array data show that the key enzyme of several steps in carbohydrate metabolism, HK1 is upregulated in preneoplastic rat lesions. Furthermore, preneoplastic rat lesions overexpress some key genes of PPP. This may indicate that the enzyme HK plays an important role for preneoplastic cells to use G6P for the generation of nucleotides to synthesize DNA for proliferation. We, therefore studied, whether blockade of HK leads to reduced DNA synthesis in preneoplastic cells. To approach this question we intended to block HK in primary HC by applying 2-deoxyglucose (2DG). For this purpose, we tried to establish an optimal experiment set-up, as is described in the following.

4.2.1. ATP level of primary HC kept in different culture media

First, we tested the impact of different culture media on the ATP level of primary HC: two different Williams media E with and without glucose, termed as WE_{old} (+G) and WE_{new} (+/-G), and RPMI 1640 with and without glucose (termed as RPMI +/-G).

Williams Medium E is a hepatocyte-specific culture medium, whereas RPMI is a standard medium frequently used for transformed cell lines. The media differ in their composition (see table 3.2.1., table 3). WE_{new} and RPMI are glucose-depleted media. WE_{old} contains D-glucose at a concentration of 11.11 mM (2000 mg/L). To enable comparison with WE_{old} we added D-glucose (11.11 mM) to WE_{new} and RPMI if required. The three media also differ in the concentration of several other amino acids, vitamins and co-factors, inorganic salts and some other components (for details see chapter 3.2.1., table 3). The three media also differ in the composition of additives, which were added before usage of the media. WE_{old} and WE_{new} were mixed with glutamax, HEPES, ascorbate, gentamycin and hormone-mix (H_2-mix). The H_2-mix contains different hormones, such as insulin, glucagon, triiodothyronine and dexamethasone. The different hormone additives may have an effect on the metabolic activity and vitality of HC. For details about additives of the media and the composition of H_2-mix see 3.2., table 2.

After rat liver perfusion and HC isolation, the cells were cultured in the three different media. ATP levels were measured using a luminescence ATP detection assay. It is based on the production of light, produced by the reaction of ATP with added luciferase and D-luciferin. The emitted light is proportional to the ATP concentration. For further details see chapter 3.5.2.

We measured the ATP level at different time points (12 h, 24 h, 48 h or 72 h). Figure 17 shows the luminescence measured in HC of the control groups (medium +G) over time.

The three media exerted different effects on the ATP levels. In WE_{new} (+G) the ATP level remained more or less constant and tend to decrease after 48 h (figure 17 (A)), whereas in WE_{old} (+G) the ATP level was lower after 48 h and tended to raise again at 72 h (figure 17 (B)). The hepatocellular ATP level in RPMI (+G) was somewhat higher after 48 h than after 24 h and declined after 72 h (figure 17 (C)).

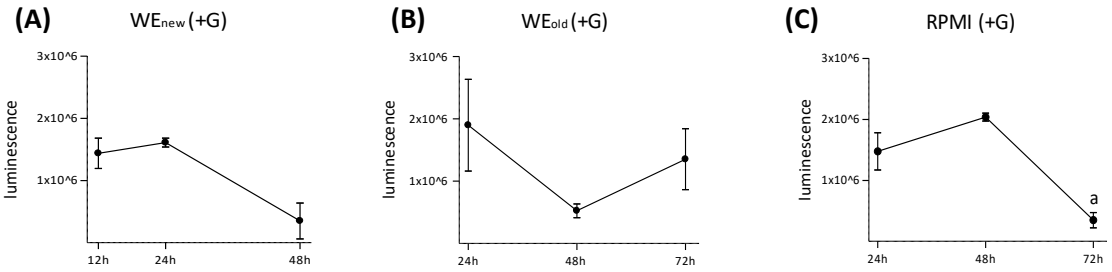


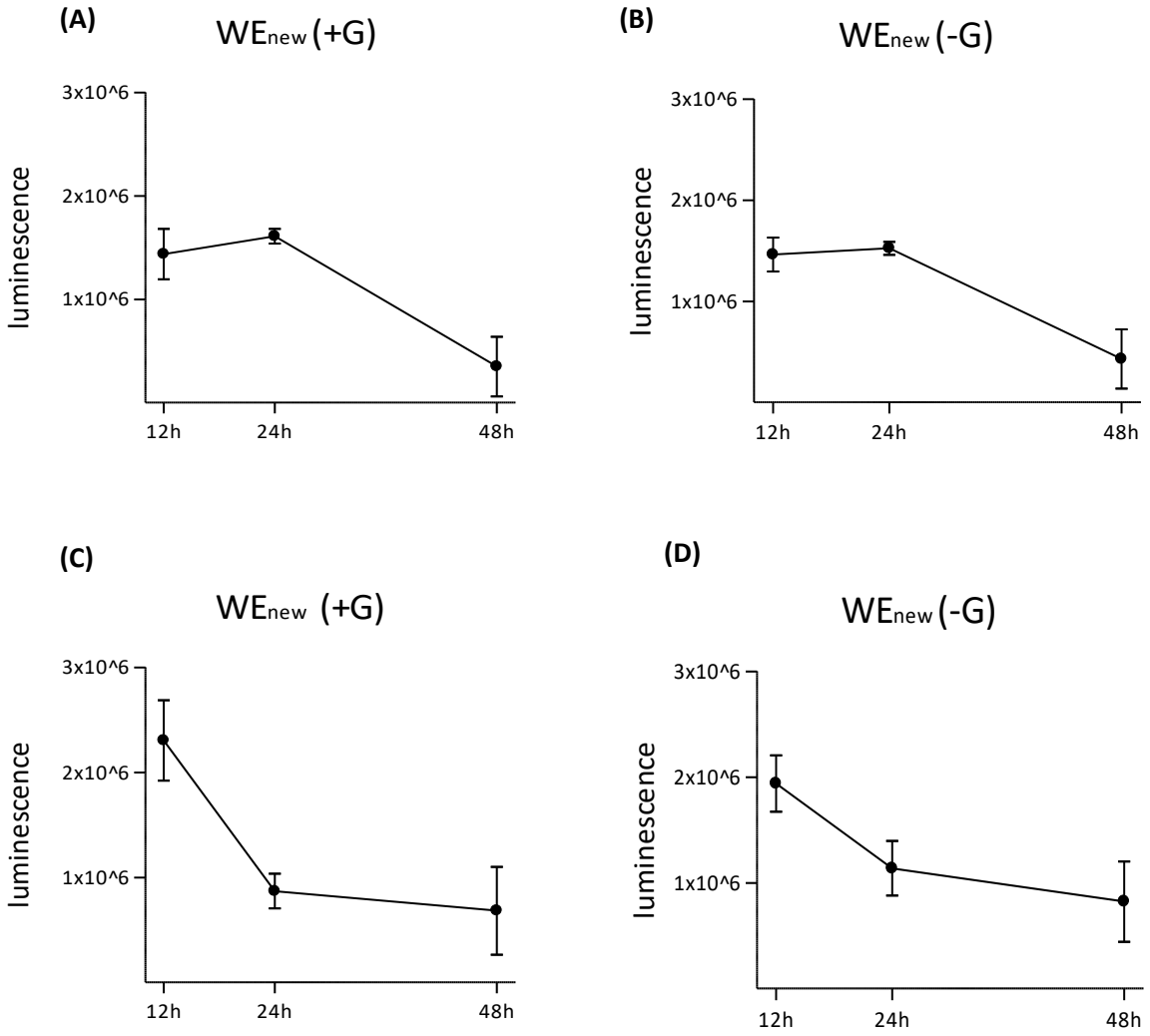
Figure 17: ATP levels in primary HC, cultured in different media (+G) for up to 72 h. *Livers of untreated rats were perfused with collagenase, HC were isolated and 4x10^5 HC/well were seeded on collagen coated 6-well plates in WE_{new} (+G), WE_{old} (+G) and RPMI (+G), which contained 10 % of FCS. After 90 min in culture, the medium was changed to the three different serum-free culture media. All media contained D-glucose at a concentration of 11.11 mM. For the 72 h measurement time point, the medium was changed after 48 h. (A) WE_{new} (+G), ATP level was measured after 12 h, 24 h or 48 h. (B) WE_{old} (+G); food was removed 12 h before cell isolation. ATP level was measured after 24 h, 48 h or 72 h. (C) RPMI (+G), food was removed 12 h before cell isolation. ATP level was measured after 24 h, 48 h or 72 h. Data derived from ≥ 3 independent cell preparations and are shown as means ±SEM. Statistics by Kruskal-Wallis test over time: (a) p < 0, 05.*

4.2.2. ATP level of primary HC kept in WE_{new} (+/-G) and RPMI (+/-G) with and without food withdrawal

Figure 18 shows the ATP level in HC kept in WE_{new} (+/-G) and RPMI (+/-G). Figure 18 (A) and (B) shows ATP levels from rats, which had access to food approximately 3 h before cell isolation. The ATP level in WE_{new} (+G) remained constant and tend to decrease after 48 h, as shown already in figure 17 (A) and again presented in figure 18 (A). A similar trend was seen under glucose-depleted conditions in WE_{new} (-G) (figure 18 (B)). Due to the similar ATP levels as well as in glucose-rich and glucose-depleted medium, it was assumed that HC may break down glycogen to fulfil energy needs, under glucose-free conditions. Thus, removing of food from rats 12 h before cell isolation was included in all further experiments. Figure 18 (C) and (D) show the ATP level of rats, after food withdrawal approximately 12 h before cell isolation. After 12 h more ATP was measured in HC, cultivated with

glucose)). After 24 h and 48 h, the ATP levels decreased after 24 h and 48 h, in both glucose-rich and -depleted conditions (compare figure 18 (C) and (D).

In RPMI (+G) the ATP level increased after 48 h and decreased after 72 h (see figure 17 (C) and 18 (E)). However, in glucose-depleted RPMI (-G) less ATP was measured (see figure 18 (F)) than in RPMI (+G) at 48 h. At 72 h the difference was no longer evident.



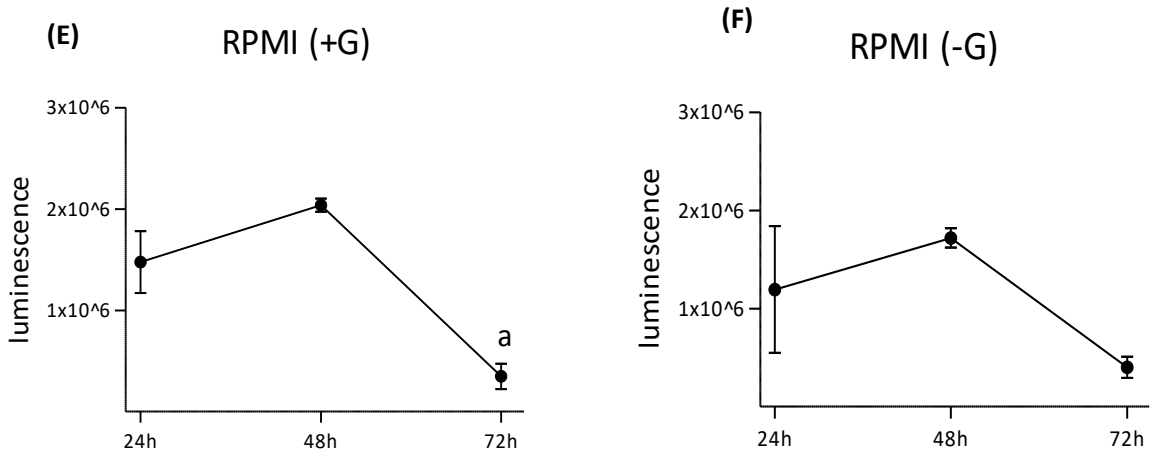


Figure 18: ATP levels in HC, cultured in WE_{new} (+/-G) and RPMI (+/-G) after different time points*. Livers of untreated rats were perfused with collagenase, HC were isolated and $4x10^5$ HC/well were seeded on collagen coated 6-well plates in WE_{new} (+/-G) and RPMI (+/-G), which contained 10 % of FCS. After 90 min in culture, the medium was changed to different serum-free culture media. The media (+G) contained 11.11 mM of D-glucose. For the 72 h measurement time point, the medium (+/-G) was changed after 48 h. (A) WE_{new} (+G); rats had access to food appr. 3 h before cell isolation. ATP level was measured after 12 h, 24 h or 48 h. (B) WE_{new} (-G); rats had access to food appr. 3 h before cell isolation. ATP level was measured after 12 h, 24 h or 48 h. (C) WEnew (+G); food was removed appr. 12 h before cell isolation. ATP level was measured after 12 h, 24 h or 48 h. (D) WE_{new} (-G); food was removed appr. 12 h before cell isolation. ATP level was measured after 12 h, 24 h or 48 h. (E) RPMI (+G); food was removed appr. 12 h before cell isolation. ATP level was measured after 24 h, 48 h or 72 h. (F) RPMI (-G); food was removed appr. 12 h before cell isolation. ATP level was measured after 24 h, 48 h or 72 h. Data derived from ≥ 3 independent cell preparations and are shown as means ±SEM. Statistics by Kruskal-Wallis test: ATP-level in HC in RPMI with glucose over time: (a) $p < 0.05$.*

4.2.3. Vitality of primary HC in WE_{new} (+/-G)

To test the impact of glucose deprivation on the vitality of primary HC, we performed a viability test after 24 h and 48 h of culture. The concept of the viability assay is based on the reduction of 3-(4, 5-dimethylthiazol-2yl)-2, 5-diphenyltetrazolium bromide (short MTT) to a purple colored formazan product by viable cells with active metabolism. Formazan has an absorbance maximum near 570 nm, which can be detected by spectrophotometry (for further details see chapter 3.5.3.).

In HC, kept in WE_{new} (+G), we measured a somewhat higher vitality than in cells cultured in WE_{new} (-G), both after 24 h and 48 h (see figure 19).

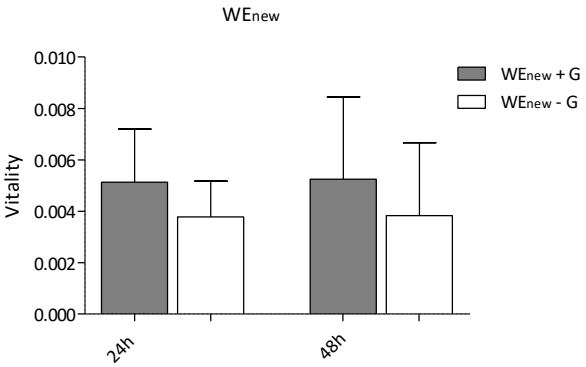


***Figure 19: Vitality of HC, cultured in WE_{new} (+/-G) after different time points**. Food was removed 12 h before cell isolation. Livers of untreated rats were perfused with collagenase, HC were isolated and 2000 HC/well were seeded on collagen coated 96-well plates in WE_{new} (+/-G), which contained 10 % of FCS. After 90 min in culture, medium (+/-G) was changed to different serum-free culture media. Viability test was performed by applying the MTT assay after 24 h and 48 h. Data derived from 3 independent cell preparations and are shown as means ±SEM.*

4.2.4. Effect of 2DG on ATP levels of HC, kept in WE_{old} (+G), WE_{new} (+/-G) and RPMI (+/-G)

In the synthetic glucose analogue, 2DG, the C2 hydroxyl group is missing oxygen. The structural similarity between 2DG and glucose allows the transport into the cell via glucose transporter. In the cytoplasm, hexokinase converts 2DG to 2DG-phosphate, which accumulates in the cell, leading to inhibition of the enzyme. The inhibition of this key enzyme results in the suppression of ATP production, and in further consequence in cell growth inhibition and cell death [85].

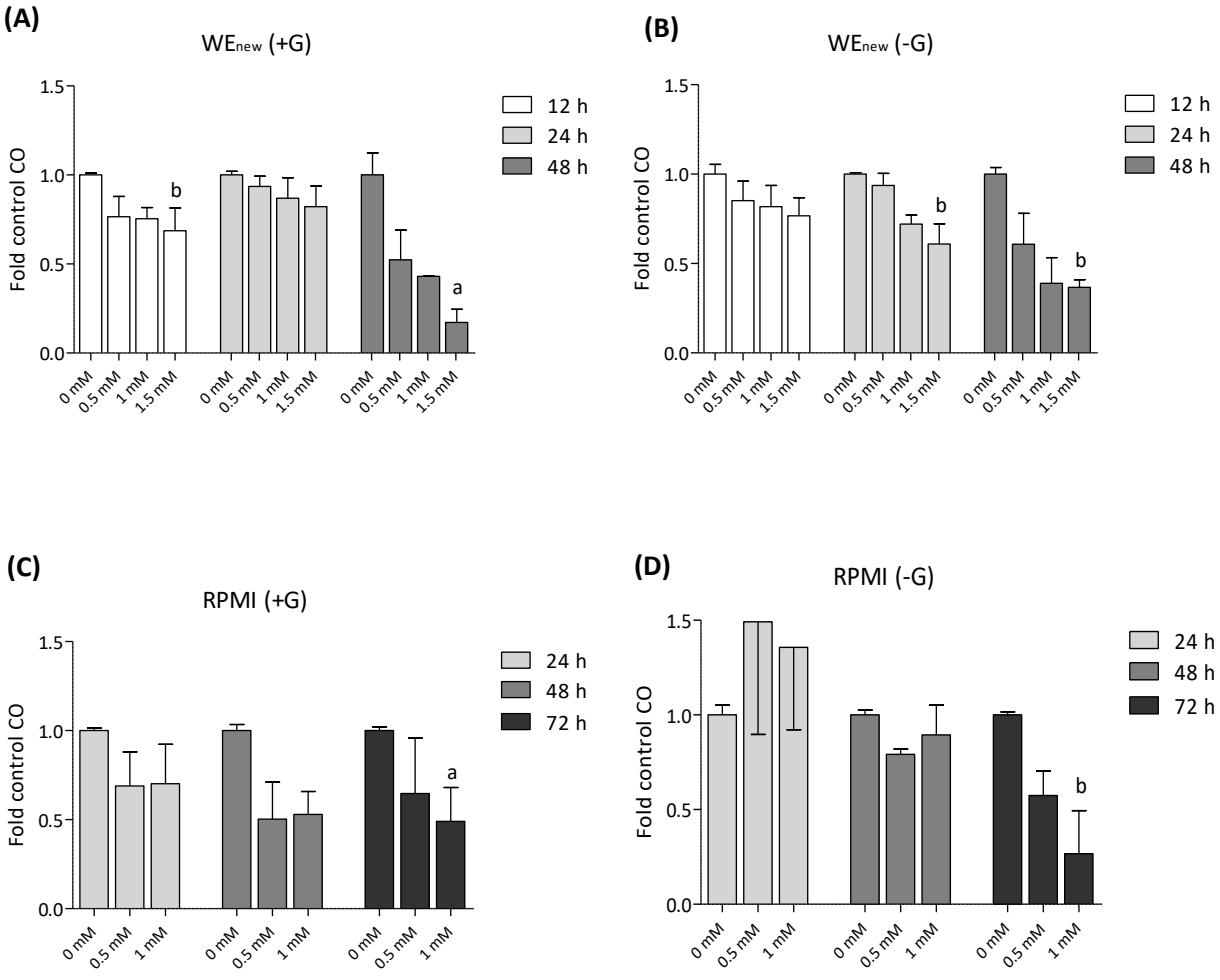
To verify the suppression of ATP production by 2DG, we cultured HC in WE_{old} (+G), WE_{new} (+/-G) and RPMI (+/-G) with different concentrations of 2DG and measured the ATP levels at several time points. Figure 20 shows the hepatocellular ATP levels in WE_{old} (+G), WE_{new} (+/-G) and RPMI (+/-G) over time. The ATP levels in HC in the various control media (media +/-G) were arbitrarily set 1. The impact of the different control media on ATP content after different time points are described in figure 17 and 18.

HC, cultured in WE_{new} (+/-G), were treated with 0.5 mM, 1 mM or 1.5 mM of 2DG for 12 h, 24 h or 48 h. Figure 20 (A) and (B) show, that the higher the concentration of 2DG, the lower ATP levels were found. Over the period of 48 h, there was an overall decrease in ATP levels in both WE_{new} (+/-G).

HC cultured in RPMI (+/-G) were treated with two different concentrations of 2DG (0.5 mM and 1 mM). Figure 20 (C) shows that after 24 h and 48 h the ATP levels in RPMI (+G) remained more or less constant. In RPMI (+G) 0.5 mM and 1 mM 2DG were almost equally effective in reducing the endogenous ATP level by about 1/3 to 1/2 within 72 h (figure 20 (C)).

After 24 h and 48 h in RPMI (-G), 0.5 mM and 1 mM 2DG appeared to be ineffective in reducing ATP level, while after 72 h the ATP levels had decreased at the higher concentration of 2DG (see figure 20 (D)).

Figure 20 (E) shows that in WE_{old} (+G) ATP levels remained more or less unaffected by 2DG for the whole observation period.



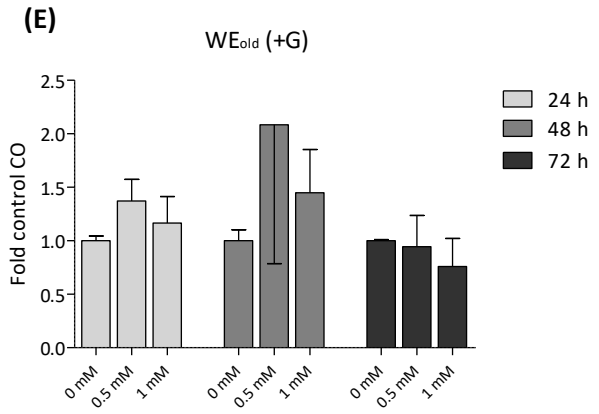


Figure 20: ATP levels in 2-DG treated HC, cultured in WE_{old} (+G), WE_{new} (+/-G) and RPMI (+/-G) after different time points*. Food was removed 12 h before cell isolation. Livers of untreated rats were perfused with collagenase, HC were isolated and 4x10^5 HC/well were seeded on collagen coated 6-well plates in WE_{old} (+G), WE_{new} (+/-G), RPMI (+/-G), which contained 10 % of FCS. After 90 min in culture, the medium (+/-G) was changed to different serum-free culture media. HC were treated with different concentrations of 2DG (0 mM, 0.5 mM, 1 mM, 1.5 mM). For the 72 h measurement time point, the medium +/- 2DG was renewed after 48 h (A) WE_{new} (+G); ATP level was measured after 12 h, 24 h or 48 h. (B) WE_{new} (-G); ATP level was measured after 12 h, 24 h or 48 h. (C) RPMI (+G); ATP level was measured after 24 h, 48 h or 72 h. (D) RPMI (-G); ATP level was measured after 24 h, 48 h or 72 h. (E) WE_{old} (+G); ATP level was measured after 24 h, 48 h or 72 h; n=4. Data derived from ≥ 3 independent cell preparations and are shown as means ±SEM. Statistics by Kruskal-Wallis test: ATP-level in HC in RPMI (+G) over dose range: (a) $p < 0.05$; (b) $p < 0.01$.*

4.2.5. Effect of 2DG on the vitality of HC

We cultured HC in WE_{new} (+/-G) and treated the cells with 0 mM and 0.5 mM of 2DG. The influence of the compound on the vitality was tested by performing a viability test after 24 h and 48 h of treatment. In figure 21 (A) the ability of the control cells to convert MTT to the colored formazan remained more or less constant over 48 h. We measured lower ATP levels in HC cultured in WE_{new} (-G) (described in section 3.2.3., figure 19) than in WE_{new} (+G). However, in WE_{new} (+G), the vitality was decreased by 0.5 mM of 2DG after 24 h and 48 h. Figure 21 (B) shows that there was less vitality of HC cultured in WE_{new} (-G) after treatment with 0.5 mM of 2DG for 24 h when compared to control. After 48 h there was a marginal decrease in ATP levels after 2DG treatment in HC cultured in WE_{new} (-G).

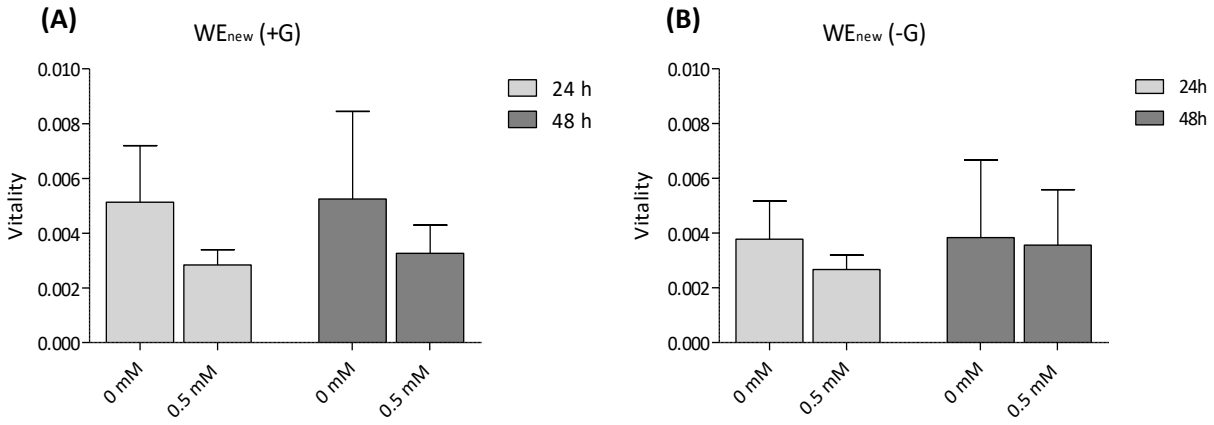


Figure 21: Vitality of 2DG-treated HC, cultured in WE_{new} (+/-G) after different time points*. Food was removed 12 h before cell isolation. Livers of untreated rats were perfused with collagenase, HC were isolated and 2000 HC/well were seeded on collagen coated 96-well plates in WE_{new} (+/-G), which contained 10 % of FCS. After 90 min in culture, the medium was changed to different serum-free culture media (+/-G) and HC were treated with 0 mM or 0.5 mM 2DG. Viability test was performed by applying the MTT assay after 24 h and 48 h. (A) WE_{new} (+G). (B) WE_{new} (-G). Data in (A) and (B) derived from 3 independent cell preparations and are shown as means ±SEM.*

4.3. Impact of 2DG on DNA synthesis of primary HC

4.3.1. DNA synthesis rate of 2DG treated primary HC kept in WE_{new} (+/-G)

The effect of 2DG comprises the inhibition of ATP production in primary HC (described in chapter 3.2.) as well as inhibition of cell growth by suppression of DNA synthesis. To examine the inhibitory effect of 2DG on DNA replication, we cultured primary HC in WE_{new} (+/-G) and treated the cells with 0 mM, 0.5 mM or 1 mM of 2DG. Since primary HC replicate rarely, we used the same protocol in presence of the potent growth factor EGF, which served to elevate the basal DNA synthesis rate. After ^{3}H-thymidine incorporation into DNA for the last 24 h in culture, the HC were fixed with formalin. Following autoradiography labelled nuclei could be detected. We did not find any DNA replication, not even in the EGF treated control group (see table 4). We speculated, whether the medium was not optimal for the cells and switched to WE_{old} (+G), as outlined in chapter 4.2.

	WE_{new} (+G)	*WE_{new} (-G)*
0 mM 2DG	0±0	0±0
0.5 mM DG	0±0	0±0
1 mM DG	0±0	0±0
0 mM + EGF	0±0	0±0
0.5 mM DG + EGF	0±0	0±0
1 mM DG + EGF	0±0	0±0

Table 4: Labelling index (LI) of unaltered primary HC, cultured in WE_{new} (+/-G), treated with 2DG. *Food was removed 12 h before cell isolation. Livers of untreated rats were perfused with collagenase. HC were isolated and 4x10^{5} HC/well were seeded onto collagen coated plates in WE_{new} (+G), which contained 10 % of FCS. After 90 min, the medium was changed to serum-free WE_{new} (+/-G), containing 0 mM, 0.5 mM and 1 mM of 2DG. After 6 h 10 ng of EGF per mL was added to the plates that served as positive control. 24 h later cells were treated with ^{3}H-thymidine and another 24 h later cells were fixed with formalin. After autoradiography, the labelling index could be determined. Data derived from 3 independent cell preparations and are shown as means ±SEM.*

4.3.2. Effect of 2DG treatment on DNA replication of unaltered and initiated primary HC in WE_{old} (+G)

We treated male rats with the NNM at a dose of 167 mg NNM/ kg body weight to induce the formation of initiated HC, which express selectively GSTp (placental glutathione S-transferase), a marker of early cancer prestages in rats. GSTp positive cells have a higher DNA synthesis rate than normal cells, both in vivo as well as in vitro [87]. Three weeks later, we perfused the liver and cultured unaltered (GSTp negative) HC and initiated (GSTp positive) HC in WE_{old} (+G) and treated them with 0 mM, 0.5 mM or 1 mM of 2DG for 48 h. In HC, treated with 2DG only, no labelled nuclei would be detected (see table 5). In parallel, the same experimental set-up was chosen and all treatment groups were exposed additionally to EGF in order to elevate the basal DNA replication rate. Under the current experimental condition, 4 % of unaltered and 7 % of GSTp positive control cells (0 mM 2DG) had incorporated ^{3}H-thymidine (see figure 22 (A)). With 0.5 mM of 2DG, the DNA synthesis rate decreased in unaltered and initiated HC by about 1/2 and with 1 mM of 2DG by about 3/4 (see figure 22 (B)).

	WE_{old} (+G)
0 mM 2DG	0±0
0.5mM DG	0±0
1mM DG	0±0

Table 5: Labelling index (LI) of unaltered primary HC, cultured in WE_{old} (+G), treated with 2DG. *Food was removed 12 h before cell isolation. Livers of untreated rats were perfused with collagenase. HC were isolated and 4x10^{5} HC/well were seeded onto collagen-coated plates in WE_{old} (+G), which contained 10 % of FCS. After 90 min, the medium was changed to serum-free WE_{old} (+G), containing 0 mM, 0.5 mM and 1 mM of 2DG. Twenty-four hours later cells were treated with ^{3}H-thymidine and another 24 h later cells were fixed with formalin. After autoradiography, the labelling index could be determined. Data derived from 2 independent cell preparations and are shown as means ±SEM.*

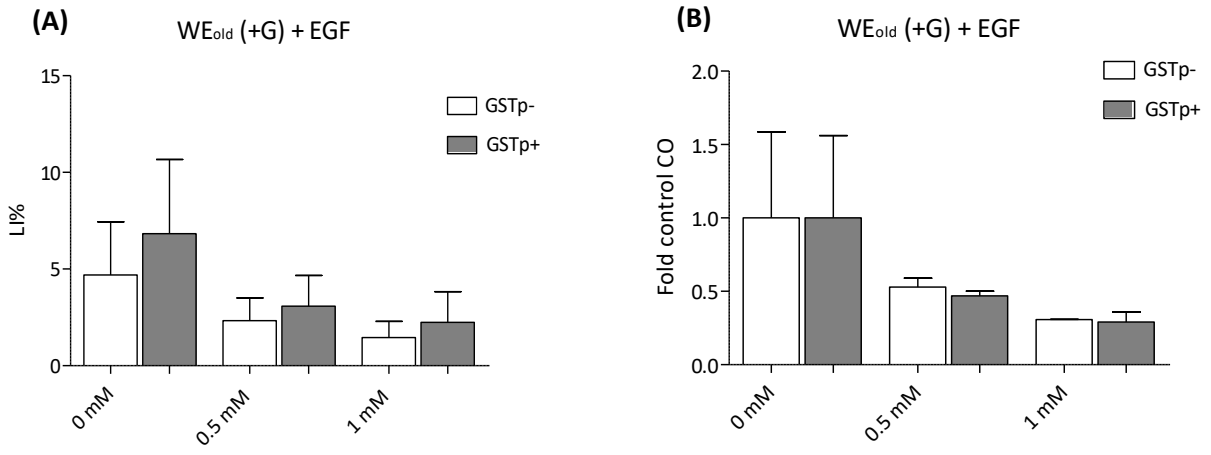


Figure 22: Labelling index (LI) of GSTp- and GSTp+ primary HC, cultured in WE_{old} (+G), treated with 2DG. *Rats were treated with a single dose of NNM (167 mg/kg). Rats were recovered for 3 weeks. Food was removed 12 h before cell isolation. Livers were perfused with collagenase. HC were isolated and $4x10^5$cells/well were seeded onto collagen-coated plates in WE_{old} (+G), which contained 10 % of FCS. After 90 min, the medium was changed to serum-free WE_{old} (+G), containing 0 mM, 0.5 mM and 1 mM of 2DG. Six hours later 30 ng of EGF per mL medium was added to the plates. Twenty-four hours later cells were treated with ^{3}H-thymidine and another 24 h later cells were fixed with formalin. After autoradiography, the labelling index could be determined. (A) WE_{old} (+G) with EGF. (B) WE_{old} (+G) with EGF. Control values were arbitrarily set 1. Data obtained are expressed as fold medium control. Data in (A) and (B) derived from 2 independent cell preparations and are shown as means ±SEM.*

4.3.3. Impact of 2DG treatment on unaltered and initiated primary HC in WE_{old} (+G) with and without EGF

Since primary HC barely replicate DNA within approximately 54 h in culture, we extended the cultivation time for further 24 h. We treated unaltered primary HC with 0 mM, 0.5 mM and 1 mM of 2DG. Six hours later we treated these cells with 30 ng of EGF per mL medium, to stimulate their DNA replication rate, which served as pre-experiment. Figure 23 shows the DNA replication rate of this unaltered primary HC, which were approximately 3 days in culture. The comparison with figure 22 (A) shows that the basal DNA replication, was marginally higher at 78 h. The 2DG-induced suppression of DNA synthesis was similar at 54 h and 78 h. At both time points, there was suppression in the DNA synthesis rate after treatment with 0.5 mM or 1 mM of 2DG.

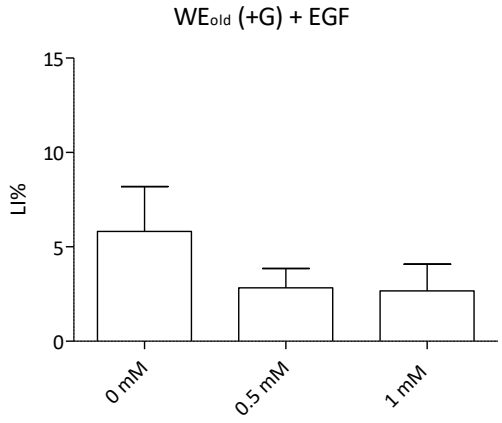


Figure 23: Labelling index (LI) of unaltered primary HC, cultured in WE_{old} (+G), treated with 2DG and EGF. *Food was removed 12 h before cell isolation. Livers of rats were perfused with collagenase. HC were isolated and $4x10^5$ HC/well were seeded onto collagen-coated plates in WE_{old} (+G), which contained 10 % of FCS. After 90 min, the medium was changed to serum-free WE_{old} (+G), containing 0 mM, 0.5 mM and 1 mM of 2-DG. After 6 h 30 ng of EGF per mL medium was added to the plates. Forty-eight hours later the treatment solution was renewed and HC were treated with ^{3}H-thymidine. Another 24 h later cells were fixed with formalin. After autoradiography, the labelling index could be determined. Data derived from 3 independent cell preparations and are shown as means ±SEM.*

Figure 24 (A) and (B) show primary HC cultured in WE_{old} (+G) without EGF. The DNA replication rate in initiated control cells was twice as high, as in unaltered control cells, which indicates the inherent growth advantage of the early pre-stages of cancer. The labelling index of the cells under this condition is not very high, i.e., 1 % of unaltered HC and somewhat over 1 % of GSTp+ HC had incorporated ^{3}H-thymidine (figure 24 (A)). The labelling index of 2DG-treated initiated cells was even eight times as high as in unaltered 2DG treated cells (see figure 24 (A) and (B)). Figure 24 (B) shows that the DNA synthesis rate in unaltered cells was halved by 0.5 mM of 2DG and tended to further decrease with 1 mM 2DG.

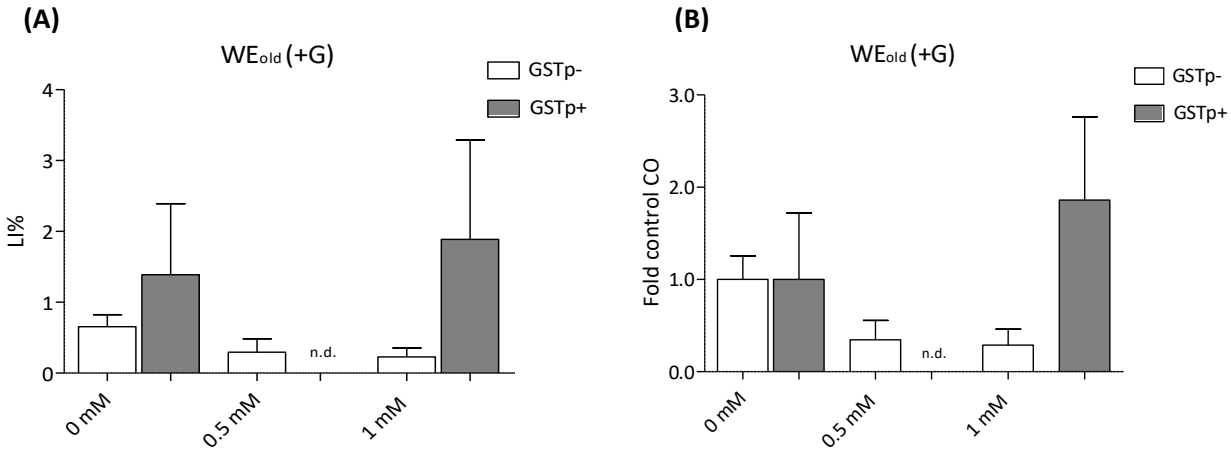


Figure 24: Labelling index (LI) of GSTp- and GSTp+ primary HC, cultured in WE_{old} (+G) treated with 2DG. *Rats were treated with a single dose of NNM (125 mg/ kg). Rats were recovered for 3 weeks. Food was removed 12 h before cell isolation. Livers were perfused with collagenase. HC were isolated and $4x10^5$ HC/well were seeded onto collagen-coated plates in WE_{old} (+G), which contained 10 % of FCS. After 90 min, the medium was changed to serum-free WE_{old} (+G), containing 0 mM, 0.5 mM and 1 mM of 2DG. Forty-eight hours later the treatment solution was renewed and HC were treated with ^{3}H-thymidine. Another 24 h later cells were fixed with formalin. After autoradiography, the labelling index could be determined. (A) WE_{old} (+G) without EGF. LI in %. (B) WE_{old} (+G) without EGF. Control values were arbitrarily set 1. Data obtained are expressed as fold medium control. Data in (A) and (B) derived from 3 independent cell preparations and are shown as means ±SEM. (n.d.) not determined.*

4.3.4. Effect of 2DG treatment on unaltered and initiated primary HC, kept in RPMI (+/-G)

Next, we examined the effect of 2DG on DNA synthesis of unaltered HC, kept in media (+/-G). Since basal DNA replication of HC was almost zero when kept in WE_{new} (+/-G), we switched to RPMI (+/-G) As a pre-experiment, we treated unaltered HC with 0 mM, 0.5 mM and 1 mM of 2DG. Six hours later we treated these cells with 30 ng of EGF per mL medium, to stimulate their DNA replication rate (figure 25). In general, the DNA replication rate of the EGF stimulated HC was much higher than without EGF (compare with figure 26). Figure 25 (A) shows, that the control group (treated with 0 mM of 2DG) had a higher labelling index than the 2DG-treated HC. However, cells treated with 1 mM of 2DG showed more incorporated ^{3}H-thymidine than cells, which were treated with 0.5 mM of 2DG. However, this was not significant. Figure 25 (B) shows that the replication rate of the control cells was lower than the cells, which were treated with 0.5 mM or 1 mM of 2DG.

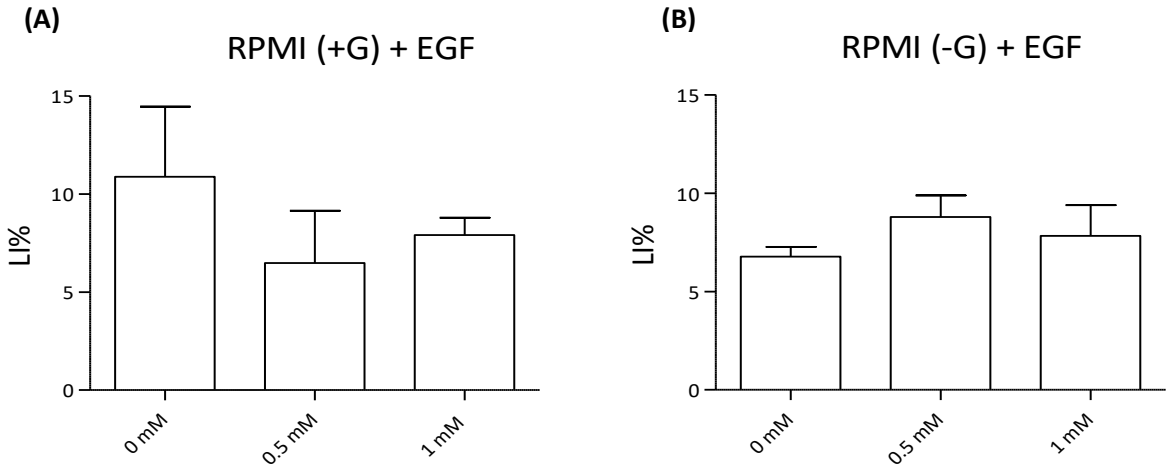


Figure 25: Labelling index (LI) of primary HC, cultured in RPMI (+/-G) treated with 2DG and EGF. *Food was removed 12 h before cell isolation. Livers were perfused with collagenase. HC were isolated and 4x10^5 HC/well were seeded onto collagen-coated plates in RPMI (+G), which contained 10 % of FCS. After 90 min, the medium was changed to serum-free RPMI (+/-G) containing 0 mM, 0.5 mM and 1 mM of 2DG. 6 h later 30 ng of EGF per mL was added. Forty-eight hours later the treatment solution was renewed and HC were treated with ^{3}H-thymidine. Another 24 h later cells were fixed with formalin. After autoradiography, the labelling index could be determined. (A) LI % of cells, kept in RPMI (+G). (B) LI % of cells, kept in RPMI (-G). Data in (A) and (B) derived from 3 independent cell preparations and are shown as means ±SEM.*

In figure 26, unaltered and initiated HC are shown, which were exposed under the same experimental conditions as the cells in the pre-experiment (shown in figure 25), except for the stimulation with EGF.

Compared with WE_{old} (+G) (see figure 24), the labelling indices were higher in RPMI (+/-G) (figure 26 (A) and (B)). The DNA replication in initiated control HC and initiated 2DG-treated HC, kept in RPMI (+G), was approximately twice as high than unaltered HC (figure 26 (A)). Figure 26 (A) and (C) show that the DNA synthesis rate of unaltered cells, kept in RPMI (+G), decreased by 1/7 with 0.5 mM of 2DG and by 1/3 with 1 mM of 2DG. Figure 26 (B) shows that the replication rate of unaltered and initiated HC, kept in RPMI (-G), was lower than in cells, kept in RPMI (+G) (compare with figure 26 (A)). The unaltered cells, kept in RPMI (-G), showed higher DNA synthesis rates than unaltered cells in RPMI (+G) (compare with figure 26 (A) and (C) with (B) and (D)), and it decreased marginally with higher 2DG concentration (figure 26 (B) and (D)).

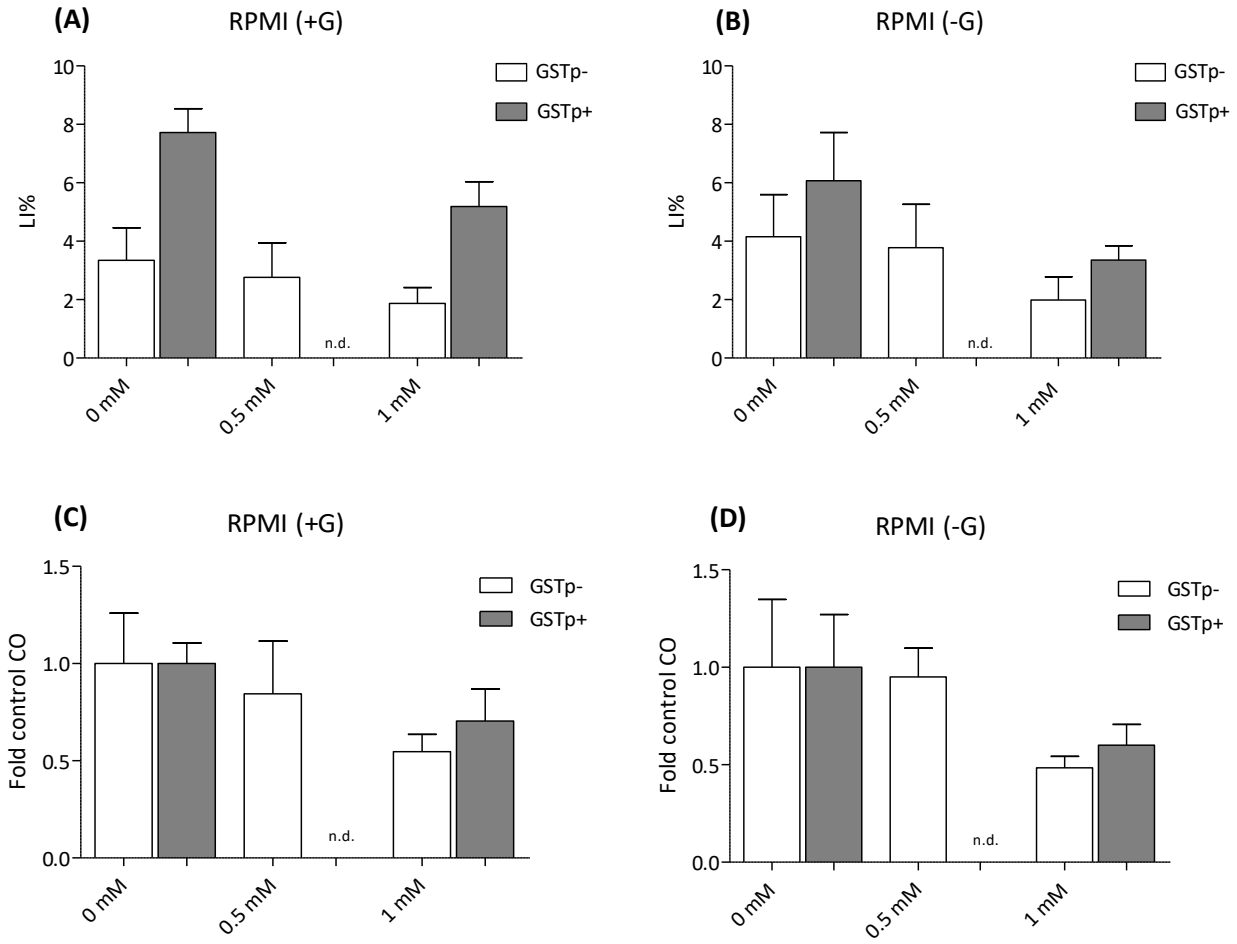


Figure 26: Labelling index (LI) of GSTp- and GSTp+ primary HC, cultured in RPMI (+/-G) treated with 2DG. *Rats were treated with a single dose of NNM (125 mg/ kg). Rats were recovered for 3 weeks. Food was removed 12 h before cell isolation. Livers were perfused with collagenase. HC were isolated and 4x10^5 HC/well were seeded onto collagen-coated plates in RPMI (+G), which contained 10 % of FCS. After 90 min, the medium was changed to serum-free RPMI (+/-G), containing 0 mM, 0.5 mM and 1 mM of 2DG. Forty-eight hours later the treatment solution was renewed and HC were treated with ^{3}H-thymidine. Another 24 h later, cells were fixed with formalin. After autoradiography, the labelling index could be determined. (A) LI % of cells, kept in RPMI (+G). (B) LI % of cells, kept in RPMI (-G). (C) RPMI (+G). Control values were arbitrarily set 1. Data obtained are expressed as fold medium control. (D) RPMI (-G). Control values were arbitrarily set 1. Data obtained are expressed as fold control. Data in (A), (B), (C) and (D) derived from 3 independent cell preparations and are shown as means ±SEM. (n.d.) not determined*

5. Discussion

5.1. Analysis of the transcriptome pattern of enzymes involved in glucose metabolism

The analysis of the transcriptome pattern of preneoplastic rat liver lesions showed deregulations of several genes, which are involved in glucose metabolism.

The enzyme hexokinase (HK) phosphorylates the incoming glucose to glucose-6-phosphate (G6P). In normal differentiated HC, the major isoform is HK4 (glucokinase), which differs from other HK isoforms (HK1 - 3) in its low affinity for glucose, its lower molecular mass and its activity is not inhibited by G6P, as it is in the other HK isoforms [88], [89]. The transcriptome pattern of preneoplastic liver foci showed upregulation of HK1. This might indicate that early prestages of cancer already induces high-level expression of HK1, which has the higher affinity for glucose than HK4 [90]. In human tumor cell lines (HepG2) the expression of the highly active HK1 or HK2 has been observed already [90]. Previous rat genome array data, done by Teresa Riegler, showed that the enzyme HK1 was increased in liver adenomas and carcinomas, which supported the observation of the isotype switch of HK, also in this rodent species. The isotype switch is part of a metabolic reprogramming of tumor cells, called Warburg effect or aerobic glycolysis. This metabolic reprogramming of cancer cells was well investigated in the past few decades. In the 1920s Otto Warburg observed already aberrations in the glucose metabolism of cancer cells. He detected that cancer cells utilize excessive amounts of glucose and ferment it to lactate, regardless of whether oxygen is present or not [91]. Since then, several aberrations of enzymes of the glucose metabolism in HCC have been described [90].

In the present work, we found that the expression of glycolytic enzymes, such as aldolase A (ALDO A) and phosphoglycerate mutase 1 (PGAM 1) are increased in preneoplastic rat liver lesions. PGAM 1 catalyzes the conversion of 3-phosphoglycerate (3PG) to 2-phosphoglycerate (2PG) and controls the intracellular levels of 2PG and 3PG. PGAM1 decreases the level of 3PG, which inhibits the enzyme phosphogluconate dehydrogenase (PGD), an important regulator of the pentose-phosphate pathway (PPP). This increases the PPP, which in further consequences elevates the DNA synthesis rate. [92], [93]. During human hepatocarcinogenesis, the enzyme aldolase may undergo an isotype switch from ALDO B, which is more prone to gluconeogenesis, to ALDO A, which tends more to glycolysis [90], [94]. ALDO A catalyzes fructose-1, 6-biphosphate (F1, 6BP) to glyceraldehyde-3-phosphate (G3P) and dihydroxyacetone phosphate (DHAP).

The product G3P may be an anti-apoptotic effector, due to the ability to inhibit caspase-3 activity, an enzyme, that has a crucial role in pro-apoptotic pathways [95]. This may indicate that already preneoplastic cells try to avoid apoptosis.

The data obtained from the preneoplastic rat liver lesions contrast to what is known from advanced tumor stages in humans. There was no considerable upregulation of the enzyme lactate dehydrogenase B (LDH B), which plays a crucial role in the Warburg effect (also known as aerobic glycolysis), by catalyzing high amounts of pyruvate to lactate. Aerobic glycolysis is characteristic for tumor cells, which utilize large amounts of glucose for fermentation to lactate. These data indicate that aerobic glycolysis is a characterization of late-stage tumors, in which tumor cells utilize large amounts of glucose and ferment it to lactate. The ATP generated during lactate generation from glucose is far less than during the oxidative phosphorylation of pyruvate in the mitochondria. This suggests that the cancer cells´ main priority is not maximizing ATP production but rather building up biomass for cell growth and proliferation using intermediates of the glycolytic pathway. The high secretion of lactate acidifies the microenvironment, which supports tumor invasion and suppresses anticancer immune effectors [96]. Furthermore, lactate may be used by surrounding cells to generate pyruvate, which is taken up by the cancer cells for fatty acid synthesis [90], [97].

Bannasch et al., (1997) [98] showed that preneoplastic rat liver foci store large amounts of glycogen (glycogenosis). These findings agree with our results, which showed that glycogenetic enzymes (GYG1, UGP2 and GBE1) are upregulated. GYG1 serves as starter molecule for de novo glycogen synthesis. UGP2 catalyzes the transfer of phosphate residues, resulting in activated UDP-glucose, which is added to the glycogen molecule by glycogen synthase. GBE1 branches the extended glycogen chain in the last step of glycogenesis [98]. The advantage of excessive glycogen storage in preneoplastic HC may be the sustained provision of glucose to fulfill the enhanced energy needs of rapidly replicating cells.

The transcriptome data of preneoplastic rat liver lesions showed that enzymes, which are involved in gluconeogenesis, are downregulated. Reyes et al., (2014) [99] reported a reduction of gluconeogenesis in HCC cells, which agrees with our findings, indicating that the suppression of gluconeogenesis already occurs in prestages of cancer. The downregulated enzymes include phosphoenolpyruvate carboxykinase 1 (PCK1), fructose-1, 6-biphosphatase (FBP1) and glucose-6-phosphatase (G6PC). PCK1 catalyzes the formation of phosphoenolpyruvate (PEP) from oxalacetate. FBP1 converts fructose-1, 6-bisphosphate (F1, 6BP) to fructose-6-phosphate (F6P). G6PC hydrolyzes G6P to glucose [15]. Due to the suppression of gluconeogenesis in preneoplastic rat liver cells, the accumulating G6P may be redirected to the PPP for generation of nucleotides, required for proliferation. In HCC cells, the suppression of gluconeogenesis may also serve for constant glycolysis.

Our finding showed, that the expression of important enzymes, involved in the PPP, such as glucose-6-phosphate dehydrogenase (G6PD), transketolase (TKT) and transaldolase 1 (TALDO 1), are increased in preneoplastic rat liver lesions, suggesting that preneoplastic liver cells are primary prone to synthesis of nucleotides, required for cell proliferation. The PPP is divided into an oxidative and a non-oxidative phase. In the irreversible oxidative phase, G6P is converted to 6-phosphogluconolactone by G6PD, then to 6-phosphogluconate, and subsequently to ribulose-5-phosphate (Ru5P) by phosphogluconate dehydrogenase (PGD) via oxidative decarboxylation. Thereby NADPH is generated. Ru5P may be either isomerized or epimerized, resulting in the generation of ribose-5-phosphate (R5P) or xylulose-5-phosphate (Xu5P). R5P is further metabolized to phosphoribosyl-phosphate, which functions as the backbone for nucleotide synthesis. In the reversible non-oxidative phase, glycolytic intermediates, such as fructose-6-phosphate (F6P) and G3P, are generated by the enzymes TKT and TALDO. Furthermore, F6P can be converted to G6P to restore the PPP [93]. Due to the upregulation of G6PD, the production of NADPH also increases, which serves as a defence against oxidative stress [100]. This indicates that the continuous supply of G6P is very important for preneoplastic HC.

In conclusion, the analysis of the transcriptome pattern of preneoplastic liver foci showed that the metabolic reprogramming already starts in early stages of cancer, which enables cells to proliferate by the utilization of glucose to synthesize nucleotides in the PPP. This indicates that glucose plays a crucial role in the stimulation of proliferation.

5.2. Impact of different culture media on ATP concentration, vitality and DNA replication of unaltered and initiated HC

5.2.1. Various compositions and components of three different culture media

Cultures of primary HC are a highly artificial model, which varies in dependence on the culture conditions applied. Therefore, we studied the role of glucose for survival and growth of unaltered and preneoplastic HC under different conditions in order to check for the robustness of data.

Williams medium E (WE_{old}, WE_{new}(+/-G)) has been developed to support long-term cultures of primary HC. RPMI 1640 is a standard medium, frequently used for transformed cell lines. The main difference between the three media is that WE_{old} contains D-glucose, which is lacking in WE_{new} and RPMI. Therefore, we added D-glucose to equalize these differences. Furthermore, profound

differences are evident with regard to the content of amino acids, vitamins, and other compounds (see table 3), which may affect metabolic activity, vitality and growth behaviour of unaltered and initiated HC (as outlined below).

5.2.2. Amino acid contents

Generally, WE_{old} and WE_{new} do not exhibit many differences in amino acid content. WE_{new} contains L-glutamine and L-glutamic acid, whereas WE_{old} contains somewhat lower amounts of L-glutamic acid and no L-glutamine. L-glutamic acid may be metabolized to L-glutamine, which may serve as alternative energy source. L-glutamine is converted to glutamate and further converted to α-ketoglutarate, which is an important intermediate of tricarboxylic acid (TCA) -cycle [101]. The functions of the TCA-cycle involve, among others, the oxidation of acetyl-CoA to CO_2. Due to this oxidation, $FADH_2$ and NADH are generated, which can be reoxidized in the electron transport chain, which in turn generates ATP. The TCA-cycle also provides intermediates for gluconeogenesis and other anabolic pathways [102]. In the present experiment, the ATP concentration of unaltered HC was similar when cultured in WE_{new} with or without glucose (see figure 18 (A) and (B)). We speculated that HC, kept in glucose-depleted conditions, either use L-glutamine as an alternative energy source or might have received energy by the breakdown of glycogen by glycogenolysis. With regard to the latter possibility, it has to be considered that HC were isolated from young animals, kept in a light-dark cycle of lights on from 6 am to 6 pm. Due to the nocturnal activity of the animals, it may be assumed that the rats consumed food approximately until 3 h before cell isolation. Due to permanent access to food, we speculated that rats may store glucose in form of glycogen in the liver. In order to exclude this possibility food was withdrawn approximately 12 h before cell isolation. Then, we compared the ATP levels of unaltered HC, kept in WE_{new} with and without glucose, and differences between ATP levels of unaltered HC became evident. We observed lower ATP levels of HC under glucose-depleted conditions than under glucose-rich conditions after 12 h. Then, the ATP levels decreased after 24 h and 48 h, in both glucose-rich and -depleted conditions (see figure 18 (A) to (D)). Furthermore, the vitality of HC, kept in glucose-depleted WE_{new}, tended to be somewhat lower than in their counterparts (WE_{new}(+G)). From this point onwards, all further experiments included food withdrawal for a period of approximately 12 h before isolation of HC.

Compared to WE_{new}, WE_{old} contains a higher level of L-cystine. L-cystine results from oxidation of L-cysteine, which is present at same concentrations in WE_{old} and WE_{new}. L-cystine consists of two L-cysteines forming a disulfide bond. L-cystine as well as L-cysteine belong to the non-essential amino acids and are important components of proteins. In proteins, the sulfur atoms may bind to thiol groups, which provide sites for redox activity and electron transfer. In cell culture, the amino acids

have an indirect protective role. L-cysteine acts as the rate-limiting amino acid for the synthesis of glutathione, which protects against reactive oxygen species (ROS). Without L-cysteine/L-cystine cells will die, because glutathione is depleted very fast [103]. SLC7a11 is expressed in HC as evident from our oligo-array data and acts as a cystine/glutamate antiporter, which is involved in the redox state of HC [104]. Accordingly, we assumed that the difference between the L-cystine content in WE_{old} and WE_{new} probably correlates with the amount of L-glutamic acid in the culture media. SLC7a11 exchanges extracellular L-cystine with intracellular L-glutamate [105], which results from preceding conversion of L-glutamic acid [101]. Thus, the higher the L-cystine level, the higher the L-glutamic acid content.

With regard to the other amino acids also distinct patterns between the various media were evident. WE_{new}/WE_{old} both contain reduced amounts of L-serine and high amounts of L-glycine, comparing with RPMI. Glycine and L-serine play roles in the metabolism of nucleic acid precursor via the tetrahydrofolate (THF) - cycle. As reported by Salazar et al. (2016) [104], the depletion of L-serine, however, and compensation with glycine, results in L-serine production from glycine, catalyzed by serine hydroxymethyltransferase. This directs metabolites away from the THF-cycle, which leads to a slow THF-cycle and in further consequences to inhibition of cell proliferation. Our results showed that the basal rate of DNA synthesis was extremely low in HC kept in WE_{new} with or without glucose for 48 h. Even addition of the potent growth factor EGF at 10 ng per ml medium was without effect. We, therefore, checked DNA synthesis of HC in WE_{old}. Similar to WE_{new}, WE_{old} did not support DNA synthesis in untreated as well as in EGF-treated HC. When the culture conditions were prolonged to 72 h, DNA synthesis became evident. However, EGF at 30ng/ml medium failed to exert any significant effect.

However, in RPMI the DNA replication was high (see figure 26). RPMI contains high levels of L-serine, which may be partly responsible for the elevated DNA replication. As mentioned above, the non-essential amino acid, L-serine is involved in the THF-cycle (see above and [104]), by donating one-carbon units, which are used for the de *novo synthesis* of adenosine, guanosine, and thymidylate (or thymidine monophosphate). Furthermore, the THF-cycle generates NADH, NADPH, as well as ATP. At physiological concentrations, L-serine activates the enzyme pyruvate kinase isoform M2 (PKM2), which catalyzes phosphoenolpyruvate to pyruvate - the last step of glycolysis [106]. RPMI also contains high amounts of L-glutamine, which may also affect DNA replication in unaltered HC, using L-glutamine as alternative energy source.

In contrast to WE_{old} and WE_{new}, RPMI contains a reduced amount of the essential amino acids L-leucine, L-lysine, L-phenylalanine, L-threonine, L-tryptophan and L-valine and reduced amounts of the non-essential amino acids glycine, L-aspartic acid, L-glutamic acid, L-proline and L-tyrosine. RPMI

lacks L-alanine and L-cysteine and contains high amounts of L-arginine, L-glutamine, L-cystine and L-hydroxyproline, which is lacking in WE.

The higher amount of L-hydroxyproline may also be partly responsible for high DNA replication in HC, kept in RPMI (figure 26). To be specific, L-hydroxyproline is generated via hydroxylation of L-proline. L-hydroxyproline, as well as L-proline, are the major amino acids in collagen proteins [107]. Primary HC are able to synthesize collagen [108]. The high content of L-hydroxyproline may support the own collagen biosynthesis of HC, which provides convenient culture conditions for HC, which may support DNA replication.

To summarize, depletion of glucose reduced somewhat vitality and ATP concentration in primary HC, when food was withdrawn approximately 12 h before HC isolation.

Furthermore, the amino acid content of culture media seems to affect ATP concentration and DNA replication in unaltered HC. L-serine and L-glutamine contents in culture media seem to be important amino acids, which may affect ATP production and DNA replication of primary HC.

5.2.3. Different vitamins and co-factors

When compared to WE_{old} and WE_{new}, RPMI is lacking some vitamins, such as ascorbic acid, calciferol, menadione (vitamin K3), vitamin A and α-tocopherol. Para-aminobenzoic acid (member of vitamin B group) is only present in RPMI. RPMI contains reduced levels of biotin, D-calcium pantothenate, and vitamin B_{12}. Our results showed that the ATP concentration was similar in HC, kept in WE as well as in RPMI, although RPMI contains higher amounts of L-serine, which also correlates with ATP production [106]. This might be caused by the reduced amounts of vitamin B_{12} in RPMI, compared with WE (see figure 17). To be specific, vitamin B_{12} is an important co-factor for the enzyme methylmalonyl-CoA mutase, which catalyzes methylmalonyl-CoA to succinyl-CoA, an intermediate of the TCA-cycle [109]. In conclusion, due to somewhat higher amounts of vitamin B_{12} in WE, more succinyl-CoA may be generated and in further consequences, ATP is generated. This may compensate the reduced amounts of L-serine in WE, as outlined above.
Other vitamins, such as choline, riboflavin and especially inositol (35 mg/L) are present in high amounts in RPMI, while the content of inositol is very low in WE_{old} and WE_{new} (2 mg/L). This low level of inositol in WE_{old} and WE_{new} may be contributed to the extremely low DNA replication in HC. Inositol phosphates, such as inositol (1, 4, 5) triphosphate (IP_3), play important roles as secondary messengers, in signal transduction pathways.

IP_3 is generated from phosphatidylinositol (4, 5) bisphosphate (PIP_2) through hydrolysis by phospholipase C (PLC), after preceding binding of hormones or growth factors to receptor tyrosine kinases (RTK) and G-protein coupled receptors (GPCR). Thus, membrane-associated PLC is activated. PLC catalyzes PIP_2 to IP_3 and diacylglycerol (DAG), which remains in the plasma membrane, thereby activating protein kinase C (PKC). IP_3 binds to IP_3-receptor (IP_3R) at the ER-membrane in order to release Ca^{2+} stores from ER into the cytosol, causing the first step of the calcium (Ca^{2+}) signaling pathway, which promotes cell cycle progression and regulates glucose and energy metabolism [110].
Although WE_{old} and WE_{new} contain higher levels of Ca^{2+} than RPMI, our results showed that DNA replication in unaltered HC, kept in RPMI, was high (see figure 26). This may be due to the growth stimulatory effect of inositol via Ca^{2+} signaling. Thus, it is not surprising that primary HC might replicate their DNA preferentially when kept in RPMI.
Anyway, under glucose-rich and glucose-depleted conditions, the difference between the DNA replication of unaltered HC was not significant (see figure 26). This may be due to high inositol levels and concurrent high Ca^{2+} signalling in RPMI because Ca^{2+} is an important regulator of the rate of glycogenesis and glycogenolysis in HC. Due to high Ca^{2+} signaling pathways, more Ca^{2+} is released from ER, which activates the enzyme glycogen phosphorylase and this leads to the breakdown of glycogen (glycogenolysis) [110].

In conclusion, the content of inositol in culture media seems to may have significant effects on DNA replication of HC. Inositols function via Ca^{2+} signaling and are involved in several processes in the cell, such as cell cycle progression and energy metabolism.

5.2.4. Hormone additives in WE_{old} and WE_{new} (+/-G)

In contrast to RPMI, WE_{old} and WE_{new} were applied together with a mix of hormones which contained insulin, glucagon, dexamethasone and triiodothyronine (T_3). This mix was developed in the past to preserve the differentiated state and metabolic functions of primary HC und long-term culture in serum-free conditions.

Dexamethasone and T_3 are ligands of nuclear receptors, which are transcription factors. After binding and activation by these ligands, nuclear receptors directly regulate the transcription of genes, involved in regulation of metabolism, development and proliferation [111].
Thyroid hormone triiodothyronine (T_3) is the active form of thyroxine (T_4). T_3 acts via its intracellular thyroid hormone receptor. In the liver, T_3 is involved in the regulation of lipid, cholesterol and carbohydrate metabolism. T_3 acts as a mediator of insulin sensitivity and gluconeogenesis in the liver

[112]. Mullur et al. (2014) [112] reviewed that T_3-treatment on target genes in the liver increases genes, which regulate glycogenolysis and gluconeogenesis.

Dexamethasone is a synthetic glucocorticoid, which is anti-inflammatory and immune suppressive. As an agonist of the glucocorticoid receptor, dexamethasone inhibits the effect of insulin in the liver and promotes gluconeogenesis. Kimura et al., (2011) [113] showed that dexamethasone has an inhibitory effect on EGF-induced DNA synthesis of primary HC of rats. This inhibitory effect of dexamethasone agrees with our results because EGF-induced DNA replication of HC was halved, when kept in WE than in RPMI, which does not contain any of these hormones (compare figure 23 and 25 (A)).

Insulin is involved in glucose homeostasis and acts via the insulin receptor, which results in a signaling cascade that promotes glucose storage (glycogenesis) and phosphorylation of glucose via regulation of the expression of the hepatic HK (HK4) [22], [23]. Parzefall et al., (1996) [114] showed that insulin has a stimulatory effect on DNA synthesis in cultured HC with and without growth stimulation. Insulin is able to induce Ca^{2+}-signals in the nucleus of isolated rat HC [115]. Thus, it seems to be surprising that there was no DNA replication of HC when kept in WE_{old} and WE_{new}, which contained insulin (see table 4 and 5).

The hormone glucagon antagonizes the mode of action of insulin. Glucagon is involved in the regulation of limiting glucose uptake and promotion of glycogen breakdown (glycogenolysis) [116]. Parzefall et al., (1996) [114] showed that glucagon had no significant effect on the growth behaviour of HC.

5.2.4. DNA replication of initiated HC, using different culture media

We treated male rats with the genotoxic compound N-nitrosomorpholine (NNM), to generate initiated HC. Initiated HC express selectively the placental form of glutathione-S-transferase (GSTp), which is not expressed in normal HC. Thus, GSTp is used as a marker for chemically induced preneoplastic rat liver lesions. The enzyme GSTp is involved in detoxification processes of electrophilic xenobiotics in the liver. Expression of GSTp of initiated HC shows the inherent chemoresistance of preneoplastic HC, which provides growth advantages, enabling initiated HC to survive under these stress conditions. The basal DNA replication rate of GSTp+ HC is ~4-fold higher than in GSTp- HC. Due to the treatment with tumor promoters or increased food intake, the DNA replication rate of GSTp+ HC increases further [117].
In pre-experiments it has been shown, that EGF induces an approximately 5-fold higher DNA synthesis rate in GSTp+ HC in WE_{old} (+G) than in HC, which were cultivated without EGF (compare figure 22 with 24).

These results make it obvious that EGF is a very strong stimulator of DNA synthesis and the insulin in the WE may promote the effect of EGF, which agrees with the observations of Parzefall et al., (1996) [114].

HC, which express GSTp, showed somewhat higher DNA synthesis rate in RPMI (+G) than in RPMI (-G). This may indicate that preneoplastic HC need glucose for DNA replication. These results agree with the analysis of transcriptome patterns of preneoplastic rat liver lesions, in which we showed that initiated HC preferentially use glucose via PPP, necessary for nucleotide synthesis (see figure 15).

5.3. Inhibition of glucose supply by glucose analogue - 2-deoxyglucose (2DG)

In order to understand the role of glucose for survival and growth of primary HC, we applied the glucose analogue 2DG. 2DG is phosphorylated by HK due to its high structural similarity to glucose. The phosphorylated 2DG accumulates in the cell, leading to inhibition of HK. In further consequence glucose metabolism is inhibited, which leads to ATP depletion, cell cycle arrest and cell death [81]. The liver HK (HK4) has a lower affinity for 2DG than for glucose [88].

5.3.1. ATP concentration, vitality and DNA replication of 2DG-treated, unaltered HC, cultured in media (+/-G)

Under glucose-rich, as well as glucose-depleted conditions, 2DG-treatment reduced ATP concentrations, vitality or DNA replication of unaltered HC. However, we have shown that 2DG at a lower concentration, such as 0.5 mM, did not affect the ATP concentrations (figure 20) or DNA replication (figure 24 and 26) significantly in unaltered HC under glucose-rich, as well as glucose-depleted conditions. This might be explained by the fact that HK4 (glucokinase), which is the main HK in HC, has a higher affinity for glucose than for 2DG, at least in glucose-rich media. Therefore, higher concentrations of 2DG were necessary to decrease the ATP concentration or DNA replication in unaltered HC. Treatment with 1 mM or 1.5 mM of 2DG for 48 h, as well as 72 h, lead to decreased ATP concentrations in unaltered HC, kept under glucose-rich and glucose-depleted conditions. Unaltered HC showed this dose-dependent reduction of DNA replication after treatment with 1 mM of 2DG.

5.3.2. DNA replication of 2DG-treated, initiated HC, cultured in media (+/-G)

In vivo studies of Wang et al. (2015) [82], showed that 2DG-treatment delayed hepatocarcinogenesis of N-diethylnitrosamine (DEN)-induced rat hepatocarcinoma and extended the survival time of these rats, by decreasing cell proliferation and increasing apoptosis. These findings agree with our results, in which DNA replication of initiated HC decreased with 1mM of 2DG, as well as under glucose-rich and -depleted conditions (see figure 26 (A) and (B)). The same effect was seen after EGF-stimulated DNA replication (see figure 22), indicating that 2DG at concentrations of 1 mM or higher may be a competent growth inhibitor. This is some evidence that 2DG might be able to inhibit the enzyme HK in initiated HC. Our results from the oligo array of preneoplastic rat liver lesions (see figure 11) show that preneoplastic HC already express the HK isoform HK1/HK2, which may have a higher affinity for 2DG. Thus, the other isoform of HK (HK1/HK2) might be more prone to inhibition by 2DG. Furthermore, Wang et al. (2015) [82] showed that application with 2DG of DEN-treated rats results in lower levels of glycolysis products and in further consequences diminished ATP production and other metabolic pathways, such as TCA-cycle, fatty acid biosynthesis and cholesterol biosynthesis. This blockage of important metabolic pathways might be the reason for the degression of cell proliferation and elevation of apoptosis of DEN-induced tumor tissue [82]. Further *in vitro* experiments with initiated primary HC have to be done, in which ATP concentration is measured after 2DG-treatment.

In general, there is evidence that 2DG has antitumoral effects on several types of cancer [81]. There are other reports, in which the 2DG-based therapy is more effective in combination with other antitumoral agents, such as DL-glyceraldehyde, tephrosin or AMPK agonist (such as metformin) [77], [83] or sorafenib, a multi-kinase inhibitor, used for therapy of advanced HCC [84]. Reyes et al. (2017) [84] published that 2DG in combination with sorafenib, drastically inhibits proliferation of a sorafenib-sensitive and -resistant HCC cell line (Hep3B, Huh7-R), by induction of cell cycle arrest. They showed that 2DG-treatment alone and in combination with sorafenib decreased the glucose consumption and lactate production in both HCC cell lines, which may result in ATP depletion. The reduced ATP levels activate AMPK, which results in inhibition of mTOR, a kinase, which regulates cell cycle progression [84] (For further details about the mode of action of AMPK, see chapter 1.3.3.).

In conclusion, the depletion of glucose in the media and/or blockage of HK by 2DG reduces the vitality, ATP-concentration and DNA replication of unaltered primary HC. However, depletion of glucose and inhibition of HK reduces DNA replication even more in initiated primary HC. This is the first evidence that early prestages of liver cancer require glucose for growth, which may explain the enhanced HCC risk in people suffering from obesity, metabolic syndrome and/or type 2 diabetes. Any

therapy, which lowers blood glucose levels, may be a promising preventive approach to diminish the enhanced HCC risk of these patients.

6. Abstract

Hepatocellular carcinoma (HCC) is one of the most common cancer entities worldwide. Hepatitis virus infections and excessive ethanol consumption are well-established risk factors for this disease. Furthermore, metabolic syndrome and/or diabetes mellitus type 2 are predisposing for the development of HCC. In the present work, the question was addressed, whether elevated serum glucose levels are involved causally in the pathogenesis of this malignancy. For this purpose, an experimental model of rat hepatocarcinogenesis was used and the impact of glucose on the growth of early liver tumor prestages was studied.

First, transcriptome patterns of preneoplastic liver lesions were analyzed by oligo arrays, using micro dissected material from rats which had been treated with a single dose of the genotoxic hepatocarcinogen N-nitrosomorpholine and the tumor promoter phenobarbital for 17 months. It was shown that the enzyme hexokinase-1, which catalyzes the formation of glucose to glucose-6-phosphate, was upregulated in preneoplastic rat liver lesions. Furthermore, the expression of key-enzymes of the pentose phosphate pathway and glycogenesis were elevated considerably, while enzymes for gluconeogenesis were downregulated. These data indicate that preneoplastic hepatocytes utilize glucose preferentially for glycogenesis and the pentose phosphate pathway to generate components for nucleotide synthesis and DNA replication.

For functional studies, rats were treated with a single dose of NNM. Three weeks later unaltered or initiated hepatocytes were isolated for culture. Initiated hepatocytes were identified by glutathione-S-transferase (GSTp) immunostaining. The effect of glucose in the medium and the inhibition of HK by 2-deoxyglucose (2DG) on (i) ATP-concentration and vitality of unaltered primary hepatocytes and (ii) on DNA synthesis of unaltered and preneoplastic primary hepatocytes was studied.

Glucose depleted media and the inhibition of HK resulted in decreased ATP concentrations and diminished vitality of unaltered primary hepatocytes. As a consequence, unaltered and initiated hepatocytes showed decreased DNA synthesis.

To conclude, early prestages of liver cancer show already deregulations in the glucose metabolism. The deprivation of glucose and/or blockage of HK by 2DG results in reduced vitality and ATP-concentration of unaltered primary HC and decreased DNA synthesis of unaltered as well as preneoplastic hepatocytes. This indicates that early cancer prestages require glucose for preferential growth. Similar mechanisms might be involved in the enhanced HCC risk for people suffering from obesity, metabolic syndrome and/or type 2 diabetes mellitus.

7. Zusammenfassung

Das hepatozelluläre Karzinom ist eine der häufigsten Krebserkrankungen weltweit. Neben Infektionen mit Hepatitis-Viren und exzessiven Alkoholkonsum sind Stoffwechselerkrankungen mit erhöhtem Blutzuckerspiegel, wie das metabolische Syndrom und/oder Diabetes mellitus Typ-2, wichtige Risikofaktoren für diese Krankheit. In der vorliegenden Arbeit wurde untersucht, ob erhöhte Glukosekonzentrationen im Serum kausal an der Entstehung von Leberkrebs beteiligt sind. In einem Nagetiermodell wurde der Effekt von Glukose auf das Wachstum von frühen Lebertumor-Vorstadien untersucht.

Im ersten Schritt wurden Transkriptommuster präneoplastischer Leberläsionen untersucht, die aus mikrodissketierten Gewebeproben und nachfolgender Oligo-Array Analyse gewonnen worden waren. Die Gewebeproben stammten von Ratten, die einmalig mit dem gentoxischen Hepatokarzinogen N-Nitrosomorpholin (NNM) und über 17 Monate mit dem Lebertumor-Promoter Phenobarbital behandelt worden waren. Es zeigte sich, dass die Expression von Hexokinase 1 (HK1), einem Enzym, das Glukose zu Glukose-6-Phosphat umwandelt, in präneoplastischen Leberläsionen im Vergleich zu unverändertem Lebergewebe deutlich erhöht war. Auch die Expression von Enzymen, die im Pentose-Phosphatweg und der Glykogenspeicherung eine Schlüsselrolle spielen, waren in präneoplastischen Leberläsionen der Ratte verstärkt, während Enzyme, die an der Glukoneogenese beteiligt sind, verminderte Expression zeigten. Die Analyse der Daten weist darauf hin, dass präneoplastische Hepatozyten Glukose vermehrt für die Glykogenese und den Pentose-Phosphatweg verwenden.

Für funktionelle Studien, wurden Ratten einmalig mit NNM behandelt. Drei Wochen später wurden unveränderte und initiierte Hepatozyten isoliert und kultiviert. Iniitiierte Heptozyten wurden mittels Glutathion-S-transferase (GSTp)-Immunfärbung identifiziert. Dann wurde der Effekt von Glukose im Zellkulturmedium und Inhibierung der HK durch 2-Deoxyglukose (2DG) auf (i) ATP-Konzentration und Vitalität von unveränderten primären Hepatozyten und (ii) auf die DNS Synthese von unveränderten und initiierten primären Hepatozyten untersucht.

Glukose-freie Medien und die Inhibierung von HK, führte zum Abfall der ATP-Konzentration und zu verringerter Vitalität in unveränderten primären Hepatozyten. Als Konsequenz, zeigten unveränderte und initiierte Hepatozyten eine verminderte DNS-Synthese.

Zusammenfassend lässt sich sagen, dass Frühstadien von Leberkrebs bereits erste Anzeichen eines deregulierten Glukosestoffwechsels zeigen. Der Entzug von Glukose und/oder die Blockierung der HK durch 2DG, bewirkte verminderte Vitalität und ATP-Konzentration in unveränderten primären Hepatozyten, und eine Reduktion der DNA-Synthese sowohl in unveränderten als auch in initiierten

Hepatozyten. Dies weist darauf hin, das bereits sehr frühe Tumorvorstadien für ihr Wachstum vermehrt Glukose benötigen. Ähnliche Mechanismen könnten auch an dem erhöhten Leberkrebsrisiko bei metabolischem Syndrom und/oder Diabetes mellitus Typ 2 beteiligt sein.

8. References

[1] R. Z. Sherif, M. D. Abdel-Misih, and M. Bloomston, “Liver Anatomy,” vol. 90, no. 4, pp. 643–653, 2010.

[2] L. Rui, “Energy Metabolism in the Liver,” *Compr Physiol*, vol. 4, no. 1, pp. 177–197, 2014.

[3] D. E. Malarkey, K. Johnson, L. Ryan, G. Boorman, and R. R. Maronpot, “New Insights into Functional Aspects of Liver Morphology,” *Toxicol. Pathol.*, vol. 33, no. 1, pp. 27–34, 2005.

[4] P. Sun, X. Zhou, S. L. Farnworth, A. H. Patel, and D. C. Hay, “Modeling human liver biology using stem cell-derived hepatocytes,” *Int. J. Mol. Sci.*, vol. 14, no. 11, pp. 22011–22021, 2013.

[5] R. Malik, S. Clare, and H. Hodgon, “The role of non-parenchymal cells in liver growth.,” *Elsevier*, vol. 13, no. 6, pp. 424–431, 2002.

[6] Z. Kmiec, “Cooperation of liver cells in health and disease,” *Adv.Anat.Embryol.Cell Biol.*, vol. 161, no. 0301–5556 (Print), p. III-151, 2001.

[7] E. N. Marieb and K. Hoehn, *Human Anatomy & Physiology*. 2013.

[8] L. J. Dixon, M. Barnes, H. Tang, M. T. Pritchard, E. Laura, and C. Clinic, “Kupffer cells in the liver,” *Compr Physiol*, vol. 3, no. 2, pp. 785–797, 2016.

[9] F. Böhm, U. A. Köhler, T. Speicher, and S. Werner, “Regulation of liver regeneration by growth factors and cytokines,” *EMBO Mol. Med.*, pp. 294–305, 2010.

[10] G. K. Michalopoulos, “Liver Regeneration,” *J Cell Physiol.*, vol. 213, no. 2, pp. 286–300, 2007.

[11] W. Bursch, B. Lauer, G. Barthej, and J. Schuppler, “Controlled death (apoptosis) of normal and putative preneoplastic cells in rat liver following withdrawal of tumor promoters,” vol. 5, no. 4, pp. 453–458, 1984.

[12] V. Hoffmann and R. Schulte-Hermann, “The Regulative Role of Food Consumption in the Induction of Rat Liver Cell Proliferation by Drugs and Environmental Pollutants,” *Arch. Toxicol.*, vol. 461, pp. 457–458, 1979.

[13] Z. Fu, E. R. Gilbert, and D. Liu, “Regulation of Insulin Synthesis and Secretion and Pancreatic Beta-Cell Dysfunction in Diabetes,” *Curr. Diabetes Rev.*, vol. 9, no. 1, pp. 25–53, 2013.

[14] M. Z. Shrayyef and J. E. Gerich, “Normal Glucose Homeostasis,” in *Principles of Diabetes Mellitus*, 2010, p. 852p.

[15] Nelson and Cox, *Principles of Biochemistry*, vol. 17, no. 8. 2011.

[16] M. Mueckler and B. Thorens, “The SLC2 (GLUT) Family of Membrane Transporters,” *Mol Asp. Med.*, vol. 34, no. 0, pp. 121–138, 2013.

[17] S. Karim, D. H. Adams, P. F. Lalor, S. Karim, D. H. Adams, and P. F. Lalor, “Hepatic expression and cellular distribution of the glucose transporter family,” *World J. Gastroenteroogy*, vol. 18, no. 46, pp. 6771–6781, 2012.

[18] A. J. Cura and A. Carruthers, “The role of Monosaccharide Transport Proteins in carbohydrate assimilation, distribution, metabolism and homeostasis,” *Compr. Physiol.*, vol. 2, no. 2, pp. 863–914, 2013.

[19] M. Hosokawa and B. Thorens, “Glucose release from GLUT2-null hepatocytes : characterization of a major and a minor pathway,” *Am J Physiol Endocrinol Metab*, pp. 794–801, 2002.

[20] R. Augustin, “The Protein Family of Glucose Transport Facilitators : It ’ s Not Only About Glucose After All,” *IUBMB Life*, vol. 62, no. May, pp. 315–333, 2010.

[21] P. Iozzo, F. Geisler, V. Oikonen, M. Ma, and T. Takala, “Insulin Stimulates Liver Glucose Uptake

in Humans: an 18F-FDG PET Study," *J. Nucl. Med.*, vol. 44, no. 5, pp. 682–690, 2003.

[22] C. Gregori, I. Guillet-Deniau, J. Girard, J.-F. Decaux, and A.-L. Pichard, "Insulin regulation of glucokinase gene expression: Evidence against a role for sterol regulatory element binding protein 1 in primary hepatocytes," *FEBS Lett.*, vol. 580, no. 2, pp. 410–414, 2006.

[23] G. K. Ganjam, "Regulation of rat Liver Glucokinase Gene Expression by Sterol Regulatory Element Binding Protein-1a and Forkhead box ClassO1 Transcription factors," 2007.

[24] Z. Cheng, Y. Tseng, and M. F. White, "Insulin signaling meets mitochondria in metabolism," *Trends endocrinol Metab.*, vol. 21, no. 10, pp. 589–598, 2010.

[25] Z. Laron, "Insulin-like growth factor 1 (IGF-1): a growth hormone," *J Clin Pathol.*, vol. 1, pp. 311–316, 2001.

[26] R. C. Baxter, "IGF binding proteins in cancer : mechanistic and clinical insights," *Nat. Publ. Gr.*, vol. 14, no. 5, pp. 329–341, 2014.

[27] M. Pollak, "The insulin and insulin-like growth factor receptor family in neoplasia: an update," *Nat. Publ. Gr.*, vol. 12, no. 3, pp. 159–169, 2012.

[28] D. H. Cohen and D. Leroith, "Obesity , type 2 diabetes , and cancer : the insulin and IGF connection," *Endocr. Relat. Cancer*, vol. 19, pp. 27–45, 2012.

[29] S. Djiogue *et al.*, "Insulin resistance and cancer : the role of insulin and IGFs," *Endocrinology*, pp. 1–17, 2013.

[30] J. M. Lizcano and D. R. Alessi, "The insulin signalling pathway," *Curr. Biol.*, pp. 236–238, 2002.

[31] A. Roux, A. Loranger, and N. Marceau, "Impact of keratin intermediate filaments on insulin-mediated glucose metabolism regulation in the liver and disease association," *FASEB J.*, vol. 30, no. 2, pp. 491–502, 2017.

[32] W. Shao and P. J. Espenshade, "Expanding roles for SREBP in metabolism," *Cell Metab.*, vol. 16, no. 4, pp. 414–419, 2012.

[33] R. H. Wong and H. S. Sul, "Insulin signaling in fatty acid and fat synthesis: a transcriptional perspective," *Curr Opin Pharmacol.*, vol. 10, no. 6, pp. 684–691, 2010.

[34] S. Guo, "Insulin signaling, resistance, and metabolic syndrome: insights from mouse models to disease mechanisms," *J Endocrinol.*, vol. 220, no. 2, pp. 1–36, 2014.

[35] K. Siddle, "Signalling by insulin and IGF receptors : supporting acts and new players," *J. Mol. Endokrinol.*, vol. 47, pp. 1–10, 2011.

[36] W. Zhang and H. T. Liu, "MAPK signal pathways in the regulation of cell proliferation in mammalian cells," *Cell Res.*, vol. 12, pp. 9–18, 2002.

[37] D. B. Shackelford and R. J. Shaw, "The LKB1 – AMPK pathway : metabolism and growth control in tumour suppression," *Nat. Rev. Cancer*, vol. 9, no. AuguST, pp. 563–575, 2009.

[38] D. G. Hardie and D. R. Alessi, "LKB1 and AMPK and the cancer-metabolism link – ten years after," *BMC Biol.*, pp. 1–11, 2013.

[39] D. Carling, "The AMP-activated protein kinase cascade – a unifying system for energy control," *Trends Biochem. Sci.*, vol. 29, no. 1, pp. 18–24, 2004.

[40] I. Kim and Y. He, "Targeting the AMP-activated protein kinase for cancer prevention and therapy," *Front. Oncol.*, vol. 3, no. July, pp. 1–12, 2013.

[41] D. M. Gwinn *et al.*, "AMPK Phosphorylation of Raptor Mediates a Metabolic Checkpoint," *Cell Press*, pp. 214–226, 2008.

[42] X. Wang and C. G. Proud, "mTORC2 is a tyrosine kinase," *Nat. Publ. Gr.*, vol. 26, no. 1, pp. 1–2, 2015.

[43] K. Inoki, T. Zhu, K. Guan, and A. Arbor, “TSC2 Mediates Cellular Energy Response to Control Cell Growth and Survival,” *Cell Press*, vol. 115, pp. 577–590, 2003.

[44] D. G. Hardie, S. A. Hawley, and J. W. Scott, “AMP-activated protein kinase – development of the energy sensor concept,” *J Physiol.*, vol. 1, pp. 7–15, 2006.

[45] V. D. Longo and M. P. Mattson, “Fasting : Molecular Mechanisms and Clinical Applications,” *Cell Metab.*, vol. 19, no. 2, pp. 181–192, 2013.

[46] K. Uchida, S. Kajimura, L. G. Riley, T. Hirano, K. Aida, and E. G. Grau, “Effects of fasting on growth hormone/insulin-like growth factor I axis in the tilapia, Oreochromis mossambicus,” *Elsevier*, vol. 134, pp. 429–439, 2003.

[47] B. Martin, M. P. Mattson, and S. Maudsley, “Caloric restriction and intermittent fasting : Two potential diets for successful brain aging,” vol. 5, pp. 332–353, 2006.

[48] D. Hyun, K. Min, H. Park, E. Kyeong, L. Yeon, and J. Choi, “The roles of FoxOs in modulation of aging by calorie restriction,” *Biogerontology*, pp. 1–14, 2015.

[49] B. Sung, S. Park, B. P. Yu, and H. Y. Chung, “Modulation of PPAR in Aging , Inflammation , and Calorie Restriction,” *J. Gerontol.*, vol. 59, no. 10, pp. 997–1006, 2004.

[50] M. Zhu, R. De Cabo, M. A. Lane, and D. K. Ingram, “Caloric Restriction modulates early events in insulin signalin in liver and skeletal muscle of rat,” *New York Acad. Sci.*, vol. 1, pp. 448–452, 2004.

[51] A. Prokesch *et al.*, “Liver p53 is stabilized upon starvation and required for amino acid catabolism and gluconeogenesis,” *FASEB J.*, no. 13, 2016.

[52] W. Borena *et al.*, “Metabolic risk factors and primary liver cancer in a prospective study of 578,700 adults,” *Int. J. Cancer*, vol. 131, no. 1, pp. 193–200, 2012.

[53] International Agency for Research on Cancer, “GLOBOCAN 2012: Estimated Cancer Incidence, Mortality and Prevalence Worldwide in 2012,” *Iarc*, 2012. [Online]. Available: http://globocan.iarc.fr/Pages/fact_sheets_cancer.aspx.

[54] Cancer Treatment Centers of America, “Types of Liver Cancer.” [Online]. Available: http://www.cancercenter.com/liver-cancer/types/.

[55] J. Ferlay, H. R. Shin, F. Bray, D. Forman, C. Mathers, and D. M. Parkin, “Estimates of worldwide burden of cancer in 2008: GLOBOCAN 2008,” *Int. J. Cancer*, vol. 127, no. 12, pp. 2893–2917, 2010.

[56] P. U. Devi, “BASICS OF CARCINOGENESIS,” *Heal. Adm.*, vol. 17, no. 1, pp. 16–24, 2005.

[57] M. Greaves and C. C. Maley, “Clonal evolution in cancer,” 2012.

[58] I. A. Siddiqui, V. Sanna, N. Ahmad, M. Sechi, and H. Mukhtar, “Resveratrol nanoformulation for cancer prevention and therapy,” *Ann. N. Y. Acad. Sci.*, pp. 1–12, 2015.

[59] S. L. Teoh and S. Das, “Tumour biology of obesity-related cancers : understanding the molecular concept for better diagnosis and treatment,” *Tumor Biol.*, pp. 14363–14380, 2016.

[60] G. Testino, S. Leone, P. Borro, “Alcohol and hepatocellular carcinoma : A review and a point of view,” *World J. Gastroenteroogy*, vol. 20, no. 43, pp. 15943–15954, 2014.

[61] E. Elamin *et al.*, “Effects of Ethanol and Acetaldehyde on Tight Junction Integrity : In Vitro Study in a Three Dimensional Intestinal Epithelial Cell Culture Model,” *PLoS One*, vol. 7, no. 4, 2012.

[62] M. C. Kew, “Aflatoxins as a cause of hepatocellular carcinoma,” *J. Gastrointest. Liver Dis.*, vol. 22, no. 3, pp. 305–310, 2013.

[63] J. F. Reichard and A. Puga, “Effects of arsenic exposure on DNA methylation and epigenetic

gene regulation," *Epigenomic*, vol. 2, no. 1, pp. 87–104, 2010.

[64] Y. Chen and H. Ahsan, "Cancer Burden From Arsenic in Drinking Water in Bangladesh," *Am. J. Public Health*, vol. 94, no. 5, pp. 13–15, 2004.

[65] A. B. Olokoba, O. A. Obateru, and L. B. Olokoba, "Type 2 Diabetes Mellitus: A Review of Current Trends," *Oman Med. J.*, vol. 27, no. 4, pp. 269–273, 2012.

[66] R. J. Klement and U. Kämmerer, "Is there a role for carbohydrate restriction in the treatment and prevention of cancer ?," *Nutr. Metab. (Lond).*, vol. 8, no. 1, p. 75, 2011.

[67] H. B. Bhatt and R. J. Smith, "Fatty liver disease in diabetes mellitus," *HepatpBiliary Surg. Nutr.*, vol. 4, no. 2, pp. 101–108, 2015.

[68] C. P. Day, "Pathogenesis of steatohepatitis," *Best Pract. Res. Clin. Gastroenterol.*, vol. 16, no. 5, pp. 663–678, 2002.

[69] J. K. Dowman, J. W. Tomlinson, and P. N. Newsome, "Pathogenesis of non-alcoholic fatty liver disease," *QJM*, no. November 2009, pp. 71–83, 2010.

[70] M. A. Ibrahim, M. Kelleni, and A. Geddawy, "Nonalcoholic fatty liver disease : Current and potential therapies," *Life Sci.*, vol. 92, no. 2, pp. 114–118, 2013.

[71] F. Nassir, R. S. Rector, G. M. Hammoud, and J. A. Ibdah, "Pathogenesis and Prevention of Hepatic Steatosis," *Gastroenterol. Hepatol. (N. Y).*, vol. 11, no. 3, pp. 167–175, 2015.

[72] A. Pellicoro, P. Ramachandran, J. P. Iredale, and J. A. Fallowfield, "Liver fibrosis and repair: immune regulation of wound healing in a solid organ," *Nat. Publ. Gr.*, vol. 14, no. 3, pp. 181–194, 2014.

[73] R. Bataller and D. A. Brenner, "Liver fibrosis," *Sci. Med.*, vol. 115, no. 2, 2005.

[74] H. L. Reeves and S. L. Friedman, "ACTIVATION OF HEPATIC STELLATE CELLS – A KEY ISSUE IN LIVER FIBROSIS," pp. 808–826, 2002.

[75] V. Hernandez-Gea and S. L. Friedman, "Pathogenesis of Liver Fibrosis," *Annu. Rev. Pathol. Mech. Dis.*, 2011.

[76] S. S. Thorgeirsson and J. W. Grisham, "Molecular pathogenesis of human hepatocellular carcinoma.," *Nat. Genet.*, vol. 31, no. august, pp. 339–346, 2002.

[77] J.-H. Cheong *et al.*, "Dual inhibition of tumor energy pathway by 2-deoxyglucose and metformin is effective against a broad spectrum of preclinical cancer models.," *Mol. Cancer Ther.*, vol. 10, no. 12, pp. 2350–62, 2011.

[78] D. Hanahan and R. A. Weinberg, "Hallmarks of cancer: The next generation," *Cell*, vol. 144, no. 5, pp. 646–674, 2011.

[79] I. Ben Sahra *et al.*, "Targeting Cancer Cell Metabolism : The Combination of Metformin and 2-Deoxyglucose Induces p53-Dependent Apoptosis in Prostate Cancer Cells," no. 15, pp. 2465–2476, 2010.

[80] H. Pelicano, D. S. Martin, R. Xu, and P. Huang, "Glycolysis inhibition for anticancer treatment," pp. 4633–4646, 2006.

[81] C. Granchi and F. Minutolo, "Anti-cancer agents counteracting tumor glycolysis," *ChemMedChem*, vol. 7, no. 8, pp. 1318–1350, 2012.

[82] Z. Wang, L. Zhang, D. Zhang, R. Sun, Q. Wang, and X. Liu, "Glycolysis inhibitor 2-deoxy-D-glucose suppresses carcinogen-induced rat hepatocarcinogenesis by restricting cancer cell metabolism," *Mol. Med. Rep.*, vol. 11, no. 3, pp. 1917–1924, 2015.

[83] Y. Choi and J. H. Lee, "The combination of tephrosin with 2-deoxy-D-glucose enhances the cytotoxicity via accelerating ATP depletion and blunting autophagy in human cancer cells,"

Cancer Biol. Ther., vol. 12, no. 11, pp. 989–996, 2011.

[84] R. Reyes, N. A. Wani, K. Ghoshal, S. T. Jacob, and T. Motiwala, "Sorafenib and 2-deoxyglucose synergistically inhibit proliferation of both sorafenib-sensitive and -resistant HCC cells by inhibiting ATP production," *Gene Expr.*, vol. 17, no. 2, pp. 129–140, 2017.

[85] D. Zhang *et al.*, "2-Deoxyglucose Reverses the Promoting Effect of Insulin on Colorectal Cancer Cells In Vitro," *PLoS ONE [Electronic Resour.*, vol. 11, no. 3, p. e0151115, 2016.

[86] T. Riegler *et al.*, "Mesenchyme-derived growth factors appear critical for promotion of preneoplastic cells by non-genotoxic hepatocarcinogens," 2015.

[87] A. Löw-Baselli, K. Hufnagl, W. Parzefall, R. Schulte-Hermann, and B. Grasl-Kraupp, "Initiated rat hepatocytes in primary culture : a novel tool to study alterations in growth control during the first stage of carcinogenesis," *Carcinogenesis*, vol. 21, no. 1, pp. 79–86, 2000.

[88] L. Agius and M. Stubbs, "Investigation of the mechanism by which glucose analogues cause translocation of glucokinase in hepatocytes: evidence for two glucose binding sites.," *Biochem. J.*, vol. 346 Pt 2, pp. 413–21, 2000.

[89] H. Han, G. Kang, J. S. Kim, B. H. Choi, and S. Koo, "Regulation of glucose metabolism from a liver-centric perspective," *Exp. Mol. Med.*, vol. 48, no. 3, pp. e218-10, 2016.

[90] N. Hay, "Reprogramming glucose metabolism in cancer: can it be exploited for cancer therapy?," *Nat. Rev. Cancer*, vol. 16, no. 10, pp. 1–15, 2016.

[91] B. Y. O. Warburg, F. Wind, and E. Negelein, "The metabolism of tumors in the body," *J. Gen. Physiol.*, 1926.

[92] T. Hitosugi *et al.*, "Phosphoglycerate mutase 1 coordinates glycolysis and biosynthesis to promote tumor growth," *Cancer Cell*, vol. 22, no. 5, pp. 585–600, 2012.

[93] K. C. Patra and N. Hay, "The pentose phosphate pathway and cancer," *Trends Biochem. Sci.*, vol. 39, no. 8, pp. 347–354, 2014.

[94] Y. Wang *et al.*, "Identification of four isoforms of aldolase B down-regulated in hepatocellular carcinoma tissues by means of two-dimensional western blotting," *In Vivo (Brooklyn).*, vol. 25, no. 6, pp. 881–886, 2011.

[95] A. Herling, M. König, S. Bulik, and H. Holzhütter, "Enzymatic features of the glucose metabolism in tumor cells," *FEBS J.*, vol. 278, pp. 2436–2459, 2011.

[96] G. Kroemer and J. Pouyssegur, "Tumor Cell Metabolism: Cancer's Achilles' Heel," *Cancer Cell*, vol. 13, no. 6, pp. 472–482, 2008.

[97] R. B. Hamanaka and N. S. Chandel, "Targeting glucose metabolism for cancer therapy," *J. Exp. Med.*, vol. 209, no. 2, pp. 211–215, 2012.

[98] P. Bannasch, F. Klimek, and D. Mayer, "Early Bioenergetic Changes in Hepatocarcinogenesis : Preneoplastic Phenotypes Mimic Responses to Insulin and Thyroid Hormone," vol. 29, no. 4, pp. 303–313, 1997.

[99] R. K. Reyes, T. Motiwala, and J. S. T., "Regulation of Glucose Metabolism in Hepatocarcinogenesis by MicroRNAs," *Gene Expr.*, vol. 16, no. 2, pp. 85–92, 2014.

[100] W. M. Frederiks, P. Vizan, K. S. Bosch, H. Vreeling-sindela, J. Boren, and M. Cascante, "Elevated activity of the oxidative and non-oxidative pentose phosphate pathway in (pre) neoplastic lesions in rat liver," pp. 232–240, 2008.

[101] C. Yang *et al.*, "Glutamine oxidation maintains the TCA cycle and cell survival during impaired mitochondrial pyruvate transport," *Mol. Cell.*, vol. 56, no. 3, pp. 414–424, 2014.

[102] I. Martínez-Reyes *et al.*, "TCA cycle and mitochondrial membrane potential are necessary for

diverse biological functions," *Mol Cell*, vol. 61, no. 2, pp. 199–209, 2016.

[103] D. R. Conrad, "cystein in cell culture.pdf." [Online]. Available: http://www.sigmaaldrich.com/life-science/cell-culture/learning-center/media-expert/cysteine.html.

[104] A. Salazar, M. Keusgen, and J. Von Hagen, "Amino acids in the cultivation of mammalian cells," *Amino Acids*, vol. 48, no. 5, pp. 1161–1171, 2016.

[105] X. Lin, H. Yang, H. Zhang, L. C. Zhou, and Z. M. Guo, "A novel transcription mechanism activated by ethanol: Induction of Slc7a11 gene expression via inhibition of the DNA-binding activity of transcriptional repressor octamer-binding transcription factor 1 (OCT-1)," *J. Biol. Chem.*, vol. 288, no. 21, pp. 14815–14823, 2013.

[106] M. Yang and K. H. Vousden, "Serine and one-carbon metabolism in cancer," *Nat. Publ. Gr.*, 2016.

[107] G. Wu *et al.*, "Proline and hydroxyproline metabolism: implications for animal and human nutrition," *Amino Acids*, vol. 40, no. 4, pp. 1053–1063, 2011.

[108] P. S. Guzelian, G. Qureshi, and R. Diegelmann, "Collagen synthesis by the hepatocyte: studies in primary cultures of parenchymal cells from adult rat liver," *Coll. Relat. Res.*, vol. 1, no. 1, pp. 83–93, 1980.

[109] L. Mahmood, "The metabolic processes of folic acid and Vitamin B12 deficiency," *J. Heal. Res. Rev.*, vol. 1, no. 1, p. 5, 2014.

[110] M. Amaya and M. Nathanson, "Calcium Signaling in the Liver," *Compr. Physiol.*, vol. 3, no. 1, pp. 515–539, 2013.

[111] J. M. Olefsky, "Nuclear Receptor Minireview Series," *J. Biol. Chem.*, vol. 276, no. 40, pp. 36863–36864, 2001.

[112] R. Mullur, Y. Liu, and G. A. Brent, "Thyroid hormone regulation of metabolism," *Physiol. Rev.*, no. 27, pp. 355–382, 2014.

[113] M. Kimura, H. Moteki, and M. Ogihara, "Inhibitory Effects of Dexamethasone on Epidermal Growth Factor- Induced DNA Synthesis and Proliferation in Primary Cultures of Adult Rat Hepatocytes," *Biol. Pharm. Bull.*, vol. 34, no. 5, pp. 682–687, 2011.

[114] W. Parzefall, E. Erber, E. Kainzbauer, "Effects of Insulin , Glucagon and Triiodothyronine on DNA Synthesis in Rat Hepatocyte Primary Cultures Induced by Liver Tumour Promoters and EGF," *Toxicol. Vitr.*, vol. 10, pp. 183–193, 1996.

[115] M. A. Rodrigues, D. A. Gomes, V. A. Andrade, M. F. Leite, and M. H. Nathanson, "Insulin Induces Calcium Signals in the Nucleus of Rat Hepatocytes," *Hepatology*, vol. 48, no. 5, pp. 1621–1631, 2008.

[116] C. J. Ramnanan, D. S. Edgerton, G. Kraft, and A. D. Cherrington, "Physiologic action of glucagon on liver glucose metabolism," *Diabetes Obes. Metab.*, vol. 13, no. Suppl 1, pp. 118–125, 2011.

[117] B. Grasl-Kraupp, W. Bursch, B. Ruttkay-Nedecky, A. Wagner, B. Lauer, and R. Schulte-Hermann, "Food restriction eliminates preneoplastic cells through apoptosis and antagonizes carcinogenesis in rat liver," *Proc. Natl. Acad. Sci. U. S. A.*, vol. 91, no. October, pp. 9995–9999, 1994.

9. Appendices

9.1. List of abbreviations

+/- G	with/without glucose
2DG	2-deoxyglucose
2DGP	2-deoxyglucose-phosphate
2PG	2-phosphoglycerate
^{3}H-thymidine	Tritium thymidine
3PG	3-phosphoglycerate
4EBP1	eIF4E binding protein 1
ACC1/2	Acetyl-CoA-carboxylase 1/2
ADH	Alcohol dehydrogenase
Akt	Proteinkinase B
ALDH	Aldehyde dehydrogenase
ALDO A/B	Aldolase A/B
AMPK	AMP-activated protein kinase
AP-1	Activator protein-1
APC	Antigen presenting cell
APS	SH2B adaptor protein 2
ATP	Adenosine triphosphate
BCIP	5-bromo-4-chloro-3-indolyl phosphate
BSA	Bovine serum albumin
Ca^{2+}	Calcium ion
CAMKKβ	Calmodulin-dependent kinase kinase β
Cbl	Casitas B-lineage lymphoma
Chk1	checkpoint kinase 1
CO	Control group
DAG	Diacylglycerol
DEPC	Diethylprocarbonate
DHAP	Dihydroxyacetone phosphate
DNA	Desoxyribonucleic adic
Dock1	Dedicator of cytokinesis protein 1

EC	Endothelial cell
ECM	Extracellular matrix
EGF	Epidermal growth factor
eIF2B	eukaryotic initiation factor 2
ENO1	Enolase 1
ER	Endoplasmatic reticulum
F1,6BP	Fructose-1, 6-bispohosphate
FBP1	Fructose-1, 6-bisphosphatase 1
FCS	Fetal calf serum
FOXO	Forkhead box O
G3P	Glyceraldehyd-3-phosphate
G6P	Glucose-6-phosphate
G6PC	Glucose-6-phosphatase
G6PD	Glucose-6-phosphate dehydrogenase
Gab1	Grb-2 associated protein 1
GAP	GTPase activating protein
GAPD	Glyceraldehyd-3-phosphate dehydrogenase
GBE1	Glucan-(1, 4-α) branching enzyme 1
GH	Growth hormone
GLUT	Glucose transporter
GPCR	G-protein coupled receptor
GPI	Glucose-6-phosphate isomerase
Grb2	Growth factor receptor-bound protein 2
GS	Glycogen synthase
GSK3	Glycogen synthase kinase 3
GSTp	Glutathione-S-transferase placental
GYG1	Glycogenin 1
H_2-mix	Hormone mix
Hb-EGF	heparin-binding EGF-like growth factor
HBSS	Hank´s balanced salt solution
HC	Hepatocyte
HCC	Hepatocellular carcinoma
HEPES	4-(2-hydroxyethyl)-1-piperazineethanesulfonic acid

HGF	Hepatocyte growth factor
HIF1α	Hypoxia-inducible factor 1α
HK	Hexokinase
HMGCR	2-hydroxy-3-methylglutaryl-CoA-reduktase
Hoechst 33258	Bisbenzimid
IGF1/2	Insulin-like growth factor 1/2
IGF1/2R	Insulin-like growth factor 1/2 receptor
IGFBP	Insulin-like growth factor -binding proteins
IL-6	Interleukin-6
IP_3	Inositol (1,4,5) triphosphate
IP_3R	IP_3 receptor
IR-A /-B	Insulin receptor A / B
IRS1/2	Insulin receptor substrate 1/2
KC	Kupffer cell
LDH B	Lactat dehydrogenase B
LI	Labelling index
LKB1	Liver kinase 1
LXR-α	liver X receptor- α
MAPK	Mitogen activated protein kinase
MEK1/2	Mitogen-activated protein kinase kinase 1/2
MEM	Minimum essential medium
mTOR	Mammalian target of rapamycin
mTORC1/2	mTOR complex 1/2
MTT	3-(4, 5-dimethylthiazol-2yl)-2, 5-diphenyltetrazolium bromide
Myc	Avian myelocytomatosis viral oncogene homolog
n.d.	not determined
NAFL	Non-alcoholic fatty liver
NAFLD	Non-alcoholic fatty liver disease
NASH	Non-alcoholic steatohepatitis
NBT	Nitroblue tetrazolium chloride
NNM	N-nitrosomorpholine
NO	Nitric oxide
NPC	Non-parenchymal cells

OAA	Oxalacetate
p70S6K	p70 ribosomal S6 kinase
PB	Phenobarbital
PBS	Phosphate buffered saline
PCK1	Phosphoenolpyruvate carboxykinase 1
PDK1	Phosphoinositide-dependent kinase 1
PDK3	Pyruvate dehydrogenase kinase 3
PFKL	Phosphofructokinase
PGAM 1	Phosphoglycerate mutase 1
PGD	Phosphoglyconate dehydrogenase
PGK1	Phosphoglycerat kinase 1
PGLS	6-phosphate gluconolactonase
PGM 1-5	Phosphoglucomutase 1-5
PI3K	Phosphoinositide 3-kinase
PIP_2	Phosphatidylinositol (4, 5) bisphosphate
PIP_3	Phosphatidylinositol (3, 4, 5) bisphosphate
PKLR	Pyruvate kinase (liver and RBC)
PKM2	Pyruvate kinase M2
PLC	Phospholipase C
PNL	Preneoplastic lesions
PPAR	Proliferator-activator receptors
PPP	Pentose phosphate pathway
PTP-1B	Protein tyrosine phosphatase 1B
R5P	Ribose-5-phosphate
Raf	Rapidly accelerated fibrosarcoma
Ras	Rat sarcoma G-protein
Rheb	Ras homolog enriched in brain
RNA	Ribonucleic acid
ROS	Reactive oxygen species
RPIA	Ribose-5-phosphate isomerase A
rpm	Rounds per minute
RPMI 1640	RPMI 1640 culture medium

R-point	Restriction point
RTK	Receptor tyrosine kinase
RXR	Retinoid X receptor
SC	Stellate cell
SEM	Standard error of the mean
SHC	Src homology 2 domain containing
SIP-solution	Standard isotonic percoll solution
SIRT1	Sirtuin 1
SLC2	solute carrier 2
SOS	Son of sevenless
SPF	Specific pathogen free
SREBP-1c	Sterol regulatory element-binding protein-1c
T2DM	Type 2 diabetes mellitus
T_3	Triiodthyronine
TALDO 1	Transaldolase 1
TCA	Tricarboxylic acid cycle
TGF-α	Transforming growth factor- α
TGF-β_1	Transforming growth factor-β_1
THF	Tetrahydrofolate
TKT	Transketolase
TNF-α	Tumor necrosis factor-α
TSC2	Tuberous sclerosis complex 2
UDP-glucose	Uridin diphosphate-glucose
UGP2	UTP glucose-1-phosphate uridylyltransferase 2
WE	Williams´ E medium
α-HCH	α-hexachlorocyclohexane

9.2. List of figures

Figure 1: Scheme of the structure of sinusoids in the liver lobule and the portal triad

Figure 2: The four major fates of glucose

Figure 3: The insulin and IGF receptor family.

Figure 4: Insulin and IGF signalling and downstream pathways and their role in cancer

Figure 5: Mode of action and regulation of AMPK

Figure 6: Estimated age-standardized incidence and mortality rates for liver cancer

Figure 7: Multistage process of hepatocarcinogenesis

Figure 8: The two hit hypothesis in the pathogenesis of NAFLD

Figure 9: Pathogenesis of liver cancer

Figure 10: (A) Molecular structure of glucose and 2DG. (B) 2DG and the inhibition of HK

Figure 11: The level of HK1-mRNA in liver foci

Figure 12: Deregulated genes, involved in glycolysis

Figure 13: Deregulated genes, involved in glycogenesis

Figure 14: Downregulation of genes, involved in gluconeogenesis

Figure 15: Upregulation of genes, involved in PPP

Figure 16: Summary of deregulated key enzymes in the glucose metabolism of preneoplastic lesions

Figure 17: ATP levels in primary HC, cultured in different media for up to 72 h

Figure 18: ATP levels in HC cultured in WE_{new} and RPMI with and without glucose after different time points

Figure 19: Vitality of HC cultured in WE_{new} with and without glucose after different time points

Figure 20: ATP levels in 2-DG treated HC cultured in WE_{old}, WE_{new} and RPMI with and without glucose after different time points

Figure 21: Vitality in HC cultured in WE_{new} with and without glucose after different time points

Figure 22: Labelling index (LI) of GSTp- and GSTp+ primary HC cultured in WE_{old}, treated with 2DG

Figure 23: Labelling index (LI) of unaltered primary HC cultured in WE_{old}, treated with 2DG and EGF

Figure 24: Labelling index (LI) of GSTp- and GSTp+ primary HC cultured in WE_{old} treated with 2DG

Figure 25: Labelling index (LI) of primary HC cultured in RPMI with and without glucose treated with 2DG and EGF

Figure 26: Labelling index (LI) of GSTp- and GSTp+ primary HC cultured in RPMI with and without glucose treated with 2DG

9.3. List of tables

Table 1: List of used reagents including suppliers

Table 2: List of used solutions, buffers and media

Table 3: List of components of WE_{old}, WE_{new} and RPMI

Table 4: Labelling index (LI) of unaltered primary HC cultured in WE_{new}, treated with 2DG

Table 5: Labelling index (LI) of unaltered primary HC cultured in WE_{old}, treated with 2DG

9.4. List of boxes

Box 1: Calculation for plating of living HC after trypan exclusion test